INVESTIGATION OF THE ROLE OF CELLULAR PRION PROTEIN IN THE INVASIVENESS AND SURVIVAL OF LS 174T COLORECTAL CANCER CELLS

By

CORNELIUS CHIENG KWANG LEE

A dissertation submitted to the Department of Biomedical Science,
Faculty of Science,
Universiti Tunku Abdul Rahman,
in partial fulfillment of the requirements for the degree of
Master of Science
March 2015

ABSTRACT

INVESTIGATION OF THE ROLE OF CELLULAR PRION PROTEIN IN THE INVASIVENESS AND SURVIVAL OF LS 174T COLORECTAL CANCER CELLS

Cornelius Chieng Kwang Lee

Cellular prion protein (PrP^C) is a glycoprotein affixed by glycosylphosphatidylinositol (GPI) to the cell surface and is abundantly expressed in the central nervous system (CNS). Emerging evidence suggests the role of PrP^C is implicated in glioblastoma, prostate cancer, breast cancer, gastric cancer, and pancreatic cancer. Therefore, the objective of this study was to investigate on the role of PrP^C in the invasiveness and survival of LS 174T colorectal cancer cells. This study reveals overexpression of PrP^C correlates with the development of a more sustainable and chemotherapeutic drug-resistant LS 174T human colorectal adenocarcinoma cell line. Overexpression of PrP^C in LS 174T cells was achieved by stable transfection. Endogenous and overexpression of PrP^C were assessed with immunoblotting and immunofluorescence microscopy. Cell growth in anchorage-dependent manner was evaluated with 3-(4,5-dimethylthiazol-2-yl)-2,5-diphenyltetrazolium bromide (MTT) assay. Overexpression of PrP^C was shown to increase viable cells in a time-dependent manner. Cell growth in anchorage-independent manner was evaluated with soft agar and anoikis assay. Overexpression of PrP^C in LS 174T cells remarkably increased the number of

colonies formed. While LS 174T cells remained resistant to anoikis, overexpression of PrP^C further exacerbated the phenomenon. Overexpression of PrP^C also increased cell motility and invasiveness properties in LS 174T cells. Cell adhesion to extracellular matrix (ECM) using collagen type-I and fibronectin coated surfaces revealed increased cell attachment in LS 174T cells overexpressing PrP^C. Overexpression of PrP^C was found to mitigate doxorubicin-induced cell cytotoxicity in LS 174T cells. Analysis of apoptotic and necrotic cells with annexin V/PI-FITC staining revealed that PrP^C overexpression attenuated apoptosis. Human apoptosis antibody array with 35 apoptosis-related proteins revealed that three inhibitor of apoptosis proteins (IAPs), Survivin, XIAP, and cIAP-1 were up-regulated in LS 174T cells overexpressing PrP^C in doxorubicin-induced apoptosis. In conclusion, the overexpression of PrP^C could enhance the invasiveness and survival of LS 174T colorectal cancer cells, indicating that PrP^C plays a role in colorectal cancer biology.

ACKNOWLEDGEMENT

This dissertation would not have been possible without the help of so many people in so many ways. My special thanks to Dr. Say Yee How, my main supervisor, who introduced this study to me. Without his guidance, mentoring, and knowledge, this study would not have been completed. I would also like to thank Dr. Chew Choy Hoong, my co-supervisor, for her advice, encouragement, and constructive criticism.

I would like to extend my gratitude to former and present biomedical science laboratory officers, Ms. Ng Shel Ling, Mr. Tie Shin Wei, and Mr. Saravanan a/l Sivasangaran for their technical assistances and supplying necessary materials in facilitating my research work.

I am proud and fortunate to express my gratitude to my family and friends for their continuous and relentless support in making everything possible. Last but not least, I would like to thank God for giving me this precious opportunity to pursue my master's study, God is great!

FACULTY OF SCIENCE

UNIVERSITI TUNKU ABDUL RAHMAN

Date: _____

SUBMISSION OF DISSERTATION

It is hereby certified that **CORNELIUS CHIENG KWANG LEE** (ID No: **11ADM01661**) has completed this dissertation entitled "**INVESTIGATION OF THE ROLE OF CELLULAR PRION PROTEIN IN THE INVASIVENESS AND SURVIVAL OF LS 174T COLORECTAL CANCER CELLS**" under the supervision of **DR. SAY YEE HOW** (Supervisor) from the Department of Biomedical Science, Faculty of Science, and **DR. CHEW CHOY HOONG** (Co-Supervisor) from the Department of Biomedical Science, Faculty of Science.

I understand that University will upload softcopy of my dissertation in pdf format into UTAR Institutional Repository, which may be made accessible to UTAR community and public.

Yours truly,

_____

(CORNELIUS CHIENG KWANG LEE)

APPROVAL SHEET

This dissertation/thesis entitled "**INVESTIGATION OF THE ROLE OF CELLULAR PRION PROTEIN IN THE INVASIVENESS AND SURVIVAL OF LS 174T COLORECTAL CANCER CELLS**" was prepared by **CORNELIUS CHIENG KWANG LEE** and submitted as partial fulfillment of the requirements for the degree of Master of Science at Universiti Tunku Abdul Rahman.

Approved by:

_____

(Associate Prof. Dr. SAY YEE HOW)
Date:……..
Supervisor
Department of Biomedical Science
Faculty of Science
Universiti Tunku Abdul Rahman

_____

(Associate Prof. Dr. CHEW CHOY HOONG)
Date:……..
Co-supervisor
Department of Biomedical Science
Faculty of Science
Universiti Tunku Abdul Rahman

DECLARATION

I hereby declare that the dissertation is based on my original work except for quotations and citations which have been duly acknowledged. I also declare that it has not been previously or concurrently submitted for any other degree at UTAR or other institutions.

Name _____

Date _____

TABLE OF CONTENTS

		Page
ABSTRACT		**ii**
ACKNOWLEDGEMENTS		**iv**
PERMISSION SHEET		**v**
APPROVAL SHEET		**vi**
DECLARATION		**vii**
LIST OF TABLES		**xiii**
LIST OF FIGURES		**xiv**
LIST OF ABBREVIATIONS		**xvii**
CHAPTERS		
1.0	**INTRODUCTION**	1
2.0	**LITERATURE REVIEW**	5
	2.1 Prion and Prion Diseases	5
	2.2 Cell Biology of PrP^C	6
	2.2.1 Expression and Functions of PrP^C	6
	2.2.2 Molecular Biology of PrP^C	7
	2.2.2.1 Human Prion Protein Gene	7
	2.2.2.2 Structure of PrP^C	9
	2.2.3 Biosynthesis of PrP^C	10
	2.2.4 PrP^C and Transmembrane Signalling	11
	2.2.5 PrP^C and Cell Adhesion	12
	2.2.6 A Role of PrP^C at Synapses	13
	2.3 An Overview of Cancer Biology	14
	2.3.1 Introduction and Prevalence of Cancer	14
	2.3.2 Hallmarks of Cancer	15
	2.3.3 Cancer and Metastasis	16
	2.3.4 Cancer and Apoptosis	18
	2.3.4.1 Extrinsic Pathway of Death	19
	2.3.4.2 Intrinsic Pathway of Death	20
	2.4 PrP^C and Programmed Cell Death	22

2.4.1 PrP^C and Oxidative Stress 22
2.4.1.1 Hypothesis 1: Direct Protection of PrP^C Against Oxidative Stress 22
2.4.1.2 Hypothesis 2: Indirect Protection of PrP^C Against Oxidative Stress 23
2.4.2 PrP^C and Copper 24
2.4.3 PrP^C and Mitochondrial Dysfunction 25
2.5 PrP^C and Tumor 26
2.5.1 PrP^C and Tumor Resistance 26
2.5.2 PrP^C and Tumor Progression 27

3.0 MATERIALS AND METHODS 29
3.1 General Chemicals and Reagents 29
3.2 List of Formula 30
3.3 Cell Culture 31
3.3.1 The Cell Lines 31
3.3.1.1 LS 174T Human Colorectal Adenocarcinoma Cell Line (CL-188) 31
3.3.1.2 HEK-293 Human Embryonic Kidney Cell Line (HCL-4517) 32
3.3.2 Cell Lines Maintenance 33
3.3.2.1 Preparation of Complete EMEM Culture Medium 33
3.3.2.2 Preparation of Reduced Serum OPTI-MEM Medium 34
3.3.2.3 Sub-culturing of Adherent Cell Lines 34
3.3.2.4 Cryopreservation and Thawing of Cells 34
3.3.3 Cell Counting 35
3.3.4 Cell Transfection Using Cationic Lipids Formulation 36
3.4 Protein Expression Analysis 37
3.4.1 Preparation of Cell Lysate 37
3.4.2 Quantitation of Total Protein 38
3.4.3 Sodium Dodecyl Sulfate Polyacrylamide Gel Electrophoresis (SDS-PAGE) 39
3.4.4 Western Blotting 40
3.4.4.1 Semi-dry Transfer 40

3.4.4.2 Blotting of PVDF Membrane 41
3.4.4.3 Stripping of PVDF Membrane for Repeated Hybridization 42
3.4.4.4 Amido Black Staining of PVDF Membrane 42
3.5 Immunofluorescence Microscopy 43
3.6 Cell Viability Assay Using 3-(4,5-dimethylthiazol-2-yl)-2,5-diphenyltetrazolium bromide (MTT) 43
3.7 Cell Growth and Proliferation Assay 44
3.8 Soft Agar Colony Formation 45
3.8.1 Preparation of Base Agar 45
3.8.2 Preparation of Top Agar 45
3.8.3 Soft Agar Maintenance and Colony Formation Analysis 46
3.9 Cell Anoikis Assay 46
3.9.1 Preparation of Poly (2-hydroxyethyl methacrylate) (poly-HEMA) plate 46
3.9.2 Evaluation of Cell Viability in poly-HEMA plate 47
3.10 Scratch Wound Assay 47
3.11 Transwell Invasion Assay 48
3.12 Cell Adhesion Assay 48
3.12.1 Preparation of The Glycoproteins Coated Plate 48
3.12.2 Cell Seeding and Evaluation of Adherent Cell 49
3.13 Cell Scattering Assay 50
3.14 *In Vitro* Multi-drug Sensitivity Assay 50
3.15 Annexin V-FITC/PI/DAPI Staining 51
3.16 Human Apoptosis Antibody Array Kit 52
3.17 Statistical Analysis 52

4.0 RESULTS 53
4.1 Immunoblotting Assessment of PrP^C Expression 53
4.2 Immunocytochemical Analysis of PrP^C Expression 55
4.3 Cell Growth and Proliferation Study 57
4.3.1 MTT Cell Proliferation Assay 57
4.3.2 Anchorage Independent Growth Evaluation 59

4.3.2.1 Cell Colony Formation Assay 59
4.3.2.2 Cell Anoikis Assay 62
4.4 Cell Migration and Invasion 64
4.4.1 Scratch Wound Assay 64
4.4.2 Transwell Invasion Assay 68
4.5 Cell Adhesion Assay 70
4.5.1 Collagen Protein as Coating Component in Adhesion Assay 70
4.5.2 Fibronectin Protein as Coating Component in Adhesion Assay 73
4.6 Qualitative Study on The Effect of PrP^C Overexpression on Epithelial Cell Scattering 75
4.7 *In Vitro* Multi-drug Sensitivity Assay 79
4.7.1 Observation of Morphological Changes in LS 174T and HEK-293 Cells Following Multi-drug Treatment 79
4.7.2 The Influence of PrP^C Overexpression on Multi-drug induced Cell Cytotoxicity 82
4.8 Quantitative Study of Cell Apoptosis Against Doxorubicin Insult 87
4.8.1 Fluorescence Microscopy Visualization of Apoptotic or Necrotic Cells Induced by Doxorubicin 87
4.8.2 Apoptotic Proteins Involved in The Overexpression of PrP^C 90
4.8.2.1 Human Apoptosis Antibody Array for LS 174T Cells 90
4.8.2.2 Human Apoptosis Antibody Array for LS 174T Cells Treated with Doxorubicin 92

5.0 DISCUSSION 94
5.1 Assessment of PrP^C Expression in Cancer and Non-cancer Cell 94
5.2 Role of PrP^C in Cell Growth and Proliferation 95
5.2.1 Anchorage-dependent Manner 95
5.2.2 Anchorage-independent Manner 96
5.3 Role of PrP^C in Cell Migration and Invasion 98
5.3.1 Two-dimensional Cell Migration and Invasion 98

5.3.2 Three-dimensional Cell Migration and Invasion 99
5.4 Role of PrP^C in Cell Adhesion Towards Extracellular Matrix Glycoproteins 101
5.5 Role of PrP^C in Cell Death Induced by Serum Deprivation 102
5.6 Role of PrP^C in Chemotherapeutic Drugs Treatment 104
5.7 Role of PrP^C in Cell Regulation Against Doxorubicin Insult 105
5.8 Signaling Pathways Involved in The Anti-apoptotic Property of PrP^C 106
5.8.1 Human Apoptosis Antibody Array for LS 174T Cells 106
5.8.2 Human Apoptosis Antibody Array for LS 174T Cells in Doxorubicin-induced Apoptosis 108
5.9 Concluding Remarks and Future Studies 115

6.0 CONCLUSIONS 117
REFERENCES 119
APPENDICES 135

LIST OF TABLES

Table		Page
3.1	List of solution formulations.	30
3.2	Effective working concentrations of G-418 sulfate towards different cell lines.	37
3.3	Protocol for 30% acrylamide/bis solution, 37.5:1.	39
3.4	Antibodies for Western blotting analysis.	42
4.1	Lethal dose values for LS 174T and HEK-293 cells treated with different cancer drugs.	85

LIST OF FIGURES

Figures		Page
2.1	Overview of PrP^{C} and PrP^{Sc} metabolism.	11
2.2	Stages of metastasis.	17
2.3	Crosstalk of extrinsic and intrinsic pathways death.	21
3.1	Cell morphology of LS 174T.	31
3.2	Cell morphology of HEK293.	32
4.1	Western blot analysis of LS 174T and HEK-293 cells.	54
4.2	Immunofluorescence microscopy depicting expression of PrP^{C} in LS 174T and HEK-293 cells.	56
4.3	Cell proliferation study via MTT.	58
4.4	Cell proliferation study via soft agar colony formation assay.	60
4.5	Colony count for soft agar colony formation assay.	61
4.6	Percentage of viable cells for anoikis assay.	63
4.7	Scratch wound assay for LS 174T cells.	65
4.8	Scratch wound assay for HEK-293 cells.	66

4.9	Open wound area count for scratch wound assay.	67
4.10	QCM™ 24-well cell invasion for LS 174T cells.	68
4.11	Fluorescent intensity analysis for matrigel invasion assay.	69
4.12	Collagen coated surface for cell adhesion assay.	72
4.13	Fibronectin coated surface for cell adhesion assay.	74
4.14	The influence of PrP^C overexpression upon serum deprivation in LS 174T cells.	76
4.15	The influence of PrP^C overexpression upon serum deprivation in HEK-293 cells.	78
4.16	The influence of PrP^C overexpression upon doxorubicin exposure in LS 174T cells.	80
4.17	The influence of PrP^C overexpression upon doxorubicin exposure in HEK-293 cells.	81
4.18	Doxorubicin treatment for LS 174T and HEK-293 cells.	83
4.19	Etoposide treatment for LS 174T and HEK-293 cells.	84
4.20	Vincristine sulfate treatment for LS 174T and HEK-293 cells.	86
4.21	Fluorescence microscopy assessment for the effect of doxorubicin on LS 174T cells.	88
4.22	Percentage of cell stained with annexin V and PI.	89

4.23	Human apoptosis antibody array for LS 174T cells treated with doxorubicin.	91
4.24	Apoptosis markers profiling for LS 174T cells.	93
5.1	Possible apoptosis signalling pathways involved in LS 174T cell overexpressing PrP^C.	109

LIST OF ABBREVIATIONS

ANOVA	Analysis of variance
APS	Ammonium persulfate
BCA	Bicinchoninic acid
BSA	Bovine serum albumin
BSE	Bovine spongiform encephalopathy
CJD	Creutzfeldt-Jakob disease
CNS	Central nervous system
CO_2	Carbon dioxide
CWD	Chronic wasting disease
cyt-c	Cytochrome C
d	Day
DIABLO	Direct IAP binding protein with low pI
DISC	Death-inducing signalling complex
ECM	Extracellular matrix
EMT	Epithelial mesenchymal transition
ER	Endoplasmic reticulum

EUE	Exotic ungulate encephalopathy
FADD	Fas-associated death domain
FFI	Fatal familial insomnia
FSE	Feline spongiform encephalopathy
GAG	Glycosaminoglycan
GPI	Glycosylphosphatidylinositol
GSS	Gerstmann-Straussler-Scheinker syndrome
h	Hour
H_2O_2	Hydrogen peroxide
HtrA2	High temperature requirement protein A
IAP	Inhibitor of apoptosis protein
kDa	Kilo Dalton
MDR	Multi-drug resistance
Mn	Manganese
MTT	3-(4,5-dimethylthiazol-2-y1)-2,5-diphenyltetrazolium
NCAM	Neural cell adhesion molecule
OD	Optical density

P-gp	P-glycoprotein
PBS	Phosphate buffer saline
PBST	Phosphate buffer saline-TWEEN 20
PFA	Paraformaldehyde
p*I*	Isoelectric point
PIC	Protease inhibitory cocktail
poly-HEMA	2-hydroxyethyl-methacrylate
PrP^{C}	Cellular prion protein
PrP^{Sc}	Scrapie form prion protein
PVDF	Polyvinylidene difluoride
RI	Relative intensity
ROS	Reactive oxygen species
rpm	Revolution per minute
RT	Room temperature
SDS-PAGE	Sodium dodecyl sulphate - polyacrylamide gel electrophoresis
SEM	Standard error of mean
SMAC	Second mitochondria-derived activator of caspase

SOD	Superoxide dismutase
t	Time
TEMED	Tetramethyl ethylenediamine
TME	Transmissible mink encephalopathy
TNF	Tumor necrosis factor
TSE	Transmissible spongiform encephalopathy
V	Volt

CHAPTER 1

INTRODUCTION

Prion is defined as a proteinaceous infectious particle that lacks nucleic acid (Prusiner et al., 1998). At least two conformational isoforms of prion protein exist; the cellular prion protein (PrP^{C}), and the infectious, misfolded, scrapie form (PrP^{Sc}) (Aguzzi et al., 2008). The structure of PrP^{C} consists of a signal peptide, five-octapeptide repeats with the sequence PHGGGWGQ, a highly-conserved hydrophobic domain, three peptide sequences forming a β-helix structure, a signal sequence for glycosylphosphatidylinositol (GPI) anchor and it is found in the cholesterol-rich lipid raft domains within the cellular membrane (Mehrpour and Codogno, 2010). PrP^{C} contains two consensus sequences for the N-linked glycosylation sites, a single unique disulphide bridge between the two cysteines in most of the structured C-terminus domains, and three glycosylation isoforms that are present simultaneously in the cell, including unglycosylated PrP, monoglycosylated PrP, and diglycosylated (Lehmann et al., 1999).

In the event of post-translational conversion, PrP^{C} is converted to misfolded PrP^{Sc} whereby a portion of its α-helical and coil structure is refolded into β sheet (Pan et al., 1993). PrP^{Sc} is responsible for transmissible neurodegenerative disorders that include Creutzfeldt-Jakob diseases (CJD), Gerstmann-Straussler-Scheinker syndrome (GSS), kuru, and fatal familial

insomnia (FFI) in humans; and scrapie and bovine spongioform encephalotpathy (BSE) in animals (Aguzzi and Polymenidou, 2004). In comparison of PrP^{Sc} and PrP^{C}, the latter is rich in α-helical secondary structure, soluble in mild detergents, proteinase-K sensitive, and exists in stable monomeric state (Stohr et al., 2008).

To date, there is a wide range of research conducted to understand the physiological functions of PrP^{C}. The major proposed functions of PrP^{C} that have been documented include cellular uptake or binding of copper ions, cytoprotective effect against apoptotic and oxidative stress, transmembrane signaling, formation and maintenance of synapses, and cellular adhesion to the extracellular matrix (Westergard et al., 2007). PrP^{C} is not only expressed abundantly in the central nervous system (CNS), but has also been detected in other non-neuronal tissue as diverse as lung, kidney, heart, muscle, lymphoid cells, gastrointestinal tract, and mammary glands (Mehrpour and Codogno, 2010). Most of the studies have targeted on the aberrant roles of PrP^{C} in neurodegenerative diseases, while the functions of PrP^{C} outside the CNS remain to be elucidated.

Cancer is a disease mainly derived from mutations in single somatic cells that deviate from the normal routes of proliferation, migrate to adjacent normal tissues, and develop metastasis on different sites from the origin (Masoudi-Nejad et al., 2014). The hallmarks of cancer comprise of six distinct biological capabilities that are acquired during the multistep development of human tumors, namely sustaining proliferative signaling, evade growth

suppressors, resist cell death, enable replicative immortality, induce angiogenesis, and activate invasion and metastasis (Hanahan and Weinberg, 2011).

Recently, several documented data indicated that PrP^C might be implicated in cancer biology. For instance, level of PrP^C was found to increase in a time-dependent manner in T98G glioblastoma cell line (Kikuchi et al., 2002). Meanwhile, PrP^C expression in prostate tumor spheroids was found to be related to the intracellular redox state and potentially participate in antioxidative defense (Sauer et al, 1999). In addition, overexpression of PrP^C causes the conversion of TNF-α-sensitive MCF7 breast adenocarcinoma cell line into TNF-α-resistant through a mechanism involving alteration of cyt-c release from mitochondria and nuclear condensation (Diarra-Mehrpour et al, 2004). PrP^C promotes invasion and metastasis (Pan et al, 2006; Liang et al., 2009a), proliferation, adhesion, and resistance to apoptosis (Liang et al., 2009a), and induction of hypoxia (Liang et al., 2007b) in SGC-7901 and MKN-45 human gastric cancer cell lines. Furthermore, the binding of pro-PrP filamin A (FLNa) disrupts FLNa function, thus this increases the aggressiveness of human pancreatic ductal adenocarcinoma cell lines (Li et al., 2009). Therefore, this has alluded to the study of possible correlation between PrP^C and other type of cancers as well.

Colorectal cancer was the third most common cancer worldwide contributing 9.7% of the total number of the new cases diagnosed in 2012 (World Cancer Research Fund International, 2014). In Malaysia, colorectal

cancer was ranked at second place, after breast cancer in the statistical report of ten most frequent cancer cases of all residence (Zainal Arrifin and Nor Saleha, 2011). In regard to the high prevalence of colorectal cancer, lacking of marker during early diagnosis might even worsen the prognosis, as early detection is extremely crucial to determine the outcome of cancer progression. Besides, by understanding the function of PrP^C in colorectal cancer biology, this study also provides a significant target for chemotherapeutic intervention in colorectal cancer. Hence, investigation of the role of PrP^C in human colorectal cancer biology was carried out using LS 174T human colorectal adenocarcinoma cell line, while HEK-293 human embryonic kidney cell line was used as representative of non-cancer cell for comparison.

Therefore, the objectives of this study were:

(a) To examine the pattern of endogenous PrP^C protein expression in LS 174T and HEK-293 cell lines, and thereby to stably overexpress PrP^C.

(b) To study the function of PrP^C overexpression on cell proliferation, growth in anchorage-independent manner, migration, invasion, and adhesion to the extracellular matrix (ECM) glycoproteins.

(c) To examine the effect of PrP^C overexpression on cell sustainability through *in vitro* multi-drug sensitivity assay in LS 174T and HEK-293 cells.

(d) To investigate the relevant apoptotic proteins involved corresponding to overexpression of PrP^C in LS 174T cells through human apoptosis antibody array study.

CHAPTER 2

LITERATURE REVIEW

2.1 Prion and Prion Diseases

The word prion refers to proteinaceous infectious particle and it is devoid of nucleic acid (Prusiner et al., 1998). PrP^{C} is converted into PrP^{Sc} through a post-translational modification whereby a portion of its α–helical and coil structure is refolded into β-sheet (Pan et al., 1993). The abnormal isoform of this protein is the causative agent of prion diseases, commonly referred to as transmissible spongiform encephalopathies (TSEs) (Aguzzi and Polymenidou, 2004). The fate of PrP, a constituent of normal mammalian cells determines the manifestation of prion diseases. Prion diseases may present as genetic, sporadic, or infectious disorders, depending on the modification of the PrP (Prusiner et al., 1998). An archetype of prion diseases was first discovered in sheep, while different kinds of prion diseases have been reported in human; for instance, kuru, CJD, GSS, and FFI. In conjunction with scrapie in sheep and goats, other examples of prion disease in animals such as BSE in cattle, transmissible mink encephalopathy (TME) in mink, feline spongiform encephalopathy (FSE) in cats and exotic ungulate encephalopathy (EUE) in several exotic ungulates that include nyala and kudu, and chronic wasting disease (CWD) in deer and elk (Gibbs and Asher, 1996). Different neurological symptoms and common histopathological features distinguish these prion diseases. In general, CJD presents as progressive dementia,

meanwhile scrapie of sheep and BSE commonly manifest as ataxic illnesses (Wells et al., 1987). In CJD, scrapie, and BSE, including other disorders commonly referred to as prion diseases, astrocytic gliosis, and spongiform degeneration are observed upon microscopic examination of the CNS. The main criteria to distinguish among prion diseases is by assessing the degree of spongiform degeneration which is quite variable, meanwhile the degree of reactive gliosis generally correlates with the degree of neuron loss (Masters and Richardson, 1978). In addition, prion diseases are frequently accompanied by the extracellular accumulation of PrP isoform associated with PrP^{Sc}, which can lead to the aggregation of fibrils in the extracellular matrix (O'Donovan et al., 2001). Even though the nature of the infectious agent and the exact pathogenic mechanisms of prion diseases are not completely explored, researchers have reported that most of the prion diseases are associated with the aberrant metabolism of the PrP^{C} (Aguzzi and Weissmann, 1997; Martins et al., 2001).

2.2 Cell Biology of PrP^{C}

2.2.1 Expression and Functions of PrP^{C}

PrP^{C} is a normal cellular protein abundantly expressed in the central nervous system, also found in several peripheral tissues, and in leukocytes (Caughey et al., 1988; Bendheim et al., 1992; Dodelet and Cashman, 1998). The normal cellular function of this ubiquitous protein remains elusive, even though it is located on the cell surface and consistent with the roles in transmembrane signaling, cell adhesion and recognition, or ligand uptake

(Harris, 1999; Linden et al., 2008; Mehrpour and Codogno, 2010). A possible role of PrP^C in synaptic function is endorsed by the suggestion that PrP-null mice displayed impaired spatial learning with altered excitatory and inhibitory neurotransmission (Collinge, 1994; Criado 2005). Likewise, PrP^C has been elucidated to play a crucial role in the processing of normal sensory information by the olfactory system (Le Pichon et al., 2009) and it may also influence odor perception (Wilson and Nixon, 2009). Although PrP-null mice displayed minor alterations in immune function, recent studies have shown that PrP^C is necessary for the self-renewal of hematopoietic stem cells (Zhang et al., 2006a; Martin-Lanneree et al., 2014). Notwithstanding, Hu and colleagues (2008) have also reviewed other physiological roles played by PrP^C including regulation of circadian rhythms, memory formation, as well as cognitive function.

2.2.2 Molecular Biology of PrP^C

2.2.2.1 Human Prion Protein Gene

Human prion protein locus designated as *PRNP* locus is located in the p12/ p13 region of chromosome 20 wherein it consisted of three genes, namely *PRNP, PRND* and *PRNT* (Makrinou et al., 2002). Study by Makrinou and colleagues in 2002 revealed that these genes located within a 55 kb region where *PRNP* spans up to 20 kbp, *PRND* harbours 3 kbp and *PRNT*. It was also reported that *PRNP* composed of two exons, which is ubiquitous but showing variable expression level, particularly the highest level was observed in CNS and testis (Makrinou et al., 2002). Mutations that have occurred within the

PRNP have often been associated to the prion diseases (Aguzzi et al., 2008). *PRNP* encodes a 253 amino acid protein with size ranging from 32-35 kDa (Aguzzi and Polymenidou, 2004). Besides, this gene is reported to be found in all known mammalian cells, mostly in the brain, myoepithelial cells, lymphocytes and also stromal cells of lymphoid organs (Aguzzi and Polymenidou, 2004; Meslin et al., 2007b; Didier et al., 2006).

The second gene, *PRND*, consisted of two exons and encodes a 179 amino acids protein, which are known as Doppel (Westergard et al., 2007). This protein bears similar structure and topology of protein with *PRNP*, whereby it shares 25% identity of amino acid sequence consisting the C-terminal domain of PrP^C but in the absence of the N-terminal hydrophobic and octarepeat regions (Westergard et al., 2007). Westergard and co-workers (2007) also reported that *PRND* is predominantly expressed in variety of tissues during fetal development. Meanwhile, Comincini and co-workers (2007) linked the overexpressed *PRND* to one kind of glial tumor, astrocytoma, where a high level of Doppel was located in the cytoplasm of the tumor cells.

Another gene that is located at this locus is *PRNT*, which encodes three alternative splicing transcripts and does not encode a protein. It is reported that this gene is expressed exclusively in adult testis (Mehrpour and Codogno, 2010). Recently, a fourth gene, which is related to the prion gene family, was discovered and it is designated as *SPRN*, which encode a protein named Shadoo. However, this gene is not located in the prion genomic locus, instead

it was discovered in both mice and human chromosomes 7 and 10, respectively (Premzl et al., 2003). The open reading frame of *SPRN* is located within a single exon and it is exclusively expressed in brain (Watts et al., 2007). Watts and colleagues in 2007 suggested that Shadoo could be related to prion-associated CNS phenomena.

2.2.2.2 Structure of PrP^C

In human tissue, PrP^C is predominantly found in cholesterol-rich lipid raft within the microdomain of membrane (Stahl and Prusiner, 1991). A study on the protein structure of prion by Stahl and Prusiner (1991) revealed that human PrP^C consists of six parts- a signal peptide (1-22 amino acids residues), five octapeptide repeats of the sequence (PHGGGWGQ) (51-91 amino acids residues), a highly conserved hydrophobic domain (106-126 amino acids residues), followed by three peptides sequences that made up α-helix structures (α1-α2-α3), two peptide sequences forming a β-helix structures and lastly a signal sequence for GPI anchor (231-253 amino acids residues). It was also reported that two consensus sequences in PrP^C are responsible for the N-linked glycosylation at T181 and T197. Concurrently, the un-, mono- and di-glycosylated PrP^C are also simultaneously present in the cell (Stahl and Prusiner, 1991). The cysteine residues located at Cys 179 and Cys 214 are responsible for the formation of disulphide bond, whereby it is essential for proper folding of protein (Stahl and Prusiner, 1991).

The octapeptide repeats region in PrP^C serves two purposes. Firstly, the histidine residues located within the octarepeat region are the copper-binding sites for copper. Copper is known as inducer for endocytosis of PrP^C (Stahl and Prusiner, 1991). Secondly, the expansion of octarepeat region (13 total repeats) is known to be associated with genetic prion diseases (Stahl and Prusiner, 1991).

2.2.3 Biosynthesis of PrP^C

PrP^C is expressed beginning in the embryogenesis (Manson et al., 1992; Harris et al., 1993; Westergard et al., 2007). The biosynthetic pathway accorded by PrP^C is very similar to majority of cell membrane proteins as well as the secreted proteins (Harris, 2001). As a typical cell surface glycoprotein, PrP^C is first imported into the endoplasmic reticulum (ER), in which nascent PrP^C is processed, glycosylated, and modified by a C-terminal GPI anchor followed by proper folding prior transport to the Golgi as shown in Figure 2.1 (Rapoport, 2007; Hebert and Molinari, 2007). As it transits the Golgi stacks, PrP^C receives further modifications to its glycans as well as GPI anchor and is then delivered to the cell surface (Chakrabarti et al., 2009). Although most cell-surface PrP^C can be found in lipid rafts, however, some of the protein is shifted to clathrin-coated pits followed by constitutive endocytosis and recycling or routed to lysosomes for degradation (Shyng et al., 1994; Gorodinsky and Harris, 1995; Naslavsky et al., 1996; Sunyach et al., 2003. Consequently, majority of PrP^C follows the conventional exocytic pathway to the cell surface as well as the endocytic pathway for turnover in the lysosome

(Chakrabarti et al., 2009). In normal cell, PrP^C biosynthesis and trafficking to the cell surface usually takes ~30 min, meanwhile, cell degradation comprised of a half-life of ~3-6 h (Caughey et al., 1989; Borchelt et al., 1990).

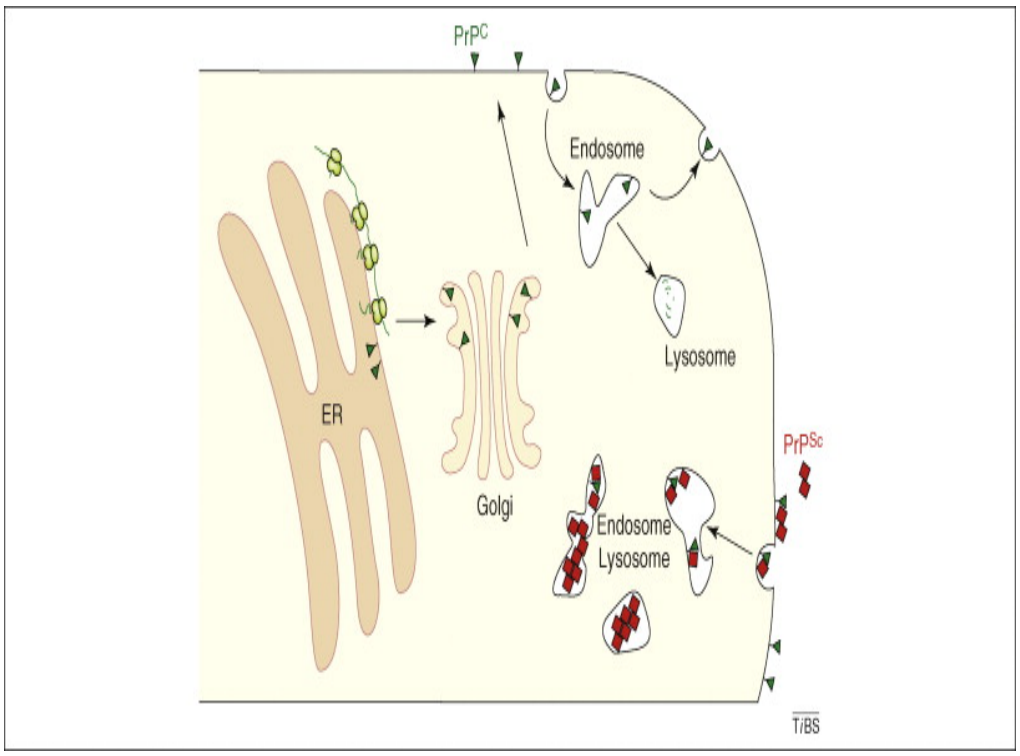

Figure 2.1: Overview of PrP^C and PrP^{Sc} metabolism
Nascent PrP (green line) is synthesized at the ER and imported into the ER lumen. Properly folded PrP (green triangle) trafficked through the Golgi to the cell surface, recycled through endosomes and eventually degraded in lysosome. The lower right shows the fates of extrinsic PrP^{Sc} (red square). PrP^C and PrP^{Sc} can both interact and internalized into endosomes. As PrP^{Sc} has a longer half-life (~24 h) for lysosomal degradation, therefore it can accumulate to a relatively higher level in intracellular compartments of the endo-lysosomal system. (Adapted from Chakrabarti et al., 2009)

2.2.4 PrP^C and Transmembrane Signalling

Up to date, there are significant researches reported that PrP^C can activate transmembrane signaling pathways implicated in several different

phenomena, which include neurite outgrowth, neuronal survival, and neurotoxicity (Westergard et al., 2007). Similar to other GPI-anchored proteins, the PrP^C resides in lipid raft domains of the plasma membrane, also known to function as molecular scaffolds for signal transduction (Tsui-Pierchala et al., 2002; Taylor and Hooper, 2006). Deletions of PrP^C in *Prn-p*$^{0/0}$ mice have been shown to reduce Akt activation, increase postischemic caspase-3 activation, and exacerbate ischemic brain injury. The level of phosphorylated Akt was declined in *Prn-p*$^{0/0}$ mice suggesting that PrP^C may intensify Akt-dependent cell survival pathways and also to prevent damage inflicted by ischemic brain injury (Weise et al., 2006). In addition, Akt activity was found reduced in neurons and brain tissue from *Prn-p*$^{0/0}$ mice as compared to *Prn-p*$^{+/+}$ mice (Vassallo et al., 2005). These suggest a potential neuroprotective effect of PrP^C in the PI3 kinase/Akt-signaling pathway, since PI3 kinase plays a pivotal role in cell survival.

2.2.5 PrP^C and Cell Adhesion

For the past two decades, numerous studies have reported that PrP^C is able to stimulate and promote the outgrowth of neurite (Chen et al., 2003; Santuccione et al., 2005; Pantera et al., 2009; Beraldo,et al., 2011; Loubet et al., 2012; Watanabe et al., 2012). The binding between PrP^C and sulfated glycosaminoglycan (GAG) (Caughey et al., 1994), which is a component of the extracellular matrix proteins, and to other matrix-related molecules such as selectins (transmembrane glycoprotein), laminin (structural component of basement membrane), laminin receptor, and stress inducible protein-1 (heat-

shock-related protein) (Rieger, et al., 1997; Graner et al., 2000; Schmitt-Ulms et al., 2001; Zanata et al., 2002; Li et al., 2007) suggested that PrP^C might participate in cell adhesion (Yang et al., 2014). Both *cis* and *trans* interactions between neural cell adhesion molecule (NCAM) at the neuronal surface as well as PrP^C promote the recruitment of NCAM to lipid rafts, that will lead to activation of fyn kinase, which is an enzyme involved in NCAM mediated signaling, thereby stimulating neurite outgrowth (Santuccione et al., 2005).

2.2.6 A Role of PrP^C at Synapses

Several experimental observations have advanced the hypothesis that PrP^C could play a role in the synaptic structure, function or maintenance. Consistent with this hypothesis is the understanding that synaptic pathology is often a notable feature of prion diseases (Jeffrey et al., 2000). In addition, studies from researchers have revealed that PrP^C is concentrated along axons as well as pre-synaptic terminals (Moya et al., 2000; Laine et al., 2001; Ford et al., 2002; Sale et al., 2002; Mironov et al., 2003; Barmada et al., 2004), and is subjected to anterograde and retrograde axonal transport (Brochelt et al., 1994; Moya et al., 2004). Furthermore, overnight exposure of cultured hippocampal neuron with recombinant PrP^C has been shown to increase neurons with differentiated axons and dendrites, as well as the number of synaptic contacts. Thus, it is evident that the full-length PrP^C could play a regulatory role in the synapse formation and it has a vital function to serve as a growth factor in the development of neuronal polarity (Kanaani et al., 2005).

2.3 An Overview of Cancer Biology

2.3.1 Introduction and Prevalence of Cancer

Cancer is a standard term used to describe diseases in which cells proliferate aggressively regardless of normal growth rates of the original tissue or organ site and continue to invade surrounding and adjoining tissues (Ray and Jablons, 2010). Most known cancers are disease of the epithelial tissue, in which during late stages the cancerous cells continue to invade the mesoderm and the endodermal layers (Cairns, 1975).

Cancer is the leading cause of death in well-developed countries and ranked at second in cause of death in developing countries. In worldwide, breast cancer in females as well as lung cancer in males are cases of the most frequently diagnosed cancers and the principal cause of cancer death for each gender followed by colorectal cancer, except in males is preceded by prostate cancer (Jemal et al., 2011). In Malaysia, colorectal cancer is ranked at second place after breast cancer followed by lung cancer in ten most frequent cancers of all residence (Zainal Arrifin and Nor Saleha, 2011).

2.3.2 Hallmarks of Cancer

For the past decade, six distinct hallmarks of cancer were proposed that provides a sturdy framework to understand the diversity of neoplastic disease. The six hallmarks include sustaining proliferative signaling, enabling replicative immortality, inducing angiogenesis, evading growth suppressors, activating invasion and metastasis, and resisting cell death (Hanahan and Weinberg, 2000).

Recent years, Hanahan and Weinberg (2011) have proposed more emerging hallmarks and enabling characteristic. As the capability is not completely generalized and fully validated, they therefore labeled them as emerging hallmarks. In the first emerging hallmark, which is deregulating cellular energetics, it involves the capability of neoplasia to alter cellular metabolism in order to effectively support cancer cells proliferation. In a subsequent emerging hallmark, which is avoiding immune destruction, it allows cancer cells to evade immunological destruction, particularly by T and B lymphocytes, natural killer cells, and macrophages (Hanahan and Weinberg, 2011). Consistent with this hallmark, Kim and colleagues (2007) have also reviewed the escape mechanisms of tumor cells from immune surveillance during tumor progression.

In addition, two consequential enabling characteristics of neoplasia, namely genome instability and mutation and tumor-promoting inflammation, were proposed to further support the acquisition of emerging hallmarks (Hanahan and Weinberg, 2011). In the process of acquiring the mutant genes

required for tumorigenesis, cancer cells tend to intensify the rates of mutation (Negrini et al., 2010; Salk et al., 2010). Nevertheless, inflammation can contribute to multiple hallmarks by nourishing tumor microenvironment, including growth factors, signaling factors, survival factors, pro-angiogenic factors, and extracellular matrix-modifying enzymes that facilitate angiogenesis, invasion, and metastasis (Karnoub and Weinberg, 2006-2007; DeNardo et al., 2010; Grivennikov et al., 2010; Qian and Pollard, 2010).

2.3.3 Cancer and Metastasis

Metastasis of cancerous cell consists of various channeling steps, whereby failure of any of the steps can lead to the shutdown of the entire metastasis mechanism (Ray and Jablons, 2010). The multistep process of invasion and metastasis has been described as a sequence of discrete steps, otherwise termed as the invasion-metastasis cascade (Fidler, 2003; Talmadge and Fidler, 2010). Figure 2.2 shows the schematic overview of metastasis process.

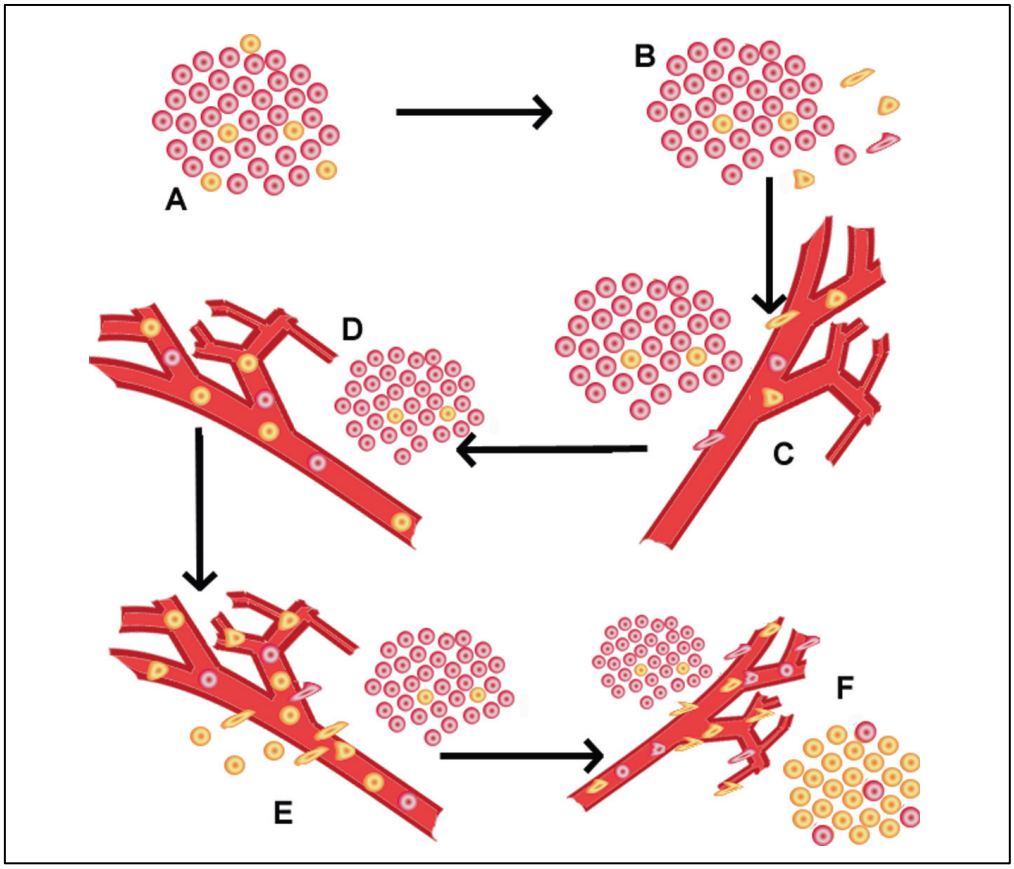

Figure 2.2: Stages of metastasis.
(A) Abnormal cell growth gives rise to tumor, (B) Detachment of tumor cells from the ECM, (C) Intravasation of tumor cells into the bloodstream, (D) Transport of tumor cells through the bloodstream, (E) Extravasation of tumor cells at distal site, (F) Growth of metastatic lesion. (Adapted from Ray and Jablons, 2010)

Increased expression of E-cadherin was well recognized as an antagonist of invasion and metastasis, notwithstanding the down regulation of E-cadherin was known to potentiate these phenotypes (Cavallaro and Christofori, 2004; Berx and van Roy, 2009). In metastasis, a prominent phase of development, referred as the "epithelial-mesenchymal transition" (EMT) where transformed epithelial cells can acquired the abilities to invade, to resist cell death, and to disseminate (Barrallo-Gimeno and Nieto, 2005; Klymkowsky and Savagner, 2009; Polyak and Weinberg, 2009; Thiery et al.,

2006; Yilmaz and Christofori, 2009). The important entity of EMT lies in which the disseminating metastatic cells have to resist cell death in anchorage-independent manner and resist to anoikis (Chiarugi and Giannoni, 2008; Ray and Jablons, 2010; Paoli et al., 2013). The ability of the metastatic cells to survive in the process is crucial as intravasating or extravasating cancer cells may not attach to the ECM at all or it is possible to encounter other non-recognized matrices on its route (Eccles and Welch, 2007). For instance, overexpression of Bcl-2 elevates the metastatic potential of breast cancer epithelial cells through the inhibition matrix-degradation-induced apoptosis; however, it does not affect primary cancer growth or cell motility (Martin and Leder, 2001; Pinkas et al., 2004). After tumor cells undergo EMT, they migrate through polarization and by extending lamellipodia or filopodia, binding specific cell surface glycoproteins or extracellular matrix ligands, further push themselves forward through actin polymerization and translocation of the of the cell body, followed by detachment of the adhesive bonds at the rear (Lauffenburger and Horwitz, 1996). Adhesion to the ECM glycoproteins can be facilitated by interactions of β-integrins that cooperate with and recruit cell surface proteases to locally degrade the ECM (Ray and Jablons, 2010).

2.3.4 Cancer and Apoptosis

Apoptosis is a term used to describe the situation where cells actively pursue a course toward cell death upon obtaining certain stimuli (Majno and Joris, 1995). Morphological distinct hallmarks of apoptosis in the nucleus are

nuclear fragmentation and chromatin condensation, usually accompanied by cell rounding, reduction in cellular volume (pyknosis) as well as retraction of pseudopodes (Kroemer et al., 2009). Chromatin condensation initiates at the periphery of the nuclear membrane, further condenses until it breaks up within a cell with an intact membrane, a feature known as karyorrhexis (Majno and Joris, 1995). During the later stage of apoptosis, some of the classic morphological features are membrane blebbing, structural alteration of cytoplasmic organelles, and loss of membrane integrity (Kroemer et al., 2009). There are a few mechanisms that contribute to evasion and apoptosis and carcinogenesis that include impaired receptor signaling pathway, defects or mutations in p53, reduced expression of caspases, increased expression of inhibitor of apoptosis proteins (IAPs), and disrupted balance of Bcl-2 family proteins (Wong, 2011).

2.3.4.1 Extrinsic Pathway of Death

The extrinsic death receptor pathway initiates when death ligands bind to a death receptor such as type 1 TNF receptor (TNFR1), Fas (CD95) and FasL (Wong, 2011). These death receptors consist of an intracellular death domain that recruits adapter proteins namely, TNF receptor-associated death domain (TRADD) and Fas-associated death domain (FADD), and cysteine proteases like caspase 8 (Schneider and Tschopp, 2000). The binding of death ligand to the death receptor results in the formation of a protein complex known as the death-inducing signaling complex (DISC) (O'Brien and Kirby, 2008). Subsequently, DISC initiates the downstream effector of caspase-8

activities (Karp, 2008). Both extrinsic and intrinsic pathway will converge at the level of pro-caspase 3.

2.3.4.2 Intrinsic Pathway of Death

Intrinsic pathway is initiated within the cell due to internal stimuli such as irreparable genetic damage, tissue hypoxia, extremely high concentrations of cytosolic Ca^{2+}level, and severe oxidative stress (Karp, 2008). Regardless of the stimuli, the pathway will result in increased mitochondrial permeability that will release the pro-apoptotic proteins such as cyt-c into the cytoplasm (Danial and Korsmeyer, 2004). There are two main groups of the Bcl-2 family proteins that regulate the pathway, namely the pro-apoptotic proteins (Bax, Bad, Bak, Bcl-Xs, Bid, Bim, Bik, and HrK) and anti-apoptotic proteins (Bcl-2, Bcl-X_L, Bfl-1, Bcl-W, and Mcl-1). The balance between these proteins will determine the initiation of apoptosis (Reed, 1997). Other apoptotic factors that are released from the mitochondrial intermembrane space into the cytoplasm are apoptosis inducing factor (AIF), Omi/high temperature requirement protein A (HtrA2), second mitochondria-derived activator of caspase (Smac), and direct IAP binding protein with low pI (DIABLO) (Kroemer et al., 2007). The function of Smac/DIABLO or Omi/HtrA 2 is to promote caspase activation by binding to IAPs, which subsequently leads to disruption of the interaction of IAPs with caspase-3 or -9 (Kroemer et al, 2007; LaCasse et al., 2008). Crosstalk of extrinsic and intrinsic pathway of death is illustrated in Figure 2.3.

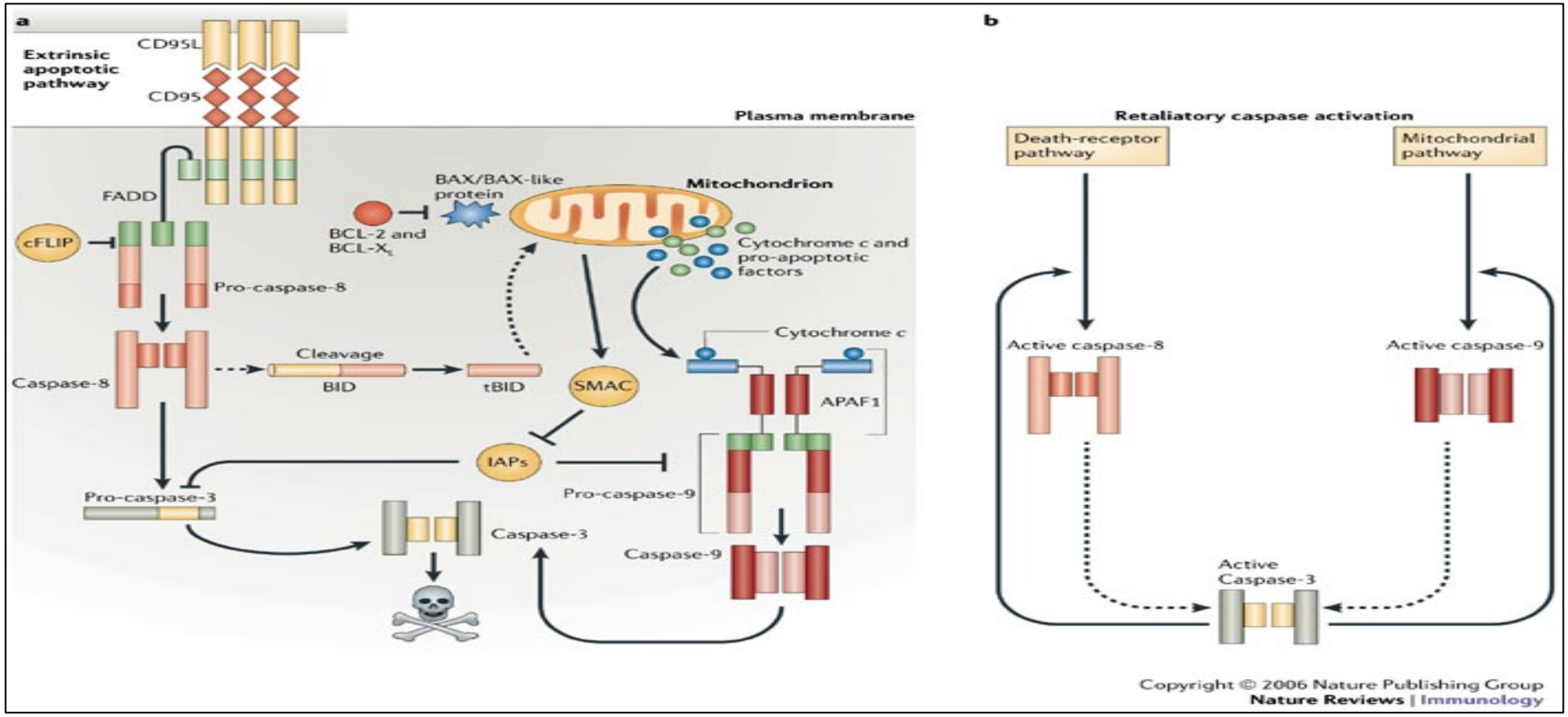

Figure 2.3: Crosstalk of extrinsic and intrinsic pathways of death.
(A) Extrinsic and intrinsic pathway of death. Extrinsic pathway is mediated by caspase-8, while the intrinsic pathway is mediated by caspase-9. In certain cells, the two pathways are interconnected by truncated BID (tBID) that is formed upon cleavage by activated caspase-8. (B) There is increasing evidence showing that the two death pathways can activate each other through the activation of caspase-9 that subsequently cleave and activate caspase-3 and in a feedback amplification loop, it activates caspase-8. (Adapted from Hotchkiss and Nicholson, 2006)

2.4 PrP^C and Programmed Cell Death

2.4.1 PrP^C and Oxidative Stress

For the past few decades, researchers have exemplified the role of PrP^C in protecting cells from oxidative stress through *in vivo* or *in vitro* studies. Perhaps the most signification observation among the study is that neurons cultured from PrP-null mice are much more susceptible to cell death than the wild-type mice in the treatment of agents that induce oxidative stress, namely, hydrogen peroxide, xanthine oxidase, and copper ions (Brown et al., 1997a, Wong et al, 2001; Brown et al, 2002). Furthermore, brain lesions induced by hypoxia and ischemia are noticeably larger in *Prn-p*$^{0/0}$ as compared to *Prn-p*$^{+/+}$ mice (McLennan et al., 2004; Sakurai Yamashita et al., 2005; Spudich et al., 2005). Since hypoxia and ischemia are causal of neuronal cell death via oxidative damage, these observations also link PrP^C to protection against oxidative stress (Westergard et al., 2007).

2.4.1.1 Hypothesis 1: Direct Protection of PrP^C Against Oxidative Stress

Direct protection of PrP^C against oxidative stress is described as a complex mechanism where PrP^C acts directly by itself to detoxify reactive oxygen species (ROS) (Westergard et al., 2007), thus it portrays a role as an antioxidant in the cellular system (Brown et al., 1999b). Consistent with this concept, recombinant PrP^C and immunoprecipitated PrP^C from brain tissue or cultured cells all exhibit a copper-dependent superoxide dismutase (SOD) activity (Brown et al., 1999a; Brown et al., 2001). However, there are controversies about the reality of this alleged SOD activity of PrP^C where no

SOD activity was detected (Hutter et al., 2003; Jones et al., 2005). Furthermore, the SOD activity measured for recombinant PrP is dependent on refolding the protein from its denatured state in the presence of supra-physiological concentrations of copper, or even small organic molecules for instance amino acids can bind to copper and show a weak dismutase activity (Westergard et al., 2007). Nevertheless, copper binds much more weakly to PrP^C as compared to the known cuproenzymes like Cu-Zn SOD (Rae et al., 1999).

2.4.1.2 Hypothesis 2: Indirect Protection of PrP^C Against Oxidative Stress

Indirect protection of PrP^C against oxidative stress is termed as a possible role of PrP^C exerts its cytoprotective effect by up-regulating other proteins for example Cu-Zn SOD or glutathione reductase that will detoxify ROS (Brown et al., 1997; Brown et al., 2002). Consistent with this observation, the activities of other anti-oxidant enzymes, for instance catalase and glutathione reductase, have been shown to exhibit a significantly lower level in *Prn-p*$^{0/0}$ mice (White et al., 1999; Waggoner et al., 2000; Klamt et al., 2001). However, there is of no certainty yet on whether PrP^C acts directly in regulating these molecules.

Besides, another possible speculation is that PrP^C acts either upstream or downstream of the ROS to exert its cytoprotective effect against oxidative stress, for example oxidative stress may activate apoptotic pathways (Halliwell, 2006). In this phenomenon, the anti-apoptotic effects of PrP^C may

contribute to the protein's ability to safeguard cells against oxidative stress (Mehrpour and Codogno, 2010). Consistent with this, neural cells from mice overexpressing PrP^C and PrP^C-knockout showed that PrP^C disrupts divalent and metal Mn uptake, thus this protects the cells from both H_2O_2- and Mn-induced oxidative stress and apoptosis (Choi et al., 2007).

2.4.2 PrP^C and Copper

Undeniably, PrP^C is well known for its copper-binding ability (Brown et al., 1997b; Stockel et al., 1998; Jackson et al., 2001; Kramer et al., 2001). The Histidine (His)-containing octapeptide repeats have a high binding affinity that binds specifically up to four Cu^{2+} ions in a pH-dependent as well as negatively cooperative manner (Walter et al., 2006). The affinity and number of Cu^{2+}-binding sites strengthen the idea that PrP^C could act as an anti-oxidant through binding of potentially harmful Cu^{2+} ions and sacrificially quenching the free radicals produced due to copper redox cycling (Mehrpour and Codogno, 2010). The octapeptide repeat region consists of a novel GAG-binding sequence and His-bound Cu^{2+} potentially act as a cofactor for intermolecular recognition reactions, thus allowing the formation of PrP^C-Cu^{2+} GAG assemblies that may serve as a crucial entities in PrP^C metabolism (Gonzalez-Iglesias et al., 2002). Consistent with the idea that PrP^C plays a protective role in respond to oxidative stress, Qin and co-workers (2009) have demonstrated that murine neuro-2a and human HeLa cells promptly respond to an elevation of intracellular copper level by up-regulating ataxia-telangiectasia mutated (ATM)- mediated transcription of PrP^C. As a result,

elevated level of PrP^C protects the cell against copper-induced oxidative stress and cell apoptosis plays an active role in the modulation of intracellular copper concentration (Qin et al., 2009).

2.4.3 PrP^C and Mitochondrial Dysfunction

Under serum deprived condition, PrP^C knockout neuronal cells were vulnerable to apoptotic cell death where the mitochondria Ca^{2+} level and apoptosis related proteins, namely p53, Bax, caspase-3, poly (ADP-ribose) polymerase (PARP) and cyt-c were significantly increased (Kim et al., 2004). Familial PrP^C mutations T183A and D178N paralleled with the human prion diseases FFI as well as familial atypical spongiform encephalopathy has been shown to partially or completely abolishes PrP's neuroprotective function against Bax (Roucou et al., 2005). The cytoprotective effect of PrP is very specific for Bax, since PrP is not able to prevent cell death mediated by Bak, tBid, staurosporine or thapsigargin. PrP has been shown to protect against Bax-mediated cell death in the human primary neurons and MCF-7 cell lines by inhibiting Bax conformational change which is the initial step in Bax activation followed by cyt-c release into the mitochondrial space. It has been proposed that PrP^C does not directly interacts with Bax to prevent cell death, but together with Bcl-2, Bax is maintained in an inactivate state. Therefore, this confers to neuroprotection in mammalian cells (Roucou et al., 2005; Roucou and LeBlanc, 2005).

2.5 PrP^C and Tumor

2.5.1 PrP^C and Tumor Resistance

Resistance to cell death is one of the essential hallmarks for cancer cells that lead to the formation of tumor (Hanahan and Weinberg, 2011). Resistance to cell death may result in aberrant expression of proteins that possess anti-apoptotic property or down-regulation of pro-apoptotic proteins that can be the sequel of either epigenetic modification or due to oncogene over-expression (Yang et al., 2014). Silencing of PrP^C expression in human breast cancer TRAIL sensitive MCF7 cell line and its two resistant counterparts; the multidrug resistant (MDR) MCF-7/AdR and TRAIL-resistant clone was shown to facilitate the activation of proapoptotic Bax by the down-regulation of Bcl-2 expression. Consequently, TRAIL-mediated apoptosis in PrP^C knocked-out cells paralleled with caspase processing, Bid cleavage and Mcl-1 degradation were more susceptible to apoptosis (Mehpour and Codogno, 2010).

As for gastric cancer investigation, gastric cancer MKN-28 cells transfected with luciferase reporter constructs of human PrP^C promoter containing heat shock element (HSE) was shown to express significantly higher luciferase activities as compared to cells transfected with the constructs containing no HSE post-hypoxia treatment (Liang et al., 2007b). The authors postulated that certain transcriptional factors was phosphorylated by ERK1/2 that will interact with HSE in the promoter of PrP^C, therefore resulting in up-regulation of PrP^C in MKN-28 cells during hypoxia. Meanwhile, down-regulation of PrP^C increased the cell susceptibility to drug-induced hypoxia.

2.5.2 PrP^C and Tumor Progression

Yu and co-workers (2012) have demonstrated that PrP knockdown in breast adenocarcinoma cells MDA-MB-435 was prone to cell death upon serum starvation, however they also exhibited drug resistance towards doxorubicin. The resistance is independent of p53 but it is associated with extracellular signal-regulated kinases (ERK) pathway. The expression of PrP that confers to drug resistance may be cell- or drug-specific, and this strengthens the suggestion that PrP might be an applicable target for molecular typing for personalized treatment (Yang et al., 2014).

A modified subtractive hybridization method have successfully identified *PRNP* being one of genes that are up-regulated from vincristine- and adriamycin-resistant gastric adenocarcinoma cell lines derived from SGC 7901 (Zhao et al., 2002). Despite of being resistant to vincristine and adriamycin treatment, cells overexpressing PrP^C are also more resistant towards etoposide, 5-fluorouracil, and cisplastin but not towards cyclophosphamide, arabinosylcytosine, and methotrexate (Du et al., 2005). It was shown that PrP^C expression up-regulated the expression of P-glycoprotein (P-gp) through multiple drug resistant (MDR)-1 upon treatment with adriamycin and vincristine (Liang et al., 2009a). Since adriamycin, vincristine, and etoposide are P-gp related drugs whereas 5-fluorouracil, cisplastin, cyclophosphamide, arabinosylcytosine, and methotrexate are P-gp non-related drugs, the resistance of cells expressing PrP^C to 5-fluorouracil and cisplastin suggests that PrP^C might be a better biomarker for diagnosing chemotherapeutic drug resistance in gastric cancer cells (Yang et al., 2014).

Furthermore, treatment of colorectal cancer cells HCT116 with anti-PrP^C specific antibodies, namely BAR221 and F89/160.15 were shown to effectively reduced the growth of cancer cells and further enhanced the efficacy of irinotecan, 5-fluorouracil, cisplastin, and doxorubicin to various degrees (McEwan et al., 2009). Thus, PrP^C might be a valid target for colorectal cancer diagnostics and treatment.

CHAPTER 3

MATERIALS AND METHODS

3.1 General Chemicals and Reagents

Tris and Phosphate Buffered Saline (PBS) tablet were purchased from MP (MP, France). Sodium Chloride (NaCl), Calcium Chloride ($CaCl_2$), Sodium Dodecyl Sulphate (SDS), and β-Mercaptoethanol were purchased from Merck (Merck, USA). Ethylenediaminetetraacetic acid (EDTA), Magnesium Chloride ($MgCl_2$), Sodium Deoxycholate, Glacial Acetic Acid and Glycerol were purchased from SYSTERM (SYSTERM, Malaysia). Bromophenol Blue, Naphthol Blue Black, Nonidet® P-40, and Tween-20 were purchased from Sigma-Aldrich (Sigma-Aldrich, USA). Phenylmethanesulfonylfluoride (PMSF) and HEPES were purchased from Bio Basic Inc. (Bio Basic Inc., Canada). Glycine was purchased from First BASE (First BASE, Singapore). Skim Milk Powder was purchased from OXOID (OXOID, UK). Methanol was purchased from Fisher Scientific (Fisher Scientific, USA).

3.2 List of Formula

Formulations for the solutions used in this study are shown in Table 3.1.

Table 3.1: List of solution formulations.

Solution	Formulation
NP-40 Cell Lysis Buffer	10 mM Tris, pH 7.8, 100 mM NaCl, 10 mM EDTA, 0.1 mM PMSF, 0.5% (w/v) Sodium Deoxycholate, 0.5% (v/v) Nonidet® P-40
Laemmli Dissociation Buffer	62.5 mM Tris, pH 6.8, 25% (v/v) Glycerol, 2% (w/v) SDS, 0.01% (w/v) Bromophenol Blue, 5% (v/v) β-Mercaptoethanol
Tris-Glycine Electrophoresis Buffer	25 mM Tris, 190 mM Glycine, 1% (w/v) SDS, pH 8.6
Phosphate Buffered Saline Tween-20 (PBS-T)	0.1% (v/v) Tween-20 in PBS
Blocking Buffer	5% (w/v) Skim Milk Powder in PBS-T
Transfer Buffer	150 mM Glycine, 20 mM Tris, 20% (v/v) Methanol
Stripping Buffer	0.4 M Glycine, 2% (v/v) Tween-20, 0.2% (w/v) SDS, pH 2.2
Amido Black Dye	0.1% (w/v) Naphthol Blue Black, 10% (v/v) Methanol, 2% (v/v) Glacial Acetic Acid
Binding Buffer	10 mM HEPES, pH 7.4, 150 mM NaCl, 5 mM KCl, 5 mM $MgCl_2$, 1.8 mM $CaCl_2$

3.3 Cell Culture

3.3.1 The Cell Lines

3.3.1.1 LS 174T Human Colorectal Adenocarcinoma Cell Line (CL-188)

LS 174T human colorectal adenocarcinoma cell line was purchased from ATCC (ATCC, USA). LS 174T cell line (Figure 3.1) was deposited by Northwestern University from a 58-year old Caucasian female who was diagnosed with Duke's type B colorectal adenocarcinoma. The adherent cell has an epithelial-like morphology with abundant of microvilli and intracytoplasmic mucin vacuoles (Tom et al., 1976). It produces large amounts of carcinoembryonic antigen (CEA) similar to the parent cell line, LS 180. LS 174T cell line proliferates in Eagle's minimum essential medium (EMEM) supplemented with 10% fetal bovine serum (FBS) and requires subcultivation in a ratio of 1:2 or 1:4 weekly.

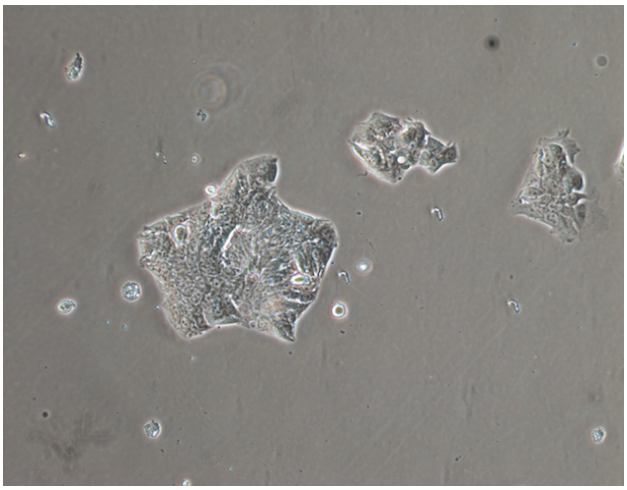

Figure 3.1: Cell morphology of LS 174T.
Image was visualized using Nikon Eclipse TS100 inverted microscope (Nikon, Japan) and acquired with NIS-Elements BR 3.0 software at 100× magnification.

3.3.1.2 HEK-293 Human Embryonic Kidney Cell Line (HCL-4517)

HEK-293 human embryonic kidney cell line (Figure 3.2) was purchased from Thermo Scientific (Thermo Scientific, USA). HEK-293 cell line was deposited by Graham F.L., and it derived from the embryonic kidney tissue of a fetus. The cell line contains adenovirus (Thomas and Smart, 2005); therefore it was handled in biosafety level-2 culture hood (Telstar Bio-IIA, Telstar, Spain). The cell line has an epithelial-like morphology and is adherent at 37 °C but some live cells were seen unattached when left at RT. HEK-293 cell line proliferates in EMEM supplemented with 10% FBS and it requires subcultivation in a ratio of 1:6 or 1:10 weekly.

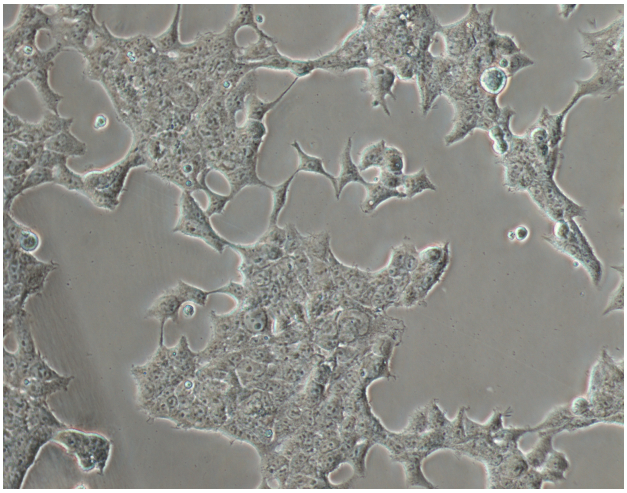

Figure 3.2: Cell morphology of HEK293.
Image was visualized using Nikon Eclipse TS100 inverted microscope and acquired with NIS-Elements BR 3.0 software at 100× magnification.

3.3.2 Cell Lines Maintenance

The cells were grown in complete EMEM (SAFC, Switzerland) supplemented with 10% (v/v) heat-inactivated FBS (PAA, Austria), and 1% (v/v) Penicillin-Streptomycin (Pen-Strep) (Millipore, USA). All cells were maintained at 37 °C in a humidified CO_2 incubator (Binder, Germany). Sub-culturing of cells was performed every 2 to 4 d depending on the cell's confluency state. Cell was examined with CKX31 inverted microscope (Olympus, USA) daily to check for any contamination or morphology aberration.

3.3.2.1 Preparation of Complete EMEM Culture Medium

To prepare a complete EMEM culture medium, 9.53 g of EMEM powder and 2.2 g of sodium bicarbonate ($NaHCO_3$) (QRec™, Canada) were measured and dissolved in 1 L of autoclaved deionized water. The pH value was adjusted to an ideal range of 7.2 to 7.6. The solution was mixed thoroughly using a stirring bar for approximately 30 min. The medium mixture was then sterilized by filtration with a filter unit of 0.2 μm cellulose acetate membrane (Sartorius, Germany) using vacuum filter system into an autoclaved Schott bottle. Aseptically, 2 mL of filtered medium was transferred to a 60 mm tissue culture dish (Orange Scientific, Belgium) and incubated in 37 °C humidified CO_2 incubator for 3 d to test for sterility while the remainder was stored at 4 °C until further usage.

3.3.2.2 Preparation of Reduced Serum OPTI-MEM Medium

To prepare reduced serum OPTI-MEM medium, a packet of OPTI-MEM powder (GIBCO™, USA) and 2.4 g of $NaHCO_3$ were dissolved in 1 L of autoclaved deionized water. The pH of the medium was adjusted to 7.0 ± 0.1 and the medium mixture was then filtered and sterilized with 0.2 μm membrane porosity using vacuum filtration system.

3.3.2.3 Sub-culturing of Adherent Cell Lines

Spent medium was decanted and the cells were washed thrice with PBS prior to trypsinization. Adequate amount of 0.05% trypsin-EDTA (GIBCO™, USA; JRS, USA) was used to detach the cells. In general, 2 mL of trypsin-EDTA was added for T_{25} culture flask, while 4 mL of trypsin-EDTA was added for T_{75} culture flask (Nunc™, Thermo Scientific, USA; Falcon®, Corning, USA). Cells were incubated for 10 to 15 min at 37 °C to allow detachment of the cells. Fresh serum-containing medium was added into the trypsinized cells to inactivate the trypsin. Cells were spun down at 1500 rpm using Heraeus Multifuge 1-SR (Thermo Scientific, USA) for 10 min. The supernatant was decanted while the pelleted cells were resuspended with complete culture medium and seeded at preferred density.

3.3.2.4 Cryopreservation and Thawing of Cells

For cryopreservation, cells reaching 80 to 90% were trypsinized and pelleted at 1500 rpm for 10 min. Freezing media containing 900 μL complete

EMEM culture medium and 100 μL dimethyl sulfoxide (DMSO) (Merck, USA) were added into cell pellet, resuspended thoroughly, and transferred to a cryovial (Nalgene, USA) for storage at −80 °C overnight prior to long-term storage in vapor phase of liquid nitrogen.

To thaw a cryopreserved cell, cryovial was removed from liquid nitrogen and thawed instantly in a pre-heated 37 °C water bath (Memmert, Germany). One part of thawed cells was then rapidly transferred to a centrifuge tube containing 9 parts of fresh EMEM culture medium to dilute the DMSO. The cells were then pelleted at 1500 rpm for 10 min, resuspended with complete EMEM culture medium, and transferred into a culture flask. The culture flask was then incubated in 37 °C humidified CO_2 incubator and medium was replaced after 2 d to remove the DMSO remnants that are cytotoxic.

3.3.3 Cell Counting

Neubauer-improved haemocytometer (Marienfeld, Germany) was used for cell counting purposes. Cells were trypsinized and pelleted at 1500 rpm for 10 min. Supernatant was decanted and adequate amount of medium was added to resuspend the cells. Carefully, 5 μL of cell suspension were aspirated and mixed gently with 5 μL of trypan blue dye (Sigma-Aldrich, USA) on a parafilm. The mixture was transferred to the haemocytometer under a thick coverslip by capillary action. The slide was observed under inverted microscope at 100× magnification and counted using a cell counter. Only cells

that fall within the 16 smaller squares and any position on the right or bottom boundary line were counted. Of note, viable cells were unstained and remained clear with a refractile ring around them while dead cells were stained with trypan blue and had no refractile ring. The concentration of the cell was calculated using the formula as follow:

$$\text{Cell Concentration} = \frac{\text{Number of Viable Cells}}{4} \times \text{Dilution Factor } (2) \times 10^4$$

The calculated cell concentration was adjusted according to the optimal seeding density for individual assay of each cell lines during plating.

3.3.4 Cell Transfection Using Cationic Lipids Formulation

Cell transfection was performed using TransPass D1 Transfection Reagent (TPD1TR) (NEB, USA) in the absence of serum. Protocol described in the manufacturer's instructions was modified accordingly. Cells were cultured in 100 mm tissue culture dish (Falcon®, Corning, USA) until 70 to 80% confluency. Five micrograms of DNA was added into 4 mL of serum-free OPTI-MEM in a 15 mL centrifuge tube for each transfection reaction. Successful clone of PrP^C cDNA into pcDNA™3.1 vector was established previously by Yap and Say (2012). TPD1TR was vortexed before aspiration to mix the frozen suspension thoroughly. An amount of 12.5 µL of TPD1TR was added into each reaction and was gently mixed well by finger flicking the tube. The mixture solution was allowed to form transfection complexes by incubating at RT for 30 min. Prior to transfection, cells were washed once

with OPTI-MEM to rinse off the FBS. The medium was replaced with the transfection mixture and was subjected to gently rocking to disperse the mixture solution evenly to the cells. Cells were then incubated in 37 °C humidified CO_2 incubator for 4 h. Following incubation, transfection medium was aspirated and replaced with complete EMEM culture medium. After 24 h post-transfection, transfected cells were treated with G-418 sulfate (A.G. Scientific, USA) at different working concentration as shown in Table 3.2 in order to obtain stable clones.

Table 3.2: Effective working concentrations of G-418 sulfate towards different cell lines.

Cell Lines	Working Concentration	Selective Marker
LS 174T	1 mg/mL for 3 weeks	Neomycin
HEK-293	2 mg/mL for 2 weeks	Neomycin

3.4 Protein Expression Analysis

3.4.1 Preparation of Cell Lysate

Cells were washed with cold PBS thrice and cell scrapper (Greiner Bio-One, Germany) was used to bring cells into suspension. Cells were centrifuged at 1500 rpm for 10 min at 4 °C. One hundred microliters of ice-cold lysis buffer was added to resuspend the pellet gently. Protease inhibitor cocktail (Sigma-Aldrich, USA) was added into the reaction mixture in a dilution factor of 1:100 and incubated on ice for 60 min. Cells were pelleted by pre-chilled centrifugation at 13,000 rpm using Sorvall Legend Micro-17R (Thermo Scientific, USA) for 10 min at 4 °C. Subsequently, cell supernatant

was transferred into a microcentrifuge tube and the protein concentration of cell lysate was quantified using Pierce® BCA Protein Assay Kit (Thermo Scientific, USA). The cell lysate was stored at −20 °C or −80 °C until further usage.

3.4.2 Quantitation of Total Protein

Bicinchoninic acid (BCA) protein assay was performed in a 96-well plate. Bovine serum albumin (BSA) standards were prepared at concentration of 0.2, 0.4, 0.6, 0.8, and 1.0 mg/mL. Working reagent was prepared by mixing 50 parts of BCA™ Reagent A (sodium carbonate, sodium bicarbonate, BCA, and sodium tartarate in 0.1 M sodium hydroxide) with 1 part of BCA™ Reagent B (4% cupric sulphate). Each unknown sample was diluted to 1:5 and 1:10 ratio and 10 µL was added in duplicate wells as well as the BSA standards. Subsequently, 200 µL of working reagent was added to each well and the 96-well plate was placed on a plate shaker for 30 sec to ensure thorough mixing of the working reagent and samples. The plate was incubated at 37 °C for 30 min and the absorbance was measured at 562 nm using Infinite® 200 PRO multimode reader (Tecan, Switzerland) and data analysis was performed using Magellan™ software.

3.4.3 Sodium Dodecyl Sulfate Polyacrylamide Gel Electrophoresis (SDS-PAGE)

To perform SDS-PAGE, a pair of glass with one slightly shorter was washed with 70% ethanol. The glasses were then inserted into a gel-casting apparatus (Bio-Rad, USA) and tightened. Table 3.3 shows the formulation for the SDS-PAGE 15% resolving gel and 4% stacking gel.

Table 3.3 Protocol for 30% acrylamide/bis solution, 37.5:1

	Resolving Gel (4%)	**Stacking Gel (15 %)**
30% Acrylamide/bis solution, 37.5:1 (Bio-Rad, USA)	4.95 mL	660 µL
0.5 M Tris, pH 6.8	−	1.26 mL
1.5 M Tris, pH 8.8	2.5 mL	−
10% SDS	100 µL	50 µL
ddH_2O	2.4 mL	3 mL
TEMED (Bio Basic Inc., Canada)	5 µL	5 µL
10% Ammonium persulfate (APS) (Sigma-Aldrich, USA)	50 µL	25 µL
Total Volume	**10 mL**	**5 mL**

Resolving gel casting solution was prepared and mixed thoroughly and aspirated into the gel cassette (Bio-Rad, USA). The cassette was filled to a level, which allowed the comb to be inserted with approximately 1 cm between the bottom of the wells and the top of the resolving gel. The gel was overlaid with 1 mL of 1-butanol (Merck, USA) to expel O_2 and create a flat interface between the resolving and stacking gels. The resolving gel was

allowed to polymerize for 30 min. Meanwhile, 1× Tris-glycine electrophoresis was prepared. A line would become visible at the top of the resolving gel as it polymerized. Butanol was removed by inverting the gel and rinsing the top of the gel with distilled water. The residual liquid was drained using filter paper. Stacking gel solution was prepared and the top of the gel cassette was filled. The comb was inserted and the stacking gel was left to polymerize for 20 min. Meanwhile, cell lysates containing desired amount of proteins (50-80 µg) were mixed with Laemmli sample buffer in 1:1 ratio and boiled at 95 °C in pre-heated water bath for 10 min. As the stacking gel has polymerized, the comb was removed and transferred to the electrophoresis tank (Bio-Rad, USA) containing the Tris-Glycine electrophoresis buffer. Subsequently, the boiled protein samples were loaded onto the polyacrylamide gel alongside with a broad range pre-stained protein molecular weight marker (Nacalai Tesque, Japan). Electrophoresis was then conducted at constant 150 V using Bio-Rad PowerPac HC (Bio-Rad, USA) for approximately 1 h and 30 min.

3.4.4 Western Blotting

3.4.4.1 Semi-dry Transfer

Polyvinylidene difluoride (PVDF) (Pall Corp., USA) membrane was cut into desired size fitting the resolving gel and was re-wetted by methanol (Merck, USA). Two pieces of thick filter paper (Bio-Rad, USA) and the PVDF membrane were immersed in the transfer buffer for 15 min. Following SDS-PAGE, the resolving gel was transferred onto the PVDF membrane, sandwiched by two pieces of thick filter paper. A centrifuge tube was rolled

over the surface of the top filter paper to exclude air bubbles. The gel was transferred using Bio-Rad Trans-Blot SD (Bio-Rad, USA) at 18 V for 30 min. Once finished, the PVDF membrane was fixed with 4% (w/v) of paraformaldehyde (PFA) (Sigma-Aldrich, USA) prior to blotting.

3.4.4.2 Blotting of PVDF Membrane

After fixation, the membrane was washed with PBS and incubated with 10 mL of blocking buffer for 1 h at RT with agitation. The membrane was washed thrice in PBS-T for 5 min each wash. Incubation with primary antibody diluted in PBS-T containing 5% BSA Fraction-V (Calbiochem, Germany) at appropriate dilutions as shown in Table 3.4 was performed for 1 h at RT or overnight at 4 °C with agitation using Stuart-SSL4 (Stuart, UK). Subsequently, the membrane was washed thrice with PBS-T for 5 min each wash before incubation with the secondary horseradish peroxidase (HRP) conjugated antibody diluted in PBS-T containing 5% BSA Fraction-V at RT for 1 h in dark with agitation. The membrane was then washed thrice with PBS-T for 5 min to remove any unbound conjugates. During the final wash, PBS-T was discarded and replaced with PBS. Bounded peroxidase conjugates were detected using Pierce® Enhanced Chemiluminescene (ECL) system (Thermo Scientific, USA). Immunofluorescence signal was visualized using ChemiDoc™ MP imaging system (Bio-Rad, USA) under auto-exposure mode, and the image was acquired using ImageLab™ version 5.1 software. Band Intensities were analyzed using ImageJ software version 1.84.

Table 3.4: Antibodies for Western blotting analysis.

Antibodies	Source	Supplier	Dilution
Anti-PrP clone 3F4	Mouse	Millipore, USA	1:8,000
Anti-actin clone C4	Mouse	Millipore, USA	1:5,000
Anti-mouse IgG	Rabbit	Calbiochem, Germany	1:10,000

3.4.4.3 Stripping of PVDF Membrane for Repeated Hybridization

For repeated hybridization, anti-actin clone C4 was used as a loading control. The blot was stripped in stripping buffer at RT for 10 min. Subsequently, membrane was washed thrice with PBS-T for 5 min each wash and incubated in anti-actin clone C4 which was pre-diluted in PBS-T containing 5% BSA for 1 h at RT.

3.4.4.4 Amido Black Staining of PVDF Membrane

Amido black dye was used to stain the total proteins on the transferred PVDF membrane. Membrane was stained with amido black dye for 10 min and rinsed under running water for 1 minute. The membrane was dried at RT and kept for future reference.

3.5 Immunofluorescence Microscopy

For surface detection of PrP^C, cells were seeded and allowed to attach on 13 mm round coverslip (H&H, Germany) for 24 h. Upon attachment to coverslips, cells were fixed with 4% (w/v) PFA in PBS for 15 min at RT and further permeabilized with 0.5% (v/v) Triton X-100 (Fisher Scientific, USA) in PBS for 5 min at RT. Cells were then blocked with 10% goat serum (Sigma-Aldrich, USA) in PBS for 20 min at RT prior to incubation with primary antibody. PrP^C was detected with anti-PrP mouse antibody (mAB) clone 3F4 (Millipore, USA) in 5% goat serum at 1:500 dilution. After overnight incubation with primary antibodies at 4 °C, cells were washed with PBS and treated with Dylight 488 goat anti-mouse IgG (Thermo Scientific, USA) in 5% goat serum at a dilution of 1:100 for 1 h in dark at RT. Prior to imaging, coverslip was mounted onto glass slides with cells facing downward using mounting agent, DPX (Merck, USA). Cells were visualized using Nikon Eclipse TS100 inverted fluorescence microscope and the image was captured with NIS-Elements BR 3.0 software.

3.6 Cell Viability Assay Using 3-(4,5-dimethylthiazol-2-yl)-2,5-diphenyltetrazolium bromide (MTT)

A total of 100 µL cells were seeded into each well of the 96-well plate (Nunc, Thermo Scientific, USA). Following 24 h of incubation, cells were treated and cultured in 37 °C humidified CO_2 incubator. Depending on treatment time-length ranging from 24 to 48 h, morphology of treated cells was observed using Nikon Eclipse TS100 inverted microscope prior to

addition of MTT (Nacalai Tesque, Japan). MTT stock solution of 5 mg/mL dissolved in PBS was prepared. The cells were then incubated at 37 °C for 4 h until purple formazan crystal has developed. Approximately 75% of the medium containing MTT was aspirated and 150 µL of DMSO was added to dissolve the formazan crystals. The plate was then incubated at 37 °C for 30 min in dark and absorbance reading was determined with Infinite® 200 PRO multimode reader at 550 nm. Cell viability was determined by using the formula as follows:

$$\text{Cell Viability} = \frac{\text{Corrected Value}}{\text{Dynamic Range}} \times 100\%$$

Corrected Value = Average OD of treated cells – Average OD of blank

Dynamic Range = Average OD of control cells – Average OD of blank

3.7 Cell Growth and Proliferation Assay

Cell suspension with a seeding density of 5×10^4 cells/mL was prepared. One hundred microliters of cell suspension was added to each well of the 96-well tissue culture plate. After 24 h of incubation in 37 °C humidified CO_2 incubator, MTT assay was performed for the first column. Following MTT assay, the 96-well tissue culture plate was returned to the incubator and MTT assay was repeated for the second column on the next day. The same process was repeated on the following column until the fifth column (5^{th} day).

3.8 Soft Agar Colony Formation Assay

3.8.1 Preparation of Base Agar

To create a basement layer of the semi-solid bilayer agar, 1% (w/v) agarose (Vivantis, USA) was sterilized by autoclave and the temperature was brought to 40 °C in water bath. After the temperature has equilibrated, 2× complete EMEM culture medium was added to the 1% (w/v) agarose in a 1:1 ratio and was mixed thoroughly. Three milliliters of bottom layer agar mixture was added to 60 mm tissue culture dish and set aside for 10 min to solidify prior to adding of top agar.

3.8.2 Preparation of Top Agar

To create a top layer of the semi-solid bilayer agar, 0.7% (w/v) agarose was prepared by autoclave and the temperature was brought to 40 °C in water bath. After the temperature has equilibrated, 2× complete EMEM culture medium was added to the 0.7% (w/v) agarose in a 1:1 ratio and was mixed thoroughly. Following that, 7.5×10^3 cells were added to the 3 mL of top layer agar mixture and was mixed thoroughly prior to adding to the solidified basement layer. After the top agar has solidified, the tissue culture dish was incubated at 37 °C in a humidified CO_2 incubator for 28 d.

3.8.3 Soft Agar Maintenance and Colony Formation Analysis

One milliliter of complete EMEM culture medium was added to the semi-solid bilayer agar every 7 d to prevent agar from desiccating as to supply nutrient to the cells. After 28 d of incubation, the agar plate was stained with 0.2% (v/v) crystal violet for 2 h and washed thrice with PBS prior to colony counting. The image was acquired with FluorChem® FC2 Imaging System (Cell Bioscience, USA) and colony count was performed using AlphaView 3.0 software.

3.9 Cell Anoikis Assay

3.9.1 Preparation of Poly (2-hydroxyethyl methacrylate) (poly-HEMA) plate

Poly-HEMA (Sigma-Aldrich, USA) was dissolved in 95% ethanol (Merck, USA) to a final concentration of 20 mg/mL poly-HEMA stock solutions by stirring vigorously. To enhance solubility, the solution was incubated at 37 °C overnight in a tightly capped bottle. On the next day, undissolved material was centrifuged at 1500 rpm for 10 min in RT. One milliliters of the poly-HEMA solution was added to each well of the 6-well tissue culture plate (Greiner Bio-One, Germany) and left open in safety cabinet for the ethanol to evaporate. The coating process was repeated twice to ensure proper coating of poly-HEMA on the surfaces. To remove any residual ethanol, the plate was washed thrice with PBS.

3.9.2 Evaluation of Cell Viability in poly-HEMA plate

After the adherent cells were trypsinized and counted, 7.5×10^4 cells in 3 mL of complete EMEM culture medium was added to the poly-HEMA coated 6-well tissue culture plate. Following 24 h of incubation in 37 °C humidified CO_2 incubator, 200 µL of cells were transferred to a 96-well tissue culture plate and proceeded with MTT assay to determine the number of viable cells.

3.10 Scratch Wound Assay

A straight line was drawn on the bottom of a 6-well tissue culture plate using a permanent extra fine marker to create a reference point. Semi-confluent cells (~70%) growing in the T_{25} culture flask were trypsinized and resuspended thoroughly every 2 d and the process was repeated for 3 times (6^{th} day) to obtain an evenly-distributed confluent monolayer growth. Cells were seeded at a density of 1.5×10^5 cells/mL in 3 mL complete EMEM culture medium in the marked 6-well tissue culture plate. The cells were dispersed gently by pipetting before incubation at 37 °C in a humidified CO^2 incubator. The cells were allowed to attach for 48 h to create a confluent monolayer growth. Using a p200 pipet tip (Axygen®, Corning, USA) a wound was created by scraping the monolayer cells vertically and perpendicular to the marking. The cells were carefully washed once with complete EMEM culture medium to remove the cell debris resulted from the scraping. Culture medium was replaced every 24 h to ensure the confluence cells received sufficient nutrients. The first image was acquired using the marking on the 6-

well tissue culture plate. Images were acquired after 24, 48, 72, and 96 h matching to the first image acquired. Visualization of image was performed using Nikon Eclipse TS100 inverted microscope and the image was acquired with NIS-Elements BR 3.0 software. TScratch software version 1.0 (CSElab, Switzerland) was used to analyze the open wound area.

3.11 Transwell Invasion Assay

Cell invasion assay was performed using QCM™ 24-well cell invasion assay kit (Fluorometric) with reference to the manufacturer's instruction (ECM 554, Chemicon® Inc., USA). Fluorescence cells were visualized using FLUOstar Omega (BMG Labtech, Germany), with 480/520 nm filter set and gain setting of 65 and data was analyzed using MARS Data Analysis software.

3.12 Cell Adhesion Assay

3.12.1 Preparation of The Glycoproteins Coated Plate

Stock solution of two glycoproteins, namely collagen type-I from the source of rat tail (Millipore, USA) and fibronectin from the source of bovine (R&D Systems, USA) was prepared at a stock concentration of 100 μg/mL. Collagen type-I was diluted in PBS to a coating concentration of 5, 10, 20, 30, and 40 μg/mL, while fibronectin was diluted in PSB to a coating concentration of 0.625, 1.25, 2.5, and 5 μg/mL. Fifty microliters of diluted glycoprotein were then added to each well of the 96-well tissue culture plate except for the

negative control. The plate was covered and incubated at 4 °C overnight to enhance coating of the glycoprotein to the solid surfaces.

3.12.2 Cell Seeding and Evaluation of Adherent Cell

To block any remaining protein binding sites on the plate, coating solution were removed and 150 µL of 1% (w/v) BSA in PBS was added per well and the plate was incubated at RT for 30 min. Meanwhile, cell suspension with seeding density of 5×10^4 cells/mL in EMEM with 2% of FBS was prepared. Prior to adding of cells, the glycoprotein coated 96-well tissue culture plate was washed thrice with PBS. Immediately after the washing step, 100 µL of cell suspension was added to each well except for the blank. The plate was then incubated in 37 °C humidified CO_2 incubator for 3 h.

After the cells have been allowed to adhere, the plate was gently washed thrice with PBS to remove any unattached cells. Fifty microliters of 95% ethanol was added to each well and incubated at RT for 10 min to fix the adherent cells. To remove the ethanol, the plate was inverted and the content was flicked out. Fifty microliters of 0.1% (v/v) crystal violet was added to each well and incubated at RT for 30 min to stain the cells. The wells were then washed thrice with dH_2O to remove excess stain. Fifty microliters of 0.2% Triton-X in dH_2O was added to each well and incubated for 10 min to lyse the cells. The absorbance was then measured at 570 nm using Infinite® 200 PRO multimode reader and data analysis was performed using Magellan™ software.

3.13 Cell Scattering Assay

Cells were seeded at a density of 5×10^4 cells in 3 mL of complete EMEM culture medium on a 6-well tissue culture plate. The cells were allowed for proper attachment prior to cell starvation. After 48 h of incubation, the medium was removed and washed thrice with PBS. Following that, the medium was replaced with OPTI-MEM with 1% Pen-Strep and in the absence of FBS. Cell scattering morphology of discrete colony was visualized using Nikon Eclipse TS100 inverted microscope and the image was acquired with NIS-Elements BR 3.0 software.

3.14 *In Vitro* Multi-drug Sensitivity Assay

A cell suspension with seeding density of 3×10^5 cells/mL in complete EMEM culture medium was prepared and 100 µL of cell suspension was added to each well of the 96-well tissue culture plate except for the blank. The plates were incubated in 37 °C humidified CO_2 incubator for 24 h prior to adding of chemotherapeutic drugs. A stock solution of 1000 µM was prepared by dissolving the chemotherapeutic drugs in the appropriate diluent. Of note, doxorubicin hydrochloride (Calbiochem®, Germany) and vincristine sulfate (Calbiochem®, Germany) were dissolved in dH_2O while etoposide (Calbiochem®, Germany) was dissolved in DMSO, filter sterilized with 0.2 µm membrane before added to the cell culture medium for treatment purposes. The reconstituted chemotherapeutic drug aliquots were stored in −20°C. Doxorubicin hydrochloride and etoposide was added at a concentration of 2, 4, 8, 16, and 32 µM, while vincristine sulfate was added at a concentration of

0.025, 0.05, and 0.1 μM. Negative control was prepared without adding chemotherapeutic drugs. The plate was incubated for 48 h followed by MTT assay.

3.15 Annexin V-FITC/PI/DAPI Staining

Cells were seeded on 13 mm round coverslips and allowed to attach for 24 h in 37°C humidified CO_2 incubator. Apoptosis was induced with exposure to 6 μM doxorubicin. Following 48 h of incubation, cells were washed with binding buffer and treated with annexin V-FITC/PI (Life Technologies, Invitrogen™, USA; Calbiochem®, Germany) at RT for 30 min, protected from light. To prepare annexin V-FITC/PI staining solution, 20 μL of annexin V-FITC and 5 μL of PI (50 mg/mL) were added to 100 μL of binding buffer. Negative control was prepared by incubating the cells in the absence of doxorubicin. Cells were then washed with binding buffer and fixed with 4% (w/v) paraformaldehyde for 10 min. After fixation, the cells were washed with binding buffer and counterstained with DAPI dihydrochloride (Calbiochem®, Germany) at RT for 10 min, protected from light. To prepare DAPI staining solution, 5 μL of DAPI (5 mg/mL) were added to 100 μL of dH_2O. Cells were then washed with binding buffer and the 13 mm round coverslips were mounted on glass slide using mounting agent, DPX. Immediately, cells were visualized using Olympus BX-41 inverted fluorescence microscope (Olympus, USA) using three different filters (NB, NG, and UV). Three random fields were captured from each slide and images were analyzed using ImageJ software version 1.84.

3.16 Human Apoptosis Antibody Array Kit

Cell apoptosis was induced with the exposure to 6 μM of doxorubicin. Human apoptosis antibody array kit was performed using Proteome Profiler™ with reference to the manufacturer's protocol (ARY009, R&D Systems, USA) with slight modification on detection method. Immunofluorescence signal was visualized using ChemiDoc™ MP imaging system under auto-exposure mode. The image was acquired using ImageLab™ version 5.1 software. Pixel densities were analyzed using ImageJ software version 1.84.

3.17 Statistical Analysis

Some results presented are from representative experiments and data were expressed as mean ± standard error of the mean (SEM) of at least two independent experiments, which were performed in at least triplicates, unless otherwise stated. Microsoft Excel® for Mac 2011 version 14.4.4 (Microsoft Corp., USA) was used to document statistical figures and statistical analysis for unpaired two-tailed Student's t-Test. Statistical Package for Social Sciences (SPSS) version 22 (SPSS Inc., USA) with one-way ANOVA followed by LSD's post hoc test for multiple comparisons was used to compare mean values. Significance level was indicated by asterisk where * denotes $p < 0.05$.

CHAPTER 4

RESULTS

4.1 Immunoblotting Assessment of PrP^C Expression

Stably transfected LS 174T overexpressing PrP^C is annotated as LS 174T-PrP, while mock-transfected LS 174T is annotated as LS 174T-3.1. Likewise, stably transfected HEK-293 overexpressing PrP^C is annotated as HEK-293-PrP, while mock-transfected HEK-293 is annotated as HEK-293-3.1. Endogenous expression and overexpression of PrP^C in LS 174T and HEK-293 cells are shown in Figure 4.1. Western blot revealed that the three glycosylation isoforms of PrP^C namely, unglycosylated PrP (27 kDa), monoglycosylated PrP (30 kDa), and diglycosylated PrP (35 kDa) were detected using anti-PrP^C antibody, clone 3F4. All the membranes were reprobed with actin antibody to confirm the equal volume of total protein loaded in each lane.

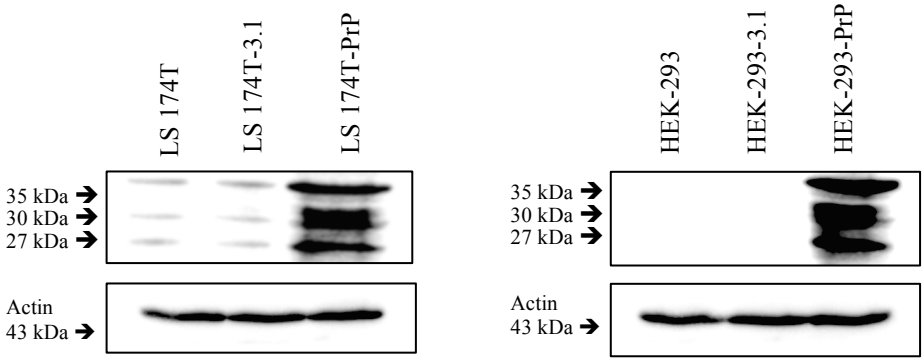

Figure 4.1: Western blot analysis of LS 174T and HEK-293 cells.
Endogenous expression and overexpression of PrP^C in LS 174T and HEK-293 cells. Images were captured using ImageLab™ software version 5.1.

4.2 Immunocytochemical Analysis of PrP^C Expression

To further confirm the overexpression efficiency of PrP^C in LS 174T and HEK-293 cells, the cells were subjected to immunofluorescence microscopy examination. As shown in Figure 4.2, the observation was very similar to the Western blot analysis. A strong emission of bright green fluorescent signaled from LS 174T -PrP and HEK-293-PrP, whereas a weak staining was noted in both LS 174T and LS 174T-3.1, and there was no immunoreactivity in HEK-293 and HEK-293-3.1.

As the endogenous expression of PrP^C in LS 174T and HEK-293 has been understood, and the overexpression of PrP^C in stably transfected LS 174T and HEK-293 has been verified, the biological roles of PrP^C were then studied in accordance to conceptual progression hallmarks of cancer.

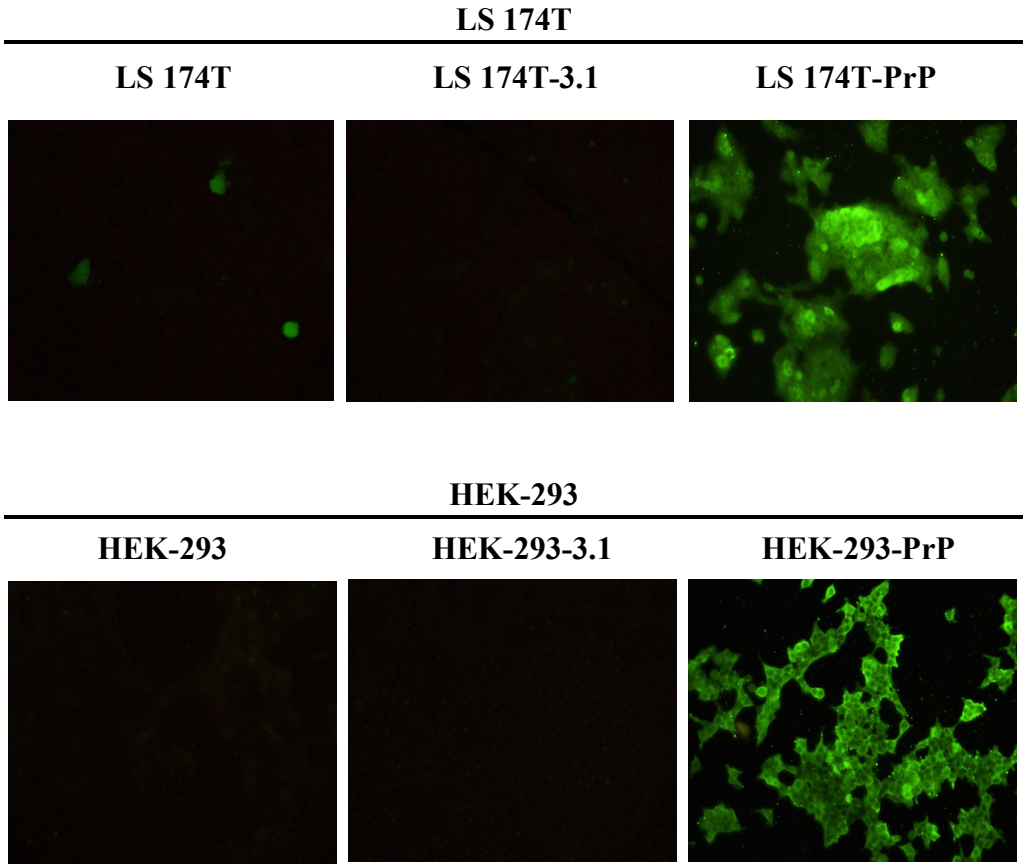

Figure 4.2: Immunofluorescence microscopy depicting expression of PrP^C in LS 174T and HEK-293 cells.
Images were acquired using NIS-Elements BR 3.0 software under Nikon Eclipse TS100 inverted fluorescence microscope at 200× magnification.

4.3 Cell Growth and Proliferation Study

The most fundamental trait of cancer cells is the ability to sustain proliferative signals, thereby resulting in uncontrolled proliferation of cells. Normal cell tends to respond to growth signals, thereby maintaining a homeostasis of cell numbers. To study the growth and proliferation of cell, it was categorized into anchorage-dependent and anchorage-independent growth evaluation.

4.3.1 MTT Cell Proliferation Assay

In anchorage-dependent growth evaluation, LS 174T-PrP has increased cell proliferation as compared to LS 174T and LS 174T-3.1. As shown in Figure 4.3(A), cell number of LS 174T-PrP has increased significantly on day 1 and increased on day 3 as compared to LS 174T and LS 174T-3.1. On day 5, cell number of LS 174T, LS 174T-3.1, and LS 174T-PrP has markedly increased by approximately 5- fold as compared to day 0. On the other hand, there was no significant difference in cell number of HEK-293, HEK-293-3.1, and HEK-293-PrP on day 1, 3, and day 5 as shown in Figure 4.3(B).

A.

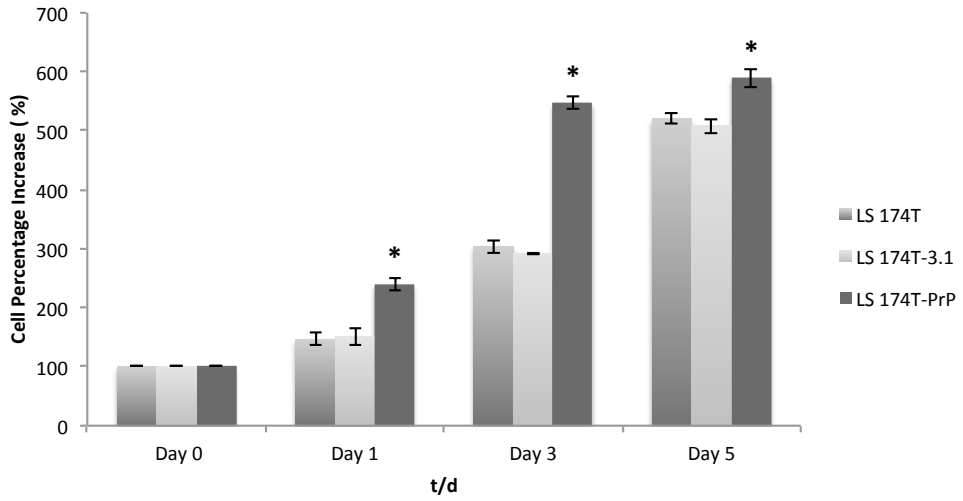

B.

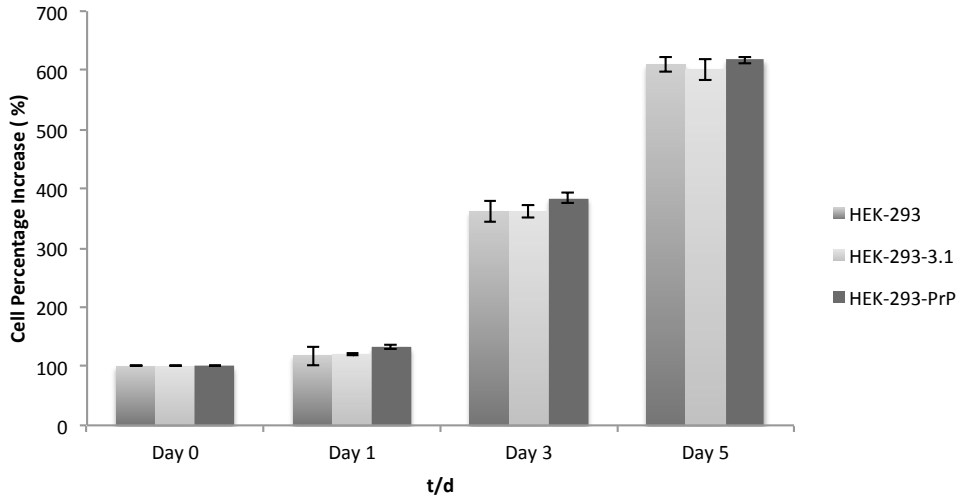

Figure 4.3: Cell proliferation study via MTT.
(A) MTT cell viability assay for LS 174T cells. (B) MTT cell viability assay for HEK-293 cells. Cell viability was calculated with the formula: (A570 of day n / A570 of day 0) ×100%. Data of percentage of cells was expressed in mean ± SEM (error bars) obtained from three independent experiments. Mean values were compared using one-way ANOVA followed by LSD's post hoc test for comparison of the means. * $p < 0.05$ as compared to LS 174T and LS 174T-3.1.

4.3.2 Anchorage Independent Growth Evaluation

4.3.2.1 Cell Colony Formation Assay

Anchorage-independent growth is one of the hallmark characteristics of cellular transformation and uncontrolled cell proliferation that can be assessed by cell colony formation assay, which is considered the most accurate and stringent *in vitro* assay for detecting malignant transformation of cells. For anchorage-independent growth evaluation, LS 174T and HEK-293 cells were subjected to growth in a semi-solid soft agar medium for 28 days. As shown in Figure 4.4, overexpression of PrP^C has increased the growth of colony formation in LS 174T cells. Image analysis has further confirmed that the colony count of LS 174T-PrP was significantly higher with an increment of approximately 1.5- fold as compared to LS 174T and LS 174T-3.1 as shown in Figure 4.5(A). As shown in Figure 4.4, there was no colony formation observed in the HEK-293-3.1 and HEK-293-PrP.

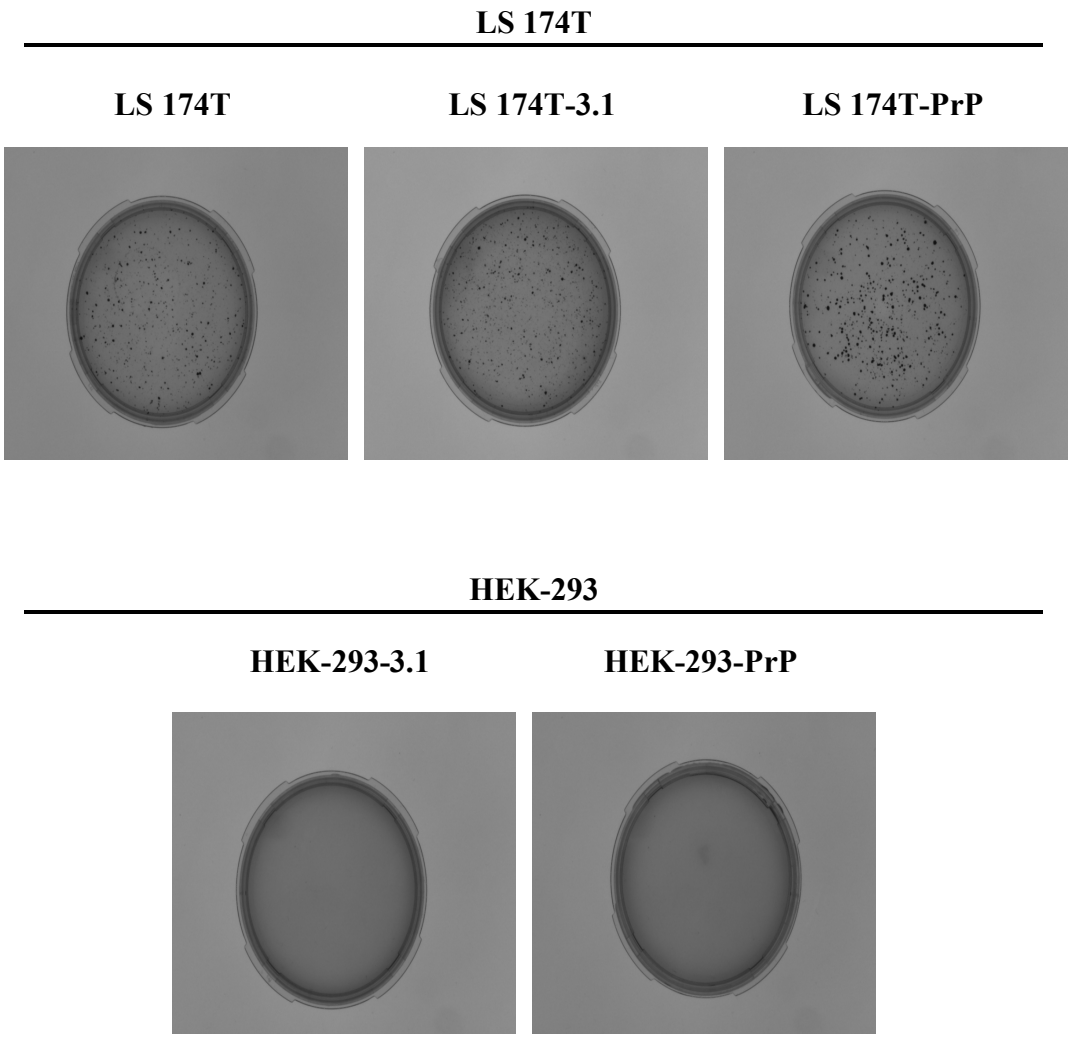

Figure 4.4: Cell proliferation study via soft agar colony formation assay. Representative images depicting colony formation of LS 174T and HEK-293 cells. Cells were cultured in a semisolid bi-layer agar medium on 60 mm culture plates. Cells were stained with 0.2% crystal violet prior to image capture. Images were acquired using FluorChem® FC2 Imaging System in the same exposure after 30 days.

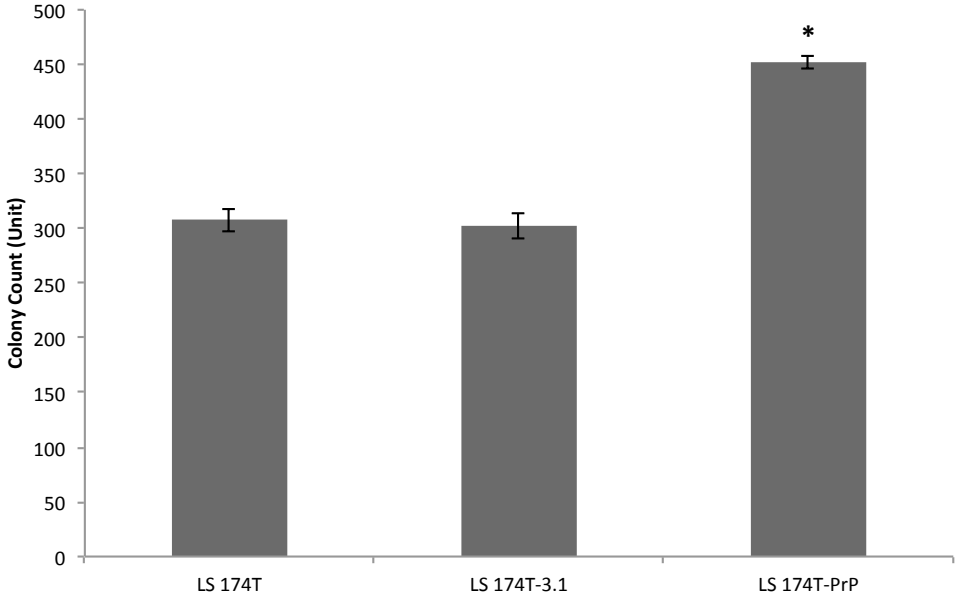

Figure 4.5: Colony count for soft agar colony formation assay.
Colony count for individual plate was performed using AlphaView 3.0 software with a standardized threshold for each plate (G=0-20000; R=65535-65535 in accordance to number of foci > 100 μm). Data of colony counts were expressed in mean ± SEM (error bars) obtained from three independent experiments. Mean values were compared using one-way ANOVA followed by LSD's post hoc test for comparison of the means. * $p < 0.05$ as compared to LS 174T and LS 174T-3.1.

4.3.2.2 Cell Anoikis Assay

To further understand the cell survival in anchorage-independent manner, percentage of viable cells remains on poly-HEMA coated surfaces was determined. As shown in Figure 4.6(A), LS 174T-PrP showed a significant difference in the percentage of cell as compared to LS 174T and LS 174T-3.1. The percentage of cells resistant to anoikis in LS 174T-PrP has markedly increased by approximately 2- fold as compared to LS 174T. Meanwhile, there was no significant difference in the percentage of viable cells for HEK-293, HEK-293-3.1, and HEK-293-PrP as shown in Figure 4.6(B). This has strengthened the understanding that up-regulation of PrP^C has increased the cell resistance to anoikis particularly in cancer cells, but has no known effect in non-cancer cells.

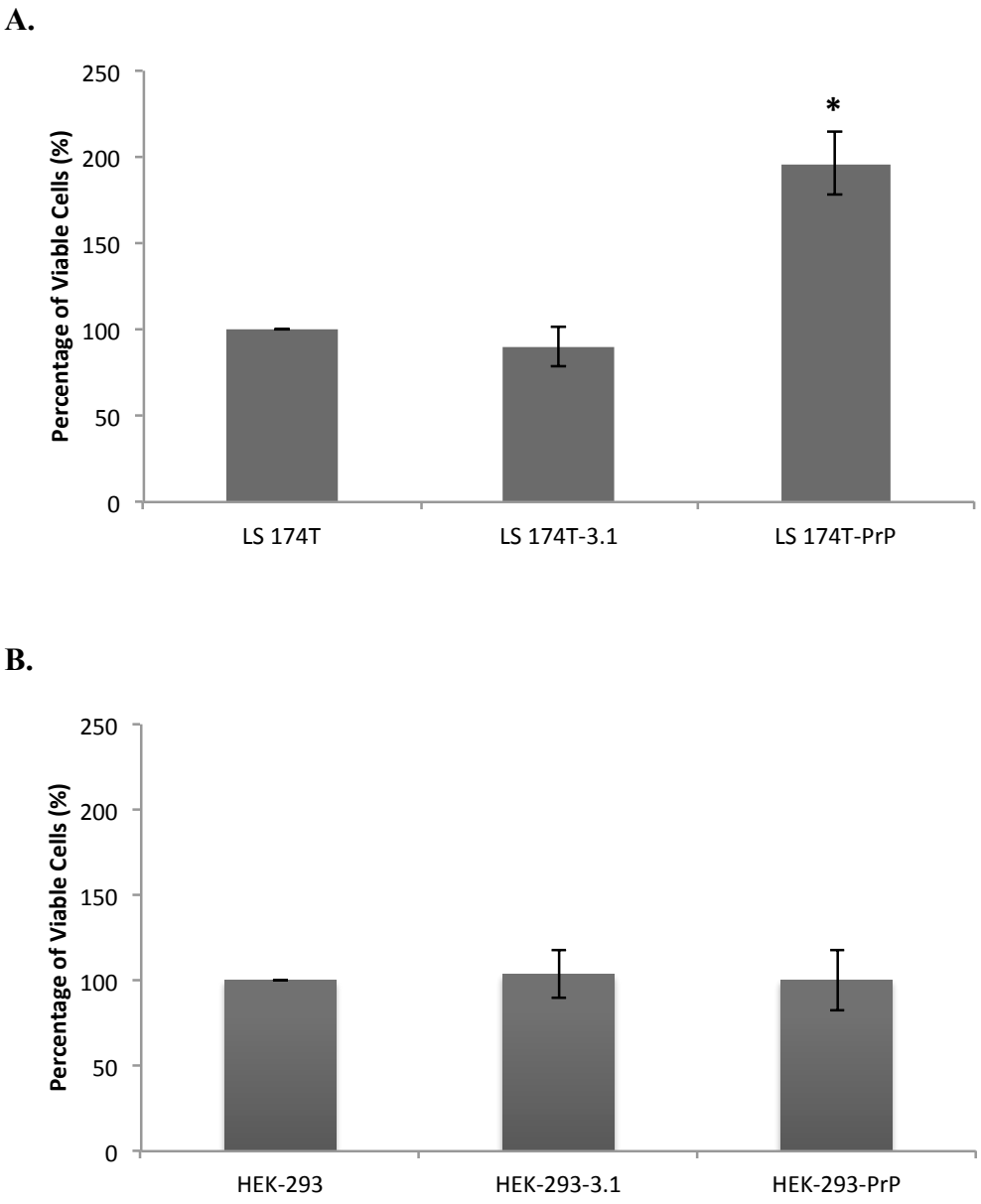

Figure 4.6: Percentage of viable cells for anoikis assay.
(A) Percentage of cell viability for LS 174T cells. O.D measurement of LS 174T-3.1 and LS 174T-PrP were normalized to LS 174T. (B) Percentage of cell viability for HEK-293 cells. O.D measurement of HEK-293-3.1 and HEK-293-PrP were normalized to HEK-293. Data of cell percentage was expressed in mean ± SEM (error bars) obtained from three independent experiments. Mean values were compared using one-way ANOVA followed by LSD's post hoc test for comparison of the means. * $p < 0.05$ as compared to LS 174T and LS 174T-3.1.

4.4 Cell Migration and Invasion

4.4.1 Scratch Wound Assay

In LS 174T cells, it was observed that the wound-healing rate increased from day 1 to day 2 as shown in Figure 4.7. On day 3, the wound closure for LS 174T-PrP was almost completed. LS 174T-PrP was able to complete wound closure on day 4. It was also observed that the cell density in LS 174T-PrP was greater as compared to LS 174T and LS 174T-3.1 from day 2 onwards. This alluded to the understanding that LS 174T-PrP has a higher proliferation rate as compared to LS 174T and LS 174T-3.1 and the observation corresponds to the earlier experiment on the cell viability MTT assay for LS 174T cells. As shown in Figure 4.9(A), image analysis has further validated that the percentage of open wound area for LS 174T-PrP on day 2, 3, 4, and 5 was significantly lower as compared to LS 174T and LS 174T-3.1.

On the other hand, there was no noticeable difference in cell migration observed between HEK-293 cells. The pattern of migration was even in HEK-293, HEK-293-3.1, and HEK-293-PrP as shown in Figure 4.8. Image analysis has further confirmed that there was no significant difference in the open wound area count for HEK-293-PrP as compared to HEK-293 and HEK-293-3.1 as shown in Figure 4.9(B).

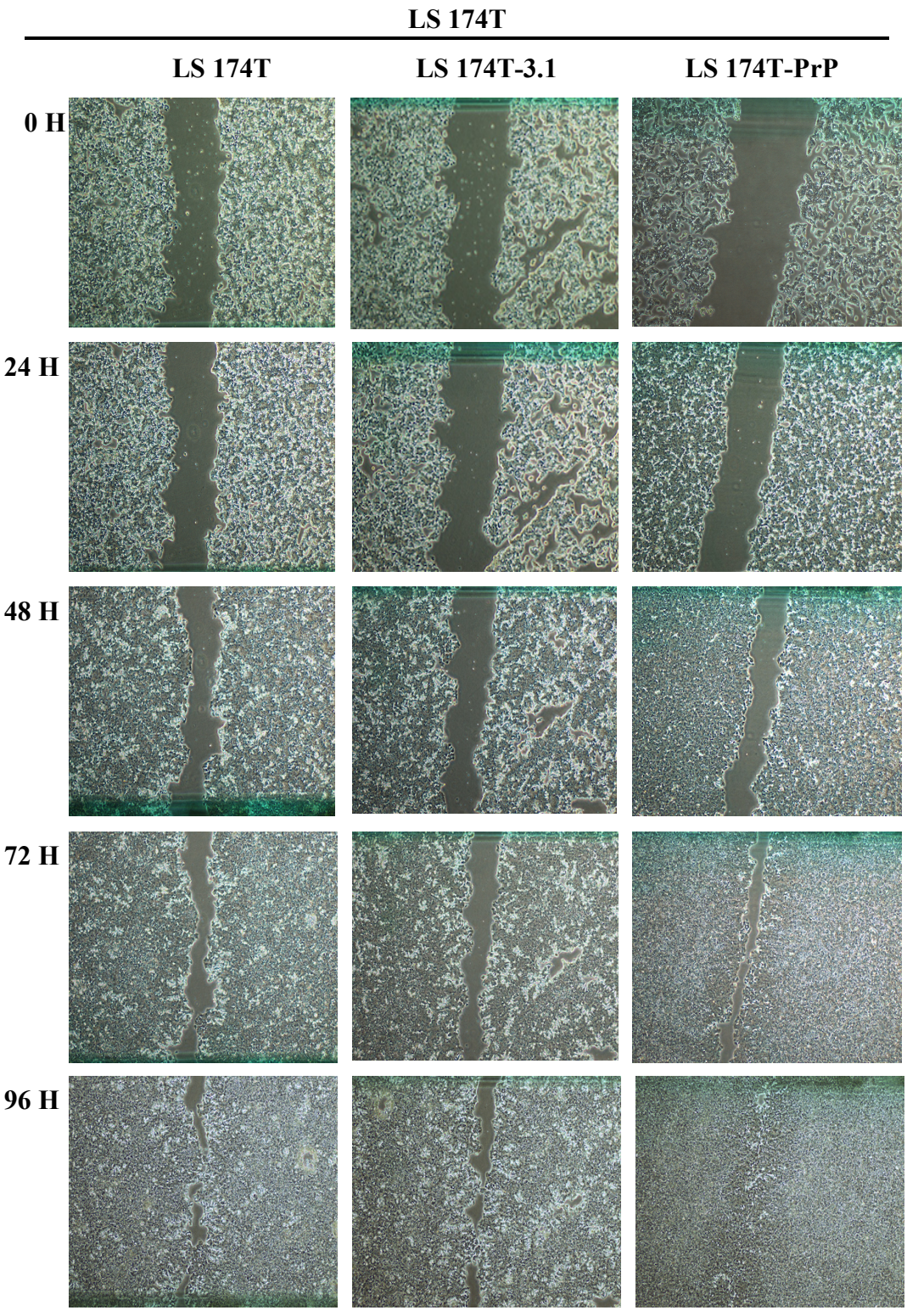

Figure 4.7: Scratch wound assay for LS 174T cells.
Wound closure for LS 174T cells was monitored from 0 h to 96 h until full closure of the wound area. Images were acquired using NIS-Elements BR 3.0 software under Nikon Eclipse TS100 inverted microscope at 40× magnification.

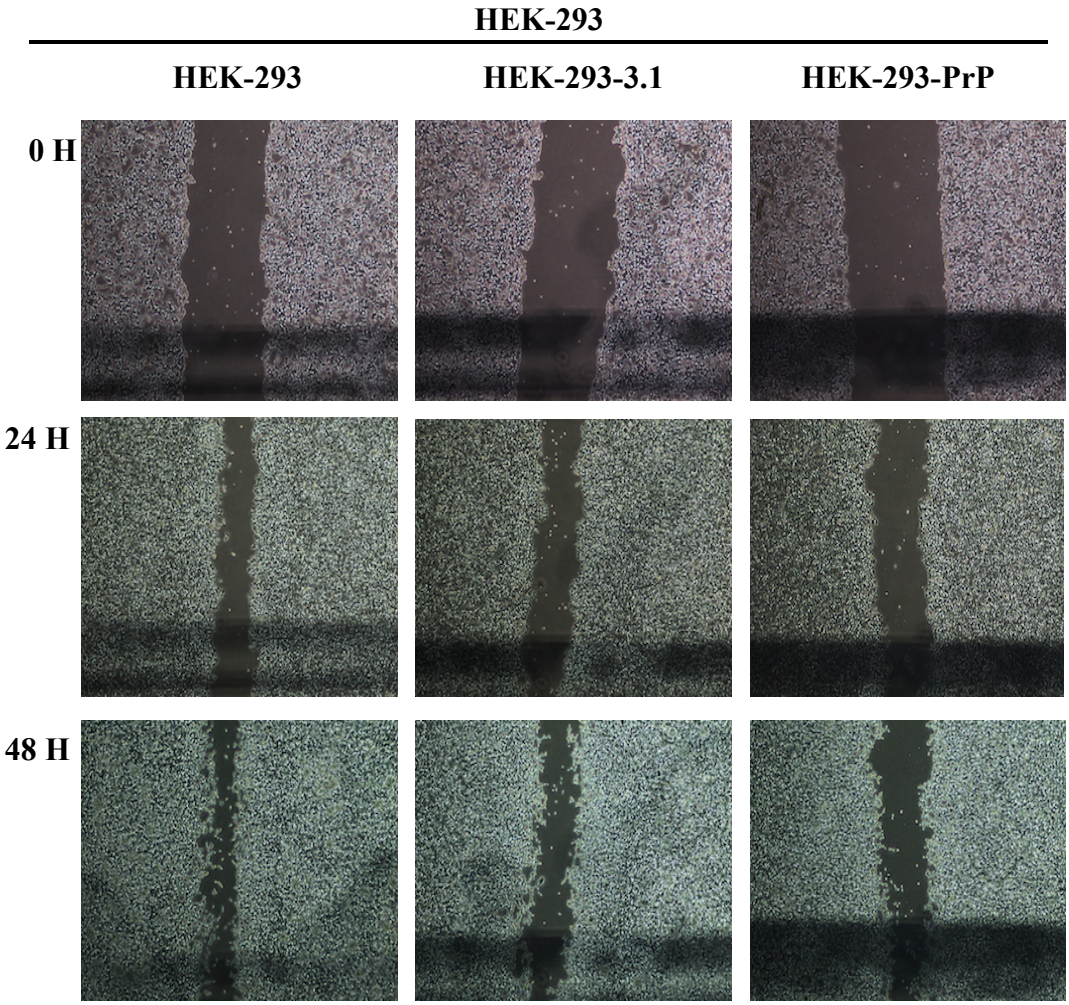

Figure 4.8: Scratch wound assay for HEK-293 cells.
Wound closure for HEK-293 cells was monitored from 0 h to 48 h. Images were acquired using NIS-Elements BR 3.0 software under Nikon Eclipse TS100 inverted microscope at 40× magnification.

A.

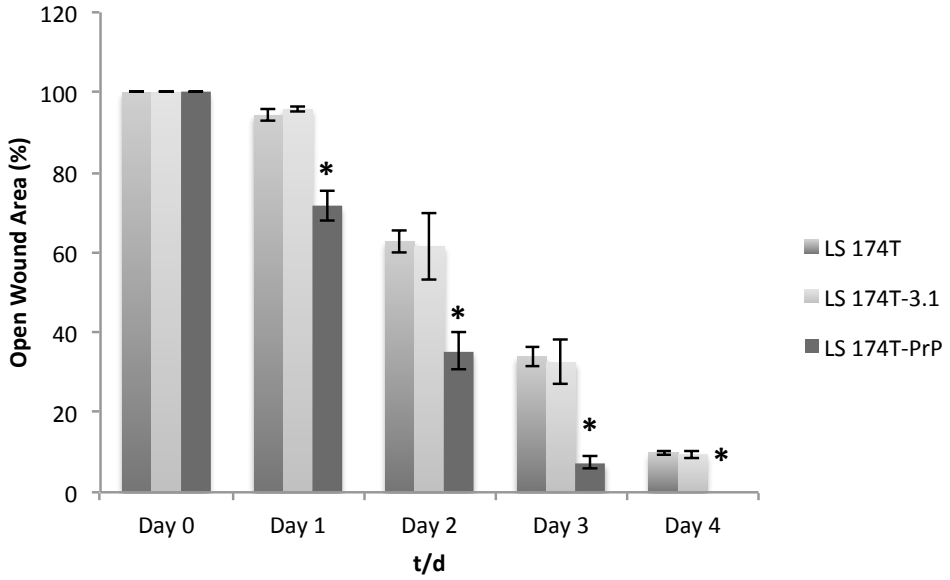

B.

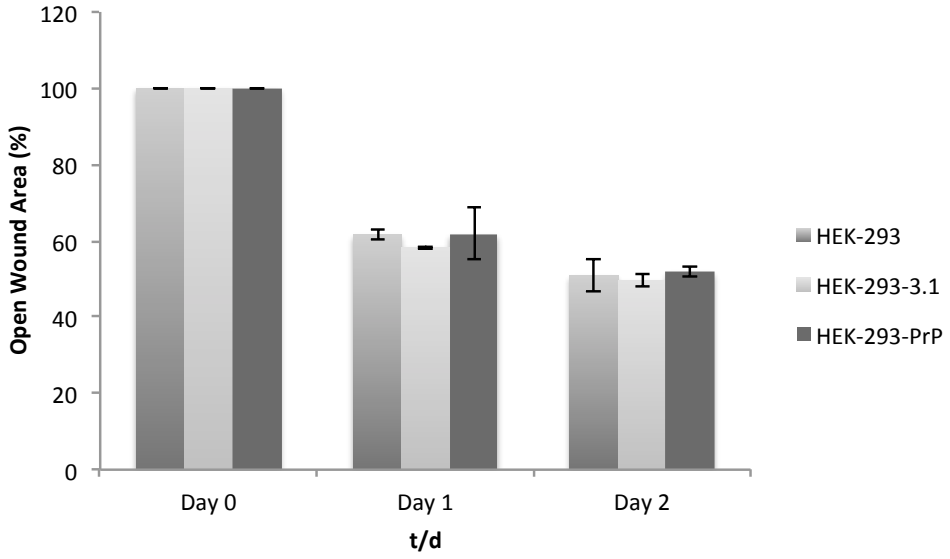

Figure 4.9: Open wound area count for scratch wound assay.
(A) Remaining area count for LS 174T cells, (B) Remaining area count for HEK-293 cells. Image analysis was performed using TScratch software version 1.0. Data of open wound area was expressed in mean ± SEM (error bars) obtained from three independent experiments. Mean values were compared using one-way ANOVA followed by LSD's post hoc test for comparison of the means. * $p < 0.05$ as compared to LS 174T and LS 174T-3.1

4.4.2 Transwell Invasion Assay

Representative images cell invasion are shown in Figure 4.10 where invasive cells with cell wall stained with crystal violet can be observed. As shown in Figure 4.11(A), LS 174T-PrP has a significantly higher relative fluorescence unit (RFU) count as compared to LS 174T and LS 174T-3.1 with an increment of cell penetration by approximately 3- fold. The above analysis construed that LS 174T-PrP has greater cell invasiveness as compared to LS 174T and LS 174T-3.1.

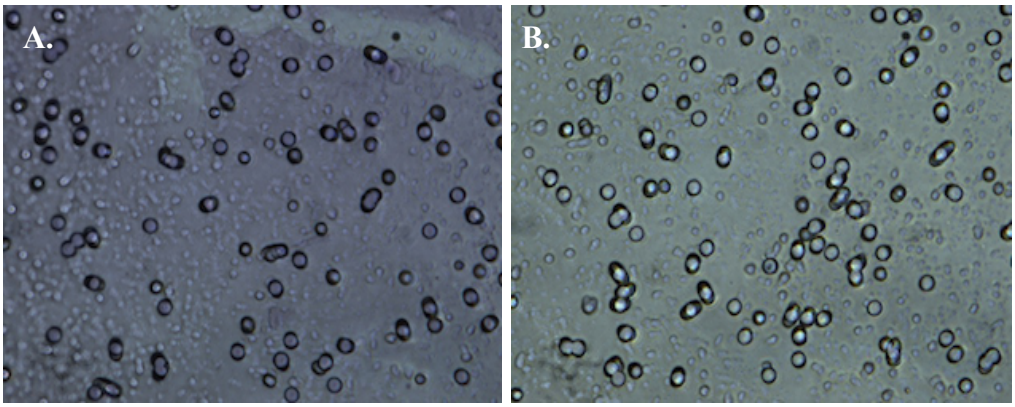

Figure 4.10: QCM™ 24-well cell invasion for LS 174T cells.
(A) LS 174T-3.1, (B) LS 174T-PrP. Invaded cells on the bottom side of the membrane were stained with 0.1% crystal violet solution. Images were acquired using NIS-Elements BR 3.0 software under Nikon Eclipse TS100 inverted microscope at 200× magnification.

A.

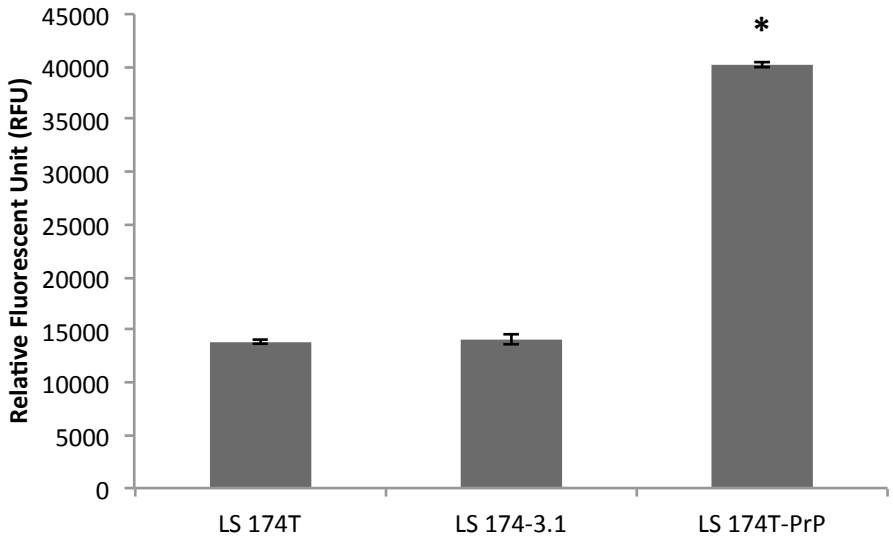

B.

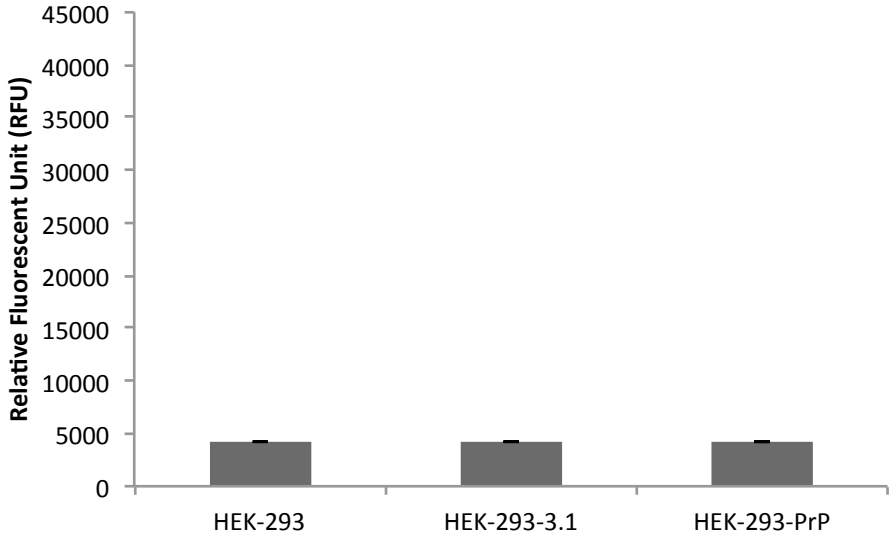

Figure 4.11: Fluorescent intensity analysis for matrigel invasion assay.
(A) Cell infiltrative analysis for LS 174T cells, (B) Cell infiltrative analysis for HEK-293 cells. Filter was set at 480/520 nm with a gain setting of 65. Data of RFU was expressed in mean ± SEM (error bars) obtained from two independent experiments. Mean values were compared using one-way ANOVA followed by LSD's post hoc test for comparison of the means. * $p <$ 0.05 as compared to LS 174T and LS 174T-3.1.

Conversely, in HEK-293 cells the fluorescence analysis for HEK-293, HEK-293-3.1, and HEK-293-PrP were less than 5000 RFU. As shown in Figure 4.11(B), there was no significant difference in the RFU of HEK-293-PrP as compared to HEK-293 and HEK-293-3.1. In non-cancer cells, the ECM occluded cell migrated through the membrane pores, therefore explaining the low RFU in HEK-293 cells as compared to LS 174T cells. This further elucidated that up-regulation of PrP^C did not result in the cell ability to develop invasiveness properties in non-cancer cells.

4.5 Cell Adhesion Assay

Since both LS 174T and HEK-293 are epithelial cells, therefore assessment of cell adhesion was stipulated at static adhesion assay only. ECM components comprised of different glycoproteins for instance collagen, elastin, laminin, and fibronectin. In this case, two popular glycoproteins namely collagen and fibronectin were used as coating components to test for the cellular attachment in LS 174T and HEK-293 cells.

4.5.1 Collagen Protein as Coating Component in Adhesion Assay

As shown in Figure 4.12(A) the attachment of LS 174T cells to collagen-coated surfaces has gradually increased as the concentration of the collagen increased. There was a significant difference in optical density (O.D) measurement for LS 174T-PrP as of 5, 10, 20, 30, and 40 μg/ml as compared to LS 174T and LS 174T-3.1. Generally, LS 174T-PrP has facilitated the cell

attachment to the collagen-coated surface approximately by 2- fold as compared to LS 174T and LS 174T-3.1.

Meanwhile, in HEK-293 cells it was observed to have a slight increase in the O.D measurement as the concentration of collagen coated increased. However, there was no significant difference in O.D measurement for HEK-293-PrP in 5, 10, 20, 30, and 40 μg/ml as compared to HEK-293 and HEK-293-3.1 as shown in Figure 4.12(B).

A.

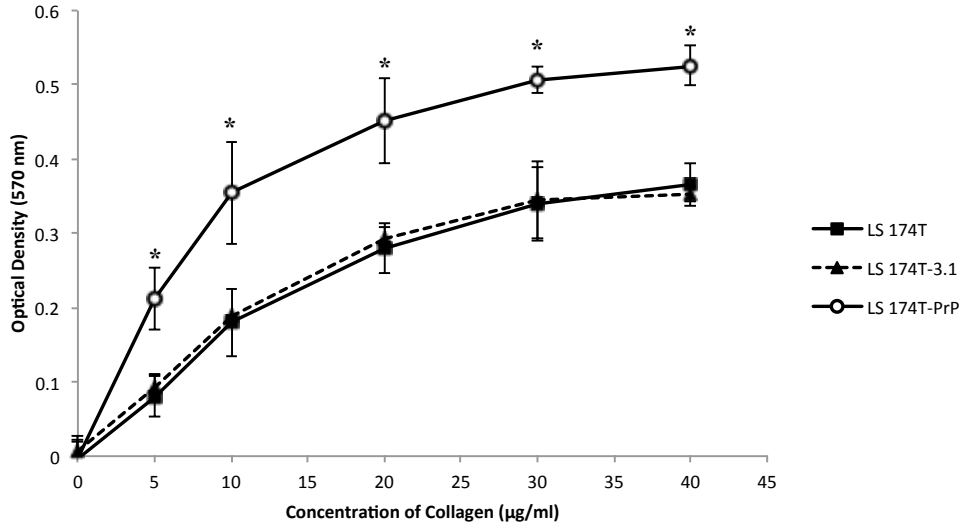

B.

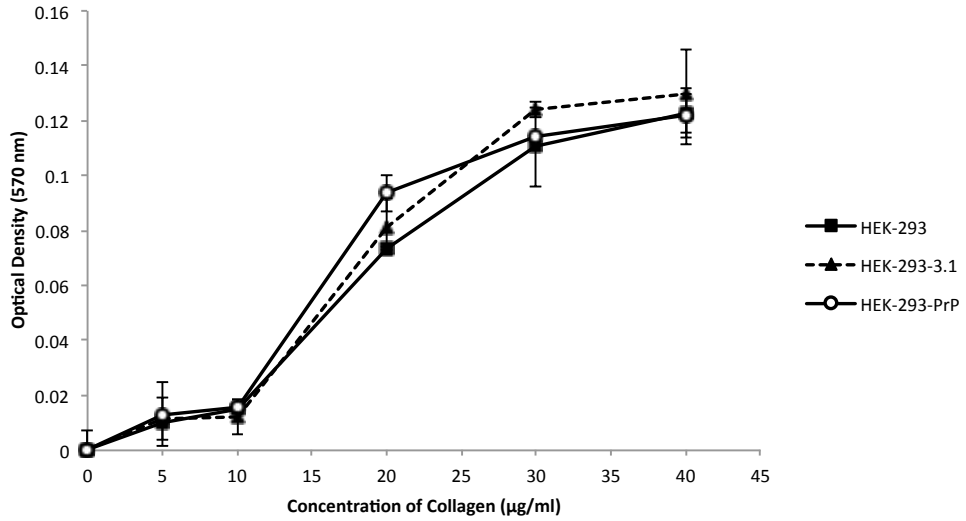

Figure 4.12: Collagen coated surface for cell adhesion assay.
(A) Absorbance reading for LS 174T cells, (B) Absorbance reading for HEK-293 cells. Absorbance reading was taken at 570 nm. Data of O.D was expressed in mean ± SEM (error bars) obtained from two independent experiments. Mean values were compared using one-way ANOVA followed by LSD's post hoc test for comparison of the means. * $p < 0.05$ as compared to LS 174T and LS 174T-3.1.

4.5.2 Fibronectin Protein as Coating Component in Adhesion Assay

In fibronectin-coated surface for the assessment of cell adhesion, the pattern of cell interaction for LS 174T cells was similar to collagen-coated surface. As shown in Figure 4.13(A) the attachment of LS 174T cells to fibronectin-coated surfaces has demonstrated a steady increment as the concentration of the fibronectin increased. There was a significant difference in O.D measurement for LS 174T-PrP as of 0.625, 1.25, 2.5, and 5 μg/ml as compared to LS 174T and LS 174T-3.1. O.D measurement for LS 174T-PrP has increased approximately 5-fold in 2.5 μg/ml and 5 μg/ml as compared to LS 174T and LS 174T-3.1. Thus, this has further revealed that PrP^C has a pivotal role in enhancing the cell adhesion to ECM components in cancer cell metastasis.

On the other hand, in HEK-293 cells it was observed to have a uniform O.D measurement in between HEK-293 cells. As shown in Figure 4.13(B), there was no significant difference in O.D measurement for HEK-293-PrP as compared to HEK-293 and HEK-293-3.1. In comparison of cell attachment and cell interaction to ECM glycoprotein-coated surfaces, cell attachment was greater in LS 174T as compared to HEK-293 cells. Thus, it validated that the up-regulation of PrP^C has increased the cell adhesion capability in cancer cells, but not in non-cancer cells.

A.

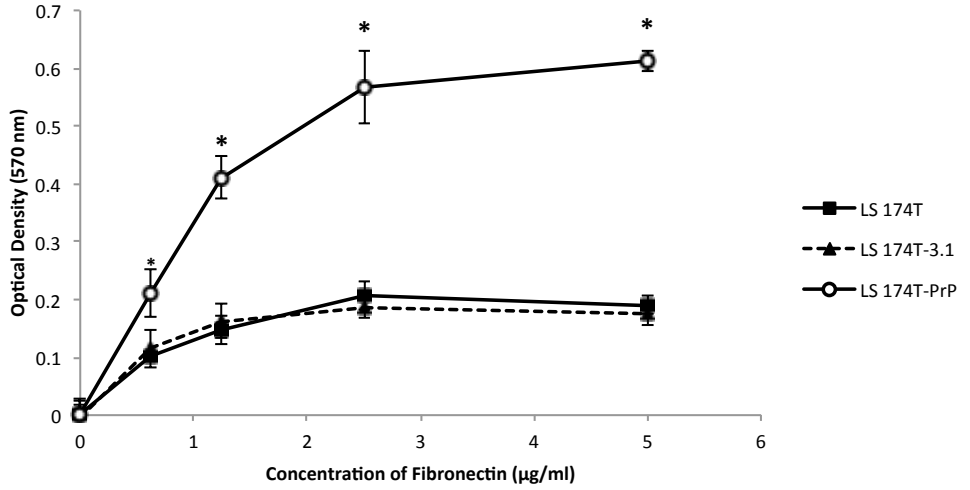

B.

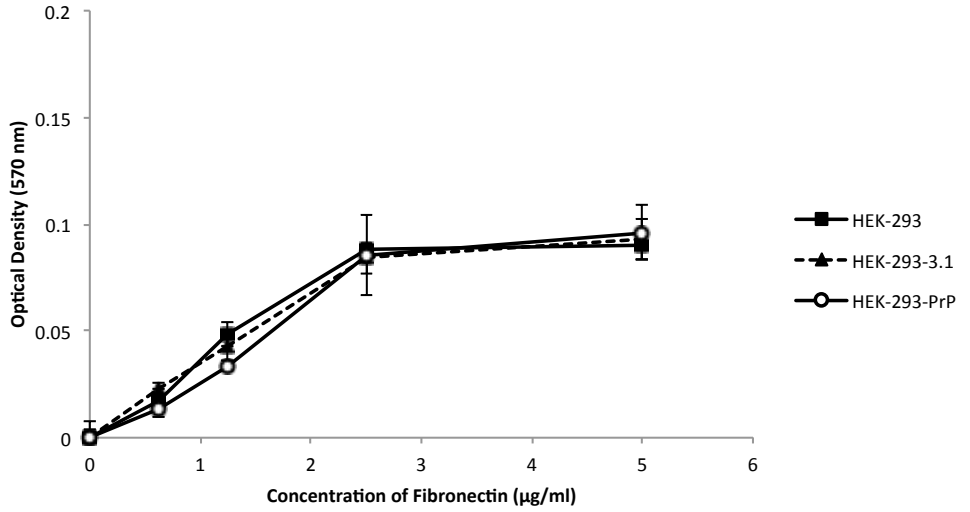

Figure 4.13: Fibronectin coated surface for cell adhesion assay.
(A) Absorbance reading for LS 174T cells, (B) Absorbance reading for HEK-293 cells. Absorbance reading was taken at 570 nm. Data of O.D was expressed in mean ± SEM (error bars) obtained from two independent experiments. Mean values were compared using one-way ANOVA followed by LSD's post hoc test for comparison of the means. * $p < 0.05$ as compared to LS 174T and LS 174T-3.1.

4.6 Qualitative Study on The Effect of PrP^c Overexpression on Epithelial Cell Scattering

In previous data, as PrP^C was overexpressed, a close relationship between the ability of LS 174T cells to migrate, invade, and attach was demonstrated. Moreover, the ability of cell to sustain is closely dependent on the growth environment. Cell resistance to apoptosis is a characteristic hallmark of cancer cells. Therefore, it is noteworthy to study the function of PrP^C in cell sustainability to altered growth environment.

In cell scattering assay, cells were subjected to starvation by replacing the complete growth medium with reduced-serum medium and the morphology of cells was observed daily. As shown in Figure 4.14, initially all cells appeared healthy with distinctive cytoplasm membrane outline and strong cell-cell contractility. However, on day 1 of cell starvation, cells have began to lose its membrane contractility and started to exhibit epithelial scattering resulting from disruption of cell-cell adhesion. Generally, LS 174T-PrP exhibited more scattering cells as compared to LS 174T and LS 174T-3.1. The contrast was even more obvious on day 2, where strong spider-like dispersion of scattering cells was observed in LS 174T-PrP. Meanwhile, LS 174T and LS 174T-3.1 were also exhibiting the same spider-like pattern of scattering cells, but apart from that it was also observed to have more apoptotic cells. This has further elucidated that PrP^C plays an important role to facilitate cell scattering in LS 174T. Potentially, it also has a correlation that increase cell migration will enhance cell scattering or vice versa.

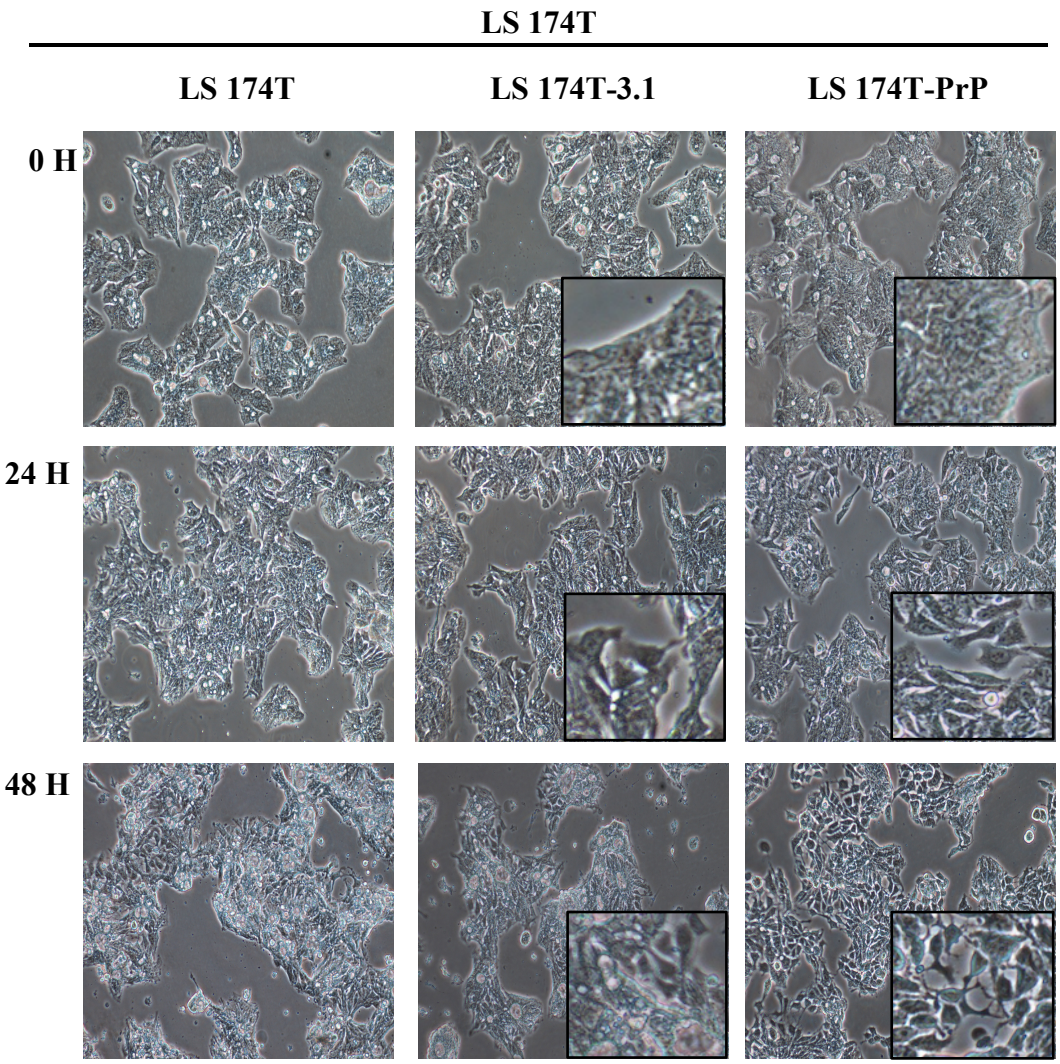

Figure 4.14: The influence of PrP^C overexpression upon serum deprivation in LS 174T cells.
Cell scattering effect was observed from 0 h to 48 h. Cell morphology changed from compact to scattered and eventually to apoptotic cells. Inset images were enlarged approximately 10× from original images. Images were acquired using NIS-Elements BR 3.0 software under Nikon Eclipse TS100 inverted microscope at 200× magnification.

Meanwhile, for HEK-293 cells, HEK-293-PrP (Figure 4.15) did not show any distinguishable increment in scattering cells as compared to HEK-293 and HEK-293-3.1. Generally, on day 1 of cell starvation, HEK-293 cells have started to exhibit apoptotic morphology such as nuclear fragmentation, cell rounding, and membrane blebbing. In non-cancer cells, during morphogenetic programs, cell-cell interactions were remodeled in order to allow certain tissue reposition; conversely inappropriate activation of these morphogenetic programs will lead to cancer invasion and metastasis (Jacob et al., 2014). In this case, there was very weak epithelial cell scattering that was observed in HEK-293 cells, suggesting up-regulation of PrP^C did not influence epithelial cell scattering in non-cancer cells.

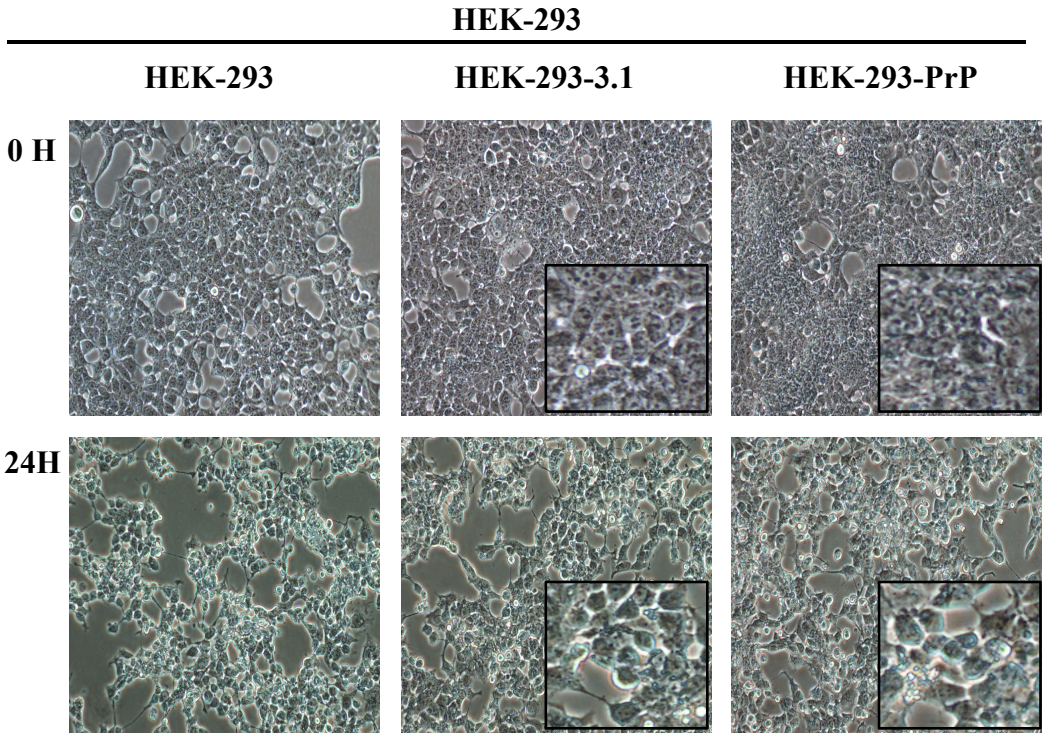

Figure 4.15: The influence of PrP^C overexpression upon serum deprivation in HEK-293 cells.
Cell scattering effect was observed from 0 h to 24 h. Cell morphology changed from compact to semi-scattered and eventually to apoptotic cells. Inset images were enlarged approximately 10× from original images. Images were acquired using NIS-Elements BR 3.0 software under Nikon Eclipse TS100 inverted microscope at 200× magnification.

4.7 *In Vitro* Multi-drug Sensitivity Assay

4.7.1 Observation of Morphological Changes in LS 174T and HEK-293 Cells Following Multi-drug Treatment

Generally, when no chemotherapeutic drug was introduced to the cells, majority of the cells displayed a standard morphology of uniform monolayer growth with a compact and distinctive membrane outline. Upon treatment with lower dose of chemotherapeutic drug, the cells started to exhibit apoptotic morphology. Cells were shrunken and accompanied by nuclear fragmentation. Upon treatment with higher dose of chemotherapeutic drug, more granulated cells could be observed. Interestingly, for LS 174T-PrP under doxorubicin treatment, lesser granulated cells were observed where majority of cells were exhibiting shrunken morphology. Representative images of LS 174T cells treated with doxorubicin are as shown in Figure 4.16. Upon exposure to etoposide and vincristine sulfate, LS 174T, LS 174T-3.1, and LS 174T-PrP displayed similar apoptotic cell morphology.

Meanwhile in HEK-293 cells, upon exposure to lower dose of chemotherapeutic drug, the cells appeared shrunken and retraction of pseudopods was observed, accompanied by cell granulation and membrane blebbing (Figure 4.17). Upon exposure to higher dose of chemotherapeutic drugs, majority of the cells underwent extensive morphology aberrations where rounded cell bodies containing only nuclei surrounded by cytoplasmic remnants were observed.

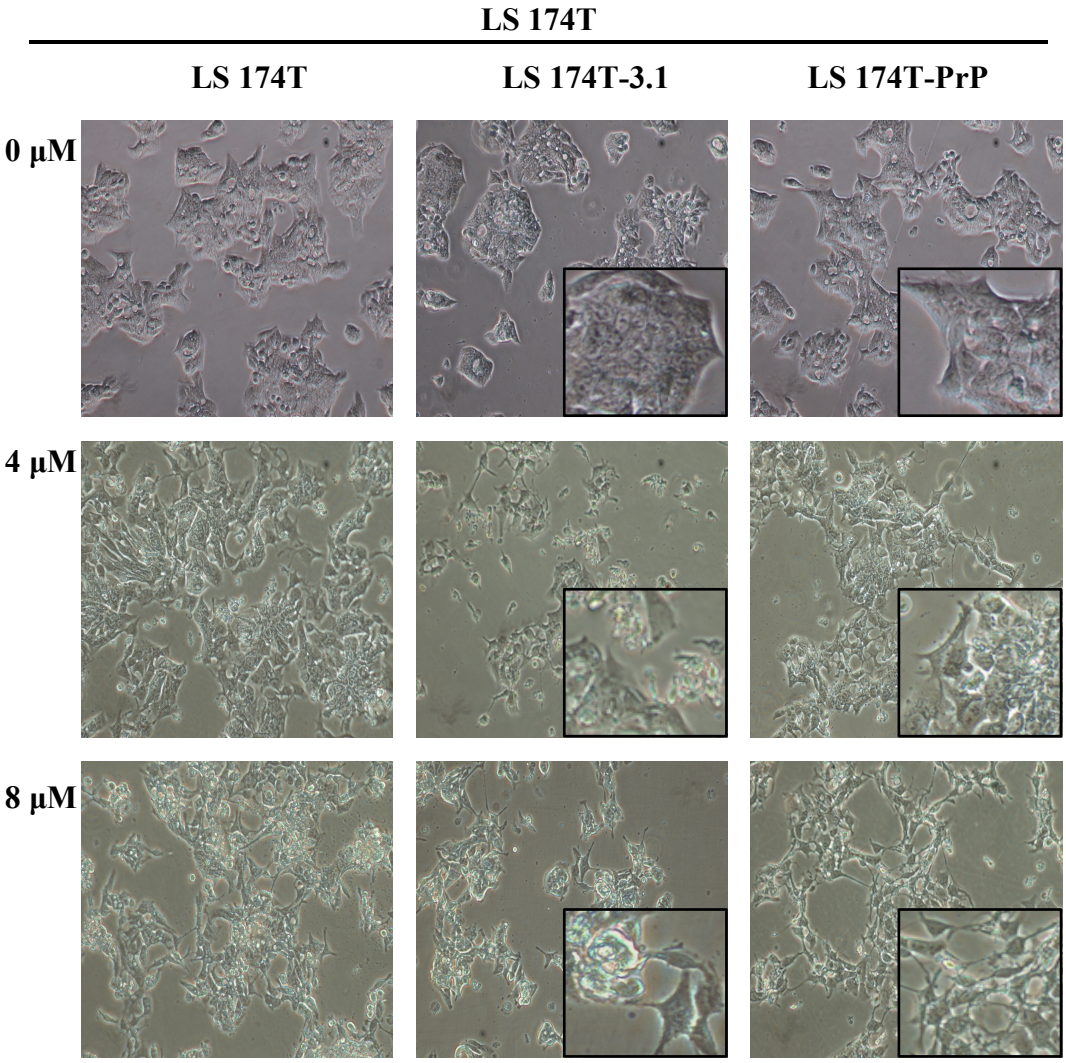

Figure 4.16: The influence of PrP^C overexpression upon doxorubicin exposure in LS 174T cells.
Representative images of LS 174T cells treated with 0, 4, and 8 µM of doxorubicin. Inset images were enlarged approximately 10× from original images. Images were acquired using NIS-Elements BR 3.0 software under Nikon Eclipse TS100 inverted microscope at 100× magnification.

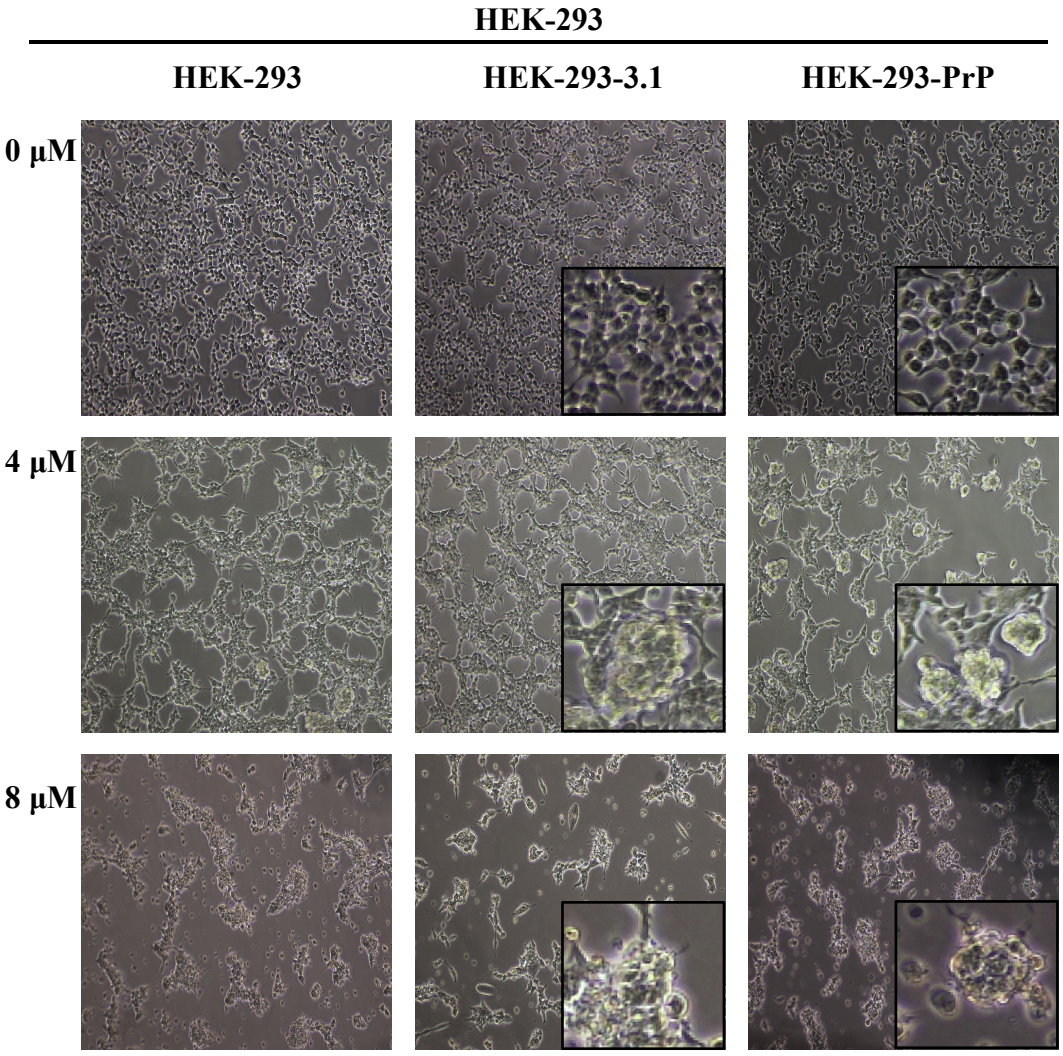

Figure 4.17: The influence of PrP^C overexpression upon doxorubicin exposure in HEK-293 cells.
Representative images of LS 174T cells treated with 0, 4, and 8 µM of doxorubicin. Inset images were enlarged approximately 10× from original images. Images were acquired using NIS-Elements BR 3.0 software under Nikon Eclipse TS100 inverted microscope at 100× magnification.

4.7.2 The Influence of PrP^C Overexpression on Multi-drug induced Cell Cytotoxicity

Briefly, LS 174T and HEK-293 cells were subjected to doxorubicin, etoposide, and vincristine sulfate treatment at increasing chemotherapeutic drug concentrations for 48 hours prior to MTT assay for the assessment of cell viability. Generally, upon exposure to the chemotherapeutic drug, a concentration-dependent decrease in cell viability was observed from the dose-response curve.

Upon exposure to doxorubicin, LS 174T-PrP showed a significant higher number of viable cells as compared to LS 174T and LS 174T-3.1. As shown in Figure 4.18(A), LC_{50} of LS 174T upon doxorubicin treatment was determined at 6 μM. Meanwhile for HEK-293 cells, overexpression of PrP^C did not show any significant difference in cell viability. As shown in Figure 4.18(B), LC_{50} of HEK-293 upon doxorubicin treatment was determined at 4 μM.

Upon exposure to etoposide, LS 174T-PrP showed a slightly higher percentage of viable cells as shown in Figure 4.19(A). However, the value was deduced insignificant as compared to LS 174T and LS 174T-3.1 after statistical analysis. Therefore, the LD_{50} for LS 174T was determined at 13 μM. Meanwhile for HEK-293 cells, no significant difference in percentage of cell viability was noted. LC_{50} of HEK-293 upon etoposide treatment was determined at 4 μM as shown in Figure 4.19(B).

A.

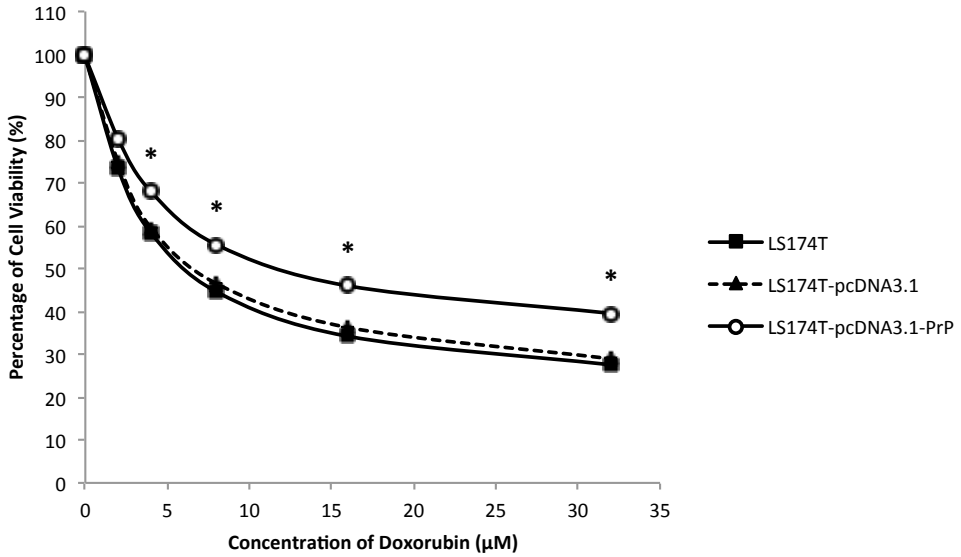

B.

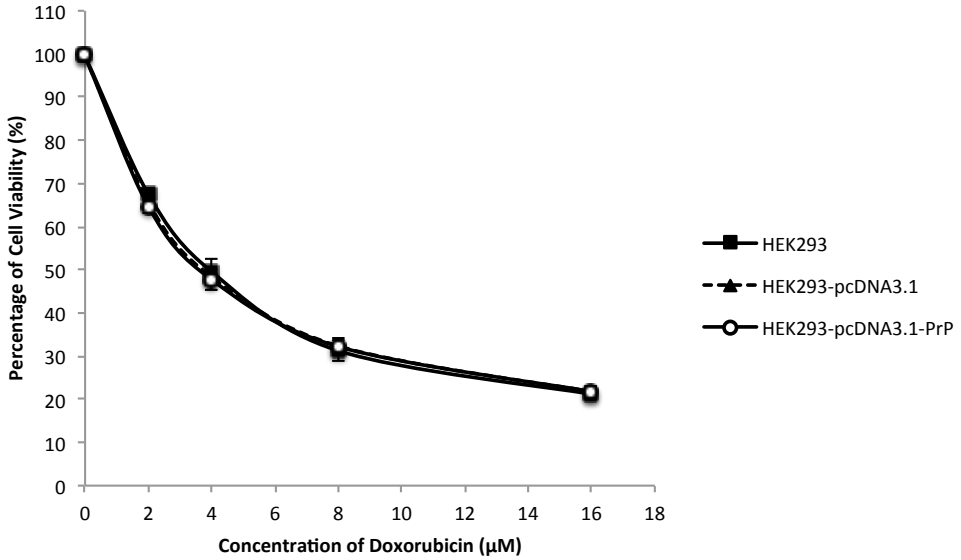

Figure 4.18: Doxorubicin treatment for LS 174T and HEK-293 cells.
(A) Dose-response curve for LS 174T cells, (B) Dose-response curve for HEK-293 cells. Data of percentage was expressed in mean ± SEM (error bars) obtained from two independent experiments. Mean values were compared using one-way ANOVA followed by LSD's post hoc test for comparison of the means. * $p < 0.05$ as compared to LS 174T and LS 174T-3.1.

A.

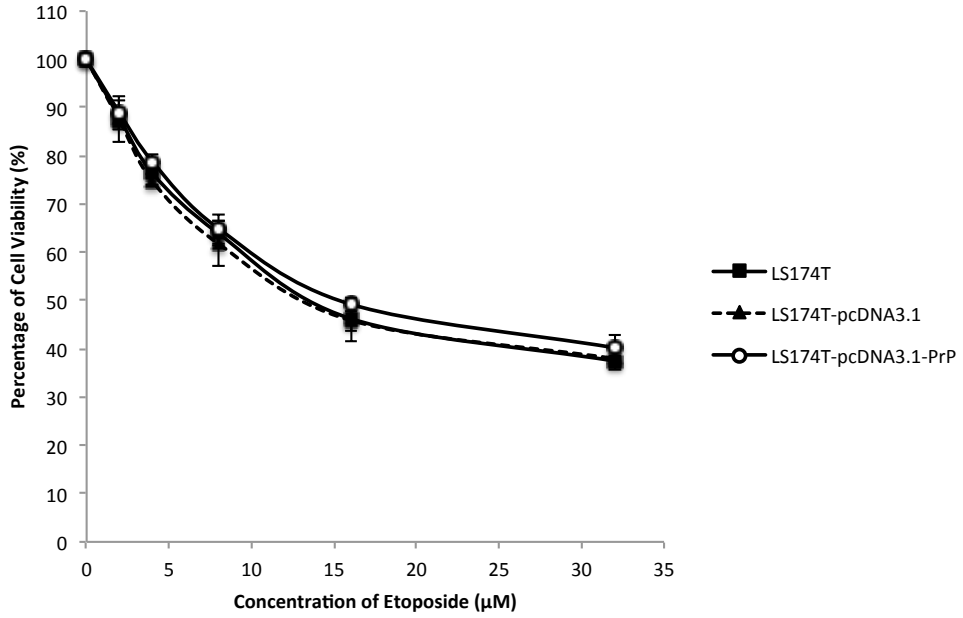

B.

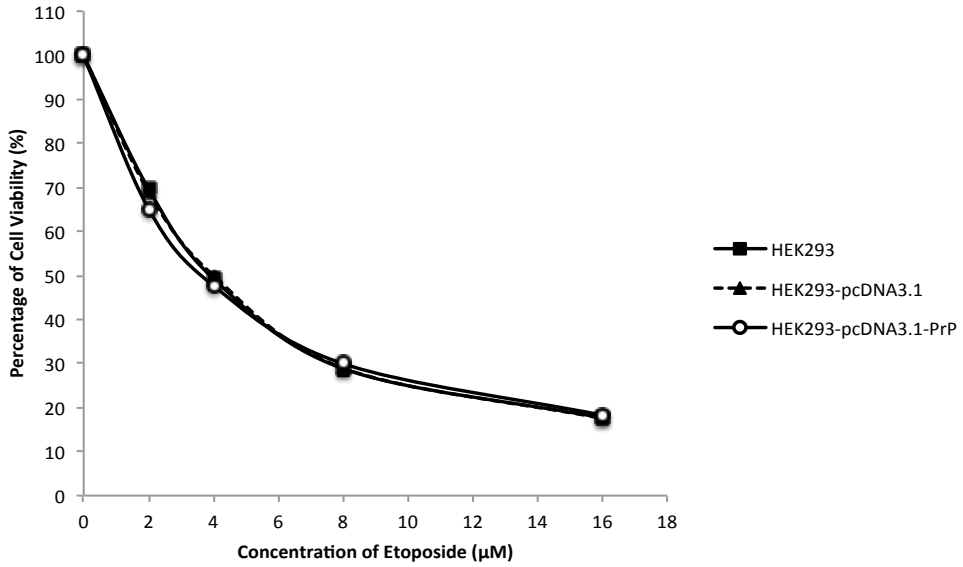

Figure 4.19: Etoposide treatment for LS 174T and HEK-293 cells.
(A) Dose-response curve for LS 174T cells, (B) Dose-response curve for HEK-293 cells. Data of percentage was expressed in mean ± SEM (error bars) obtained from two independent experiments. Mean values were compared using one-way ANOVA followed by LSD's post hoc test for comparison of the means. No significant difference in LS 174T and HEK-293 cells treated with etoposide.

Upon exposure to vincristine sulfate, LS 174T-PrP showed no significant percentage difference of viable cells. As shown in Figure 4.20(A), the LD_{50} of LS 174T was determined at 0.07 μM. Similarly, for HEK-293 cells, no significant percentage difference of viable cells was exhibited. As shown in Figure 4.20(B), the LD_{50} of HEK-293 was determined at 0.02 μM.

It was demonstrated that only one out of three chemotherapeutic drugs tested on LS 174T cells, which was doxorubicin, showed a significant increase in the percentage of viable cells in LS 174T-PrP. Up-regulation of PrP^C has no effect on cell viability in etoposide and vincristine sulfate treated LS 174T cells. As for HEK-293, up-regulation of PrP^C showed no effect in promoting cell survival or cell apoptosis on any of the chemotherapeutic drugs experimented. Therefore, doxorubicin was used as a standard parameter of triggering apoptosis in LS 174T cells to further investigate the role of PrP^C in cancer cells conferred to drug-resistance. Lethal dose values for LS 174T and HEK293 cells treated with three different cancer drugs as shown in Table 4.1.

Table 4.1 Lethal dose values for LS 174T and HEK-293 cells treated with different cancer drugs.

Cancer Drugs	**LD_{50} of LS 174T (μM)**	**LD_{50} of HEK-293 (μM)**
Doxorubicin	6	4
Etoposide	13	4
Vincristine Sulfate	0.07	0.02

A.

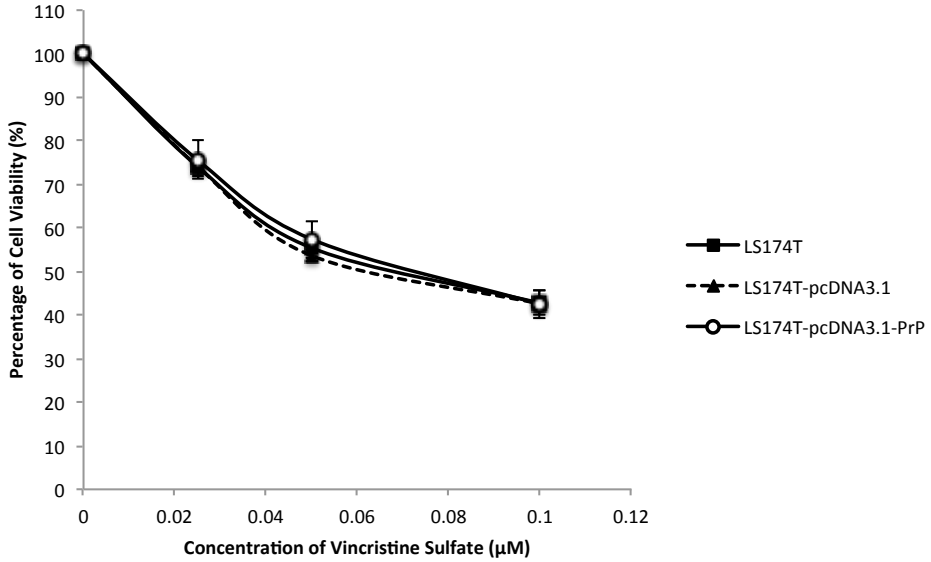

B.

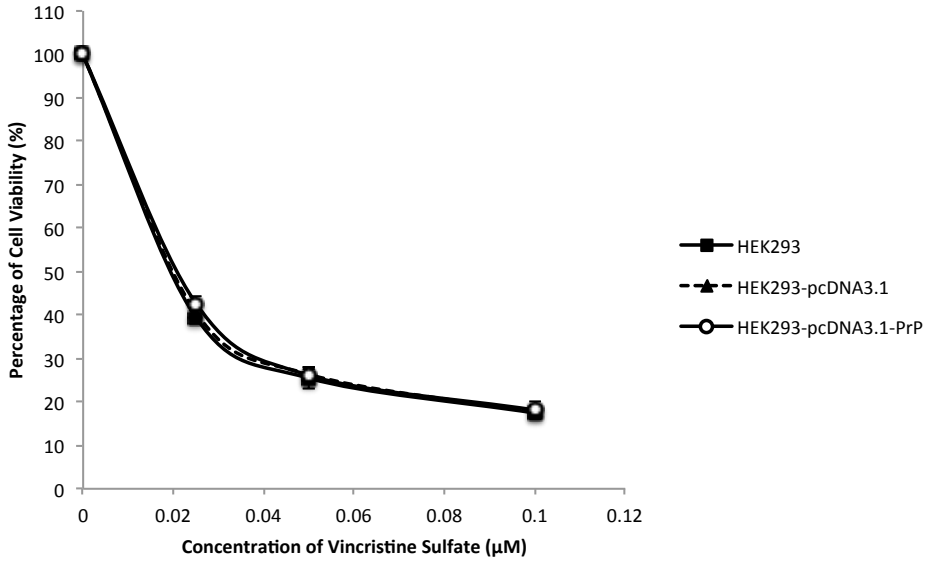

Figure 4.20: Vincristine sulfate treatment for LS 174T and HEK-293 cells.

(A) Dose-response curve for LS 174T cells, (B) Dose-response curve for HEK-293 cells. Data of percentage was expressed in mean ± SEM (error bars) obtained from two independent experiments. Mean values were compared using one-way ANOVA followed by LSD's post hoc test for comparison of the means. No significant difference in LS 174T and HEK-293 cells treated with vincristine sulfate.

4.8 Quantitative Study of Cell Apoptosis Against Doxorubicin Insult

To determine the effect of PrP^C overexpression on the cellular response to doxorubicin-induced cell death, LD_{50} of LS 174T at 6 μM was used as a standard of cell cytotoxicity. Influence of PrP^C overexpression in apoptosis study was categorized into whole cell assessment via fluorescence staining and cell lysates assessment via the human apoptosis antibody array kit.

4.8.1 Fluorescence Microscopy Visualization of Apoptotic or Necrotic Cells Induced by Doxorubicin

Cells bound with annexin V will show a green fluorescence staining of the plasma membrane. Cells that have lost membrane integrity with condensed or fragmented nucleus will show red fluorescence staining of the nucleus. DAPI counterstain was used to bind DNA so as the overall view of the cells can be compared with annexin V or PI.

As shown in Figure 4.21, LS 174T and LS 174T-3.1 were observed to have numerous cells stained with green fluorescence and red fluorescence. Green fluorescence indicates apoptotic cells while red fluorescence indicates necrotic cells. Notably, for LS 174T-PrP, only a few cells expressed green fluorescence and almost null for PI stain. Meanwhile, blue fluorescence of DAPI stain for all LS 174T cells was uniformed. The morphology of doxorubicin treated LS 174T cells were observed to have mostly shrunken with retracted pseudopods as compared to the untreated control that displayed intact cytoplasmic integrity.

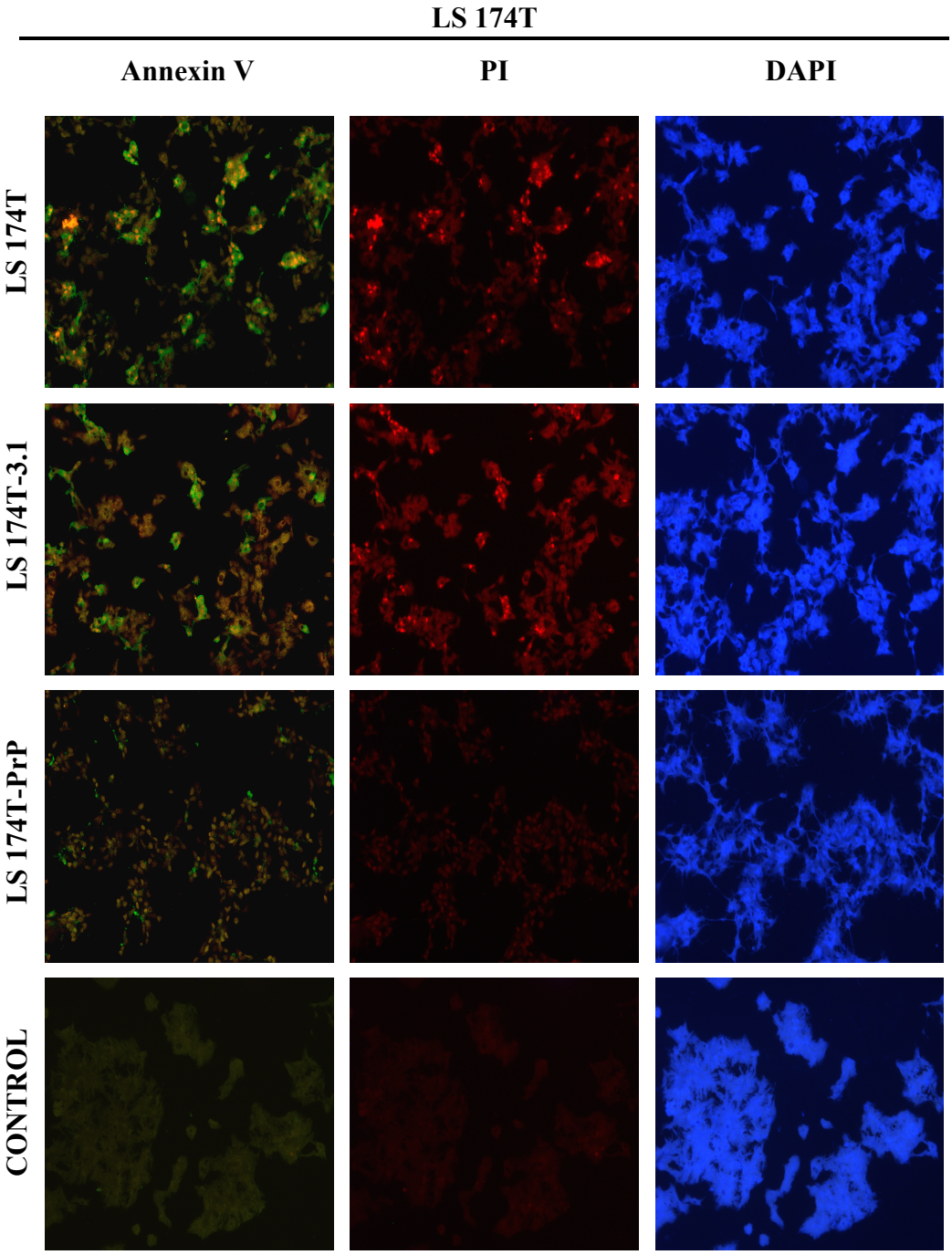

Figure 4.21: Fluorescence microscopy assessment for the effect of doxorubicin on LS 174T cells.
Green fluorescence images were resulted from annexin V stain. Red fluorescence images were resulted from PI stain. Blue fluorescence images were resulted from DAPI stain. Orange fluorescence images were resulted from indirect fluorescence stain of PI when viewed under NB filter. Images were acquired under the same field with different filters (NB, NG, and UV) using Analysis LS Research software version 3.0 at 100× magnification.

Furthermore, image analysis further confirmed that the percentage of cell stained with annexin V and PI for LS 174T-PrP was significantly lower as compared to LS 174T and LS 174T-3.1. As shown in Figure 4.22, the percentage of cells stained with annexin V increased by almost 4- fold in LS 174T and LS 174T-3.1 as compared to LS 174T-PrP. Approximately 10% of LS 174T and LS 174T -3.1 were necrotic cells while only 0.1% of LS 174T-PrP was recognized as necrotic cell.

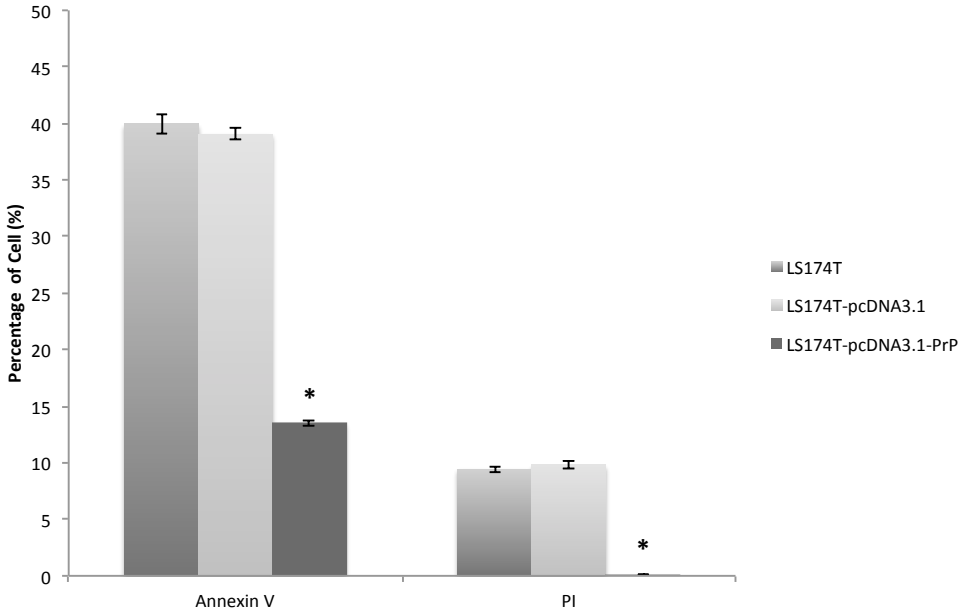

Figure 4.22: Percentage of cell stained with annexin V and PI.
Percentage of cell stained with annexin V or PI was determined by comparing the cells stained with annexin V or PI against cells stained with DAPI. Fluorescence intensity was analyzed using ImageJ software version 1.84. Data of cell percentage was expressed in mean ± SEM (error bars) of two independent experiments. Mean values were compared using one-way ANOVA followed by LSD's post hoc test for comparison of the means. * $p < 0.05$ as compared to LS 174T and LS 174T-3.1.

4.8.2 Apoptotic Proteins Involved in The Overexpression of PrP^C

4.8.2.1 Human Apoptosis Antibody Array for LS 174T Cells

To further understand the relevant apoptotic proteins that were involved in cell cycle regulation that has promoted cell survival, LS 174T and LS 174T-PrP were subjected to apoptosis antibody array. As shown in Figure 4.23, probes that can be distinguished with unaided eyes are highlighted.

Proteome profiling analysis has further revealed that there were more apoptotic markers that have significant difference in pixel densities as shown in Figure 4.24(A). Expression of SMAC/Diablo, TRAIL-R2/DR5, and pro-caspase-3 increased significantly in LS 174T as compared to LS 174T-PrP cells. Meanwhile, expression of Survivin, FADD, HO-2/HMOX2, HSP60, and cyt-c increased significantly in LS 174T-PrP as compared to LS 174T.

There was no significant difference in the protein expression of XIAP, TRAIL-R1/DR4, TRAIL R2/DR5, FAS/TNFRSF6/CD95, HSP27, HSP70, and HtrA2/Omi. Other apoptotic markers such as PON2, p21/CIP1/CDKN1A, p27/KIP1, p53 (S15), p53 (S46), p53 (S392), Rad17 (S635), TNFR1/TNFRSF1A, HIF-1α, HO-1/HMOX1/HSP32, Livin, Bad, Bax, Bcl-2, Bcl-x, cleaved caspase-3, Catalase, cIAP-1, cIAP-2, Claspin, and Clusterin showed a relatively low expression.

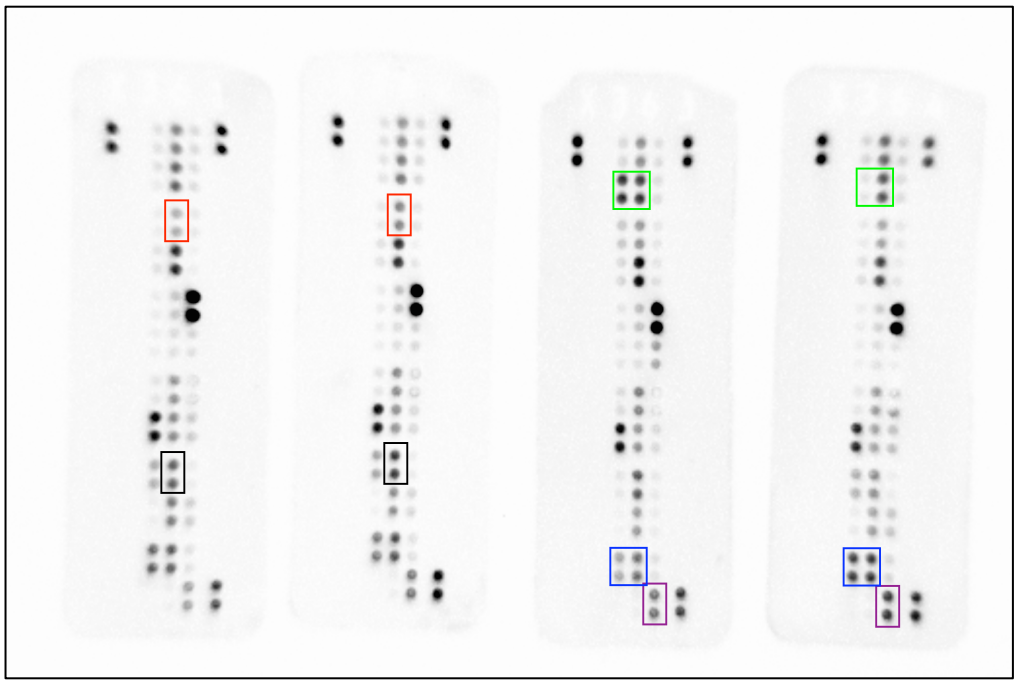

Figure 4.23: Human apoptosis antibody array for LS 174T cells treated with doxorubicin.
Red box refers to duplicate of FADD protein. Black box refers to duplicate of HSP60 protein. Green box refers to duplicate of p21/CIP1/CDKN1A and TRAIL-R2/DR5 protein. Blue box refers to duplicate of XIAP and HtrA2/Omi protein. Purple box refers to duplicate of cyt-c. Images were viewed using ChemiDoc™ MP Imaging System under auto-exposure mode and acquired using ImageLab™ software version 5.1. Refer to Appendix A for detailed coordinates and labels.

4.8.2.2 Human Apoptosis Antibody Array for LS 174T Cells Treated with Doxorubicin.

Doxorubicin treated LS 174T cells are designated as DOX-LS 174T and DOX-LS 174T-PrP. As demonstrated earlier, PrP^C was able to protect LS 174T against doxorubicin insult. Therefore it is crucial to understand the relevant apoptotic protein that confers to apoptosis resistance.

Proteome profiling analysis further revealed that there were more apoptotic markers that have significant difference in pixel densities as shown in Figure 4.24(B). Expression of p21/CIP1/CDKN1A, p27/KIP1, p53 (S15), SMAC/Diablo, TRAIL-R1/DR4, TRAIL-R2/DR5, FADD, FAS/TNFRSF6/CD95, HO-2/HMOX2, HSP60, pro-caspase-3, and cleaved caspase-3 increased significantly in DOX-LS 174T as compared to DOX-LS 174T-PrP. Meanwhile, expression of Survivin, XIAP, HtrA2/Omi, cIAP-1, and cyt-c increased significantly in DOX-LS 174T-PrP as compared to DOX-LS 174T.

There was no significant difference in protein expression of HSP27 and HSP70. Other apoptotic markers such as PON2, p53 (S46), p53 (S392), Rad17 (S635), TNFR1/TNFRSF1A, HIF-1α, HO-1/HMOX1/HSP32, Livin, Bad, Bax, Bcl-2, Bcl-x, Catalase, cIAP-2, Claspin, and Clusterin showed a relatively low expression.

A.

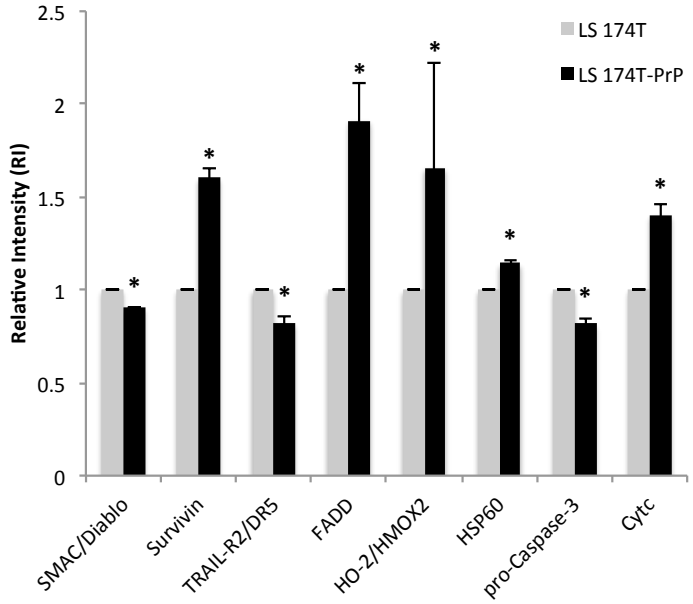

B.

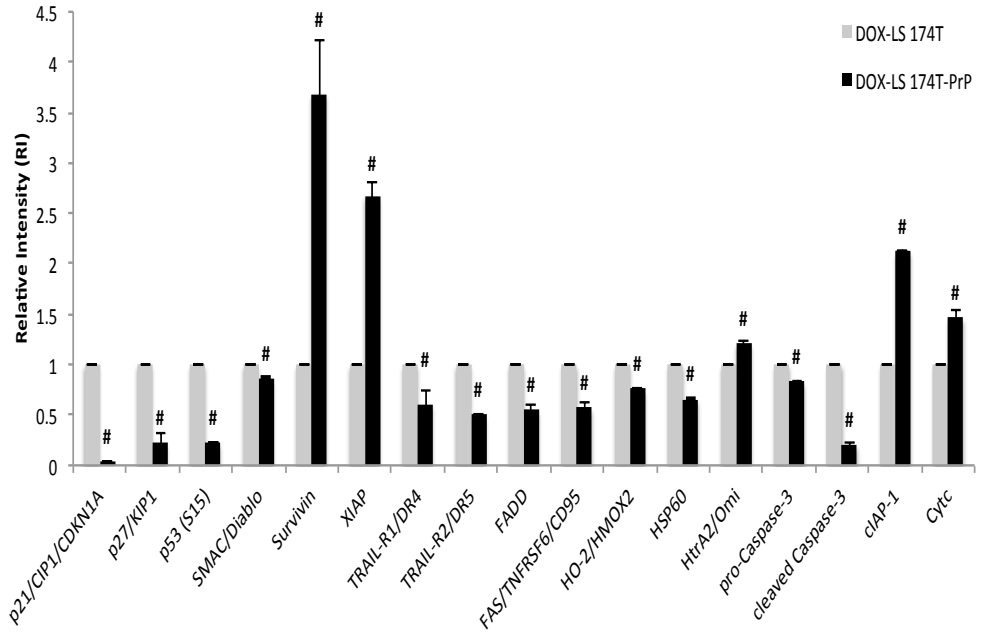

Figure 4.24: Apoptosis markers profiling for LS 174T cells.
(A) LS 174T cells. Refer to Appendix B for detailed intensity analysis. (B) LS 174T cells with exposure to doxorubicin. Refer to Appendix C for detailed intensity analysis. Refer to Appendix D for comparison of LS 174T and DOX-LS 174T. Pixel densities were analyzed using ImageJ software version 1.84. Data of intensity was expressed in mean ± SEM (error bars) obtained from two independent experiments. An unpaired two-tailed Student's t-Test using Microsoft Excel® for Mac 2011 was used for statistical analysis. * $p < 0.05$ in comparison of LS 174T and LS 174T-PrP. # $p < 0.05$ in comparison of DOX-LS 174T and DOX-LS 174T-PrP.

CHAPTER 5

DISCUSSION

5.1 Assessment of PrP^C Expression in Cancer and Non-cancer Cell

To understand the role of PrP^C in cancer cell and non-cancer cell, endogenous expression of PrP^C was determined prior to transfection. Faint protein bands were detected indicating low endogenous expression of PrP^C in LS 174T cell. Meanwhile in HEK-293 cells, the endogenous expression of PrP^C was almost null or extremely weak to be detected from immunoblotting. PrP^C is expressed most abundantly in the central nervous system (CNS), but has also been detected in other non-neuronal tissues as diverse as lymphoid cells, lung, heart, kidney, gastrointestinal tract, muscle, and mammary glands (Mehrpour and Codogno, 2010).

In this study, both LS 174T and HEK-293 cells with low endogenous expression of PrP^C was forced to overexpress PrP^C by transfection via the cationic lipid formulation, TPD1TR. Western blotting antibody probing with anti-prion protein antibody, clone 3F4 has revealed that overexpression of PrP^C resulted in three protein bands, namely unglycosylated PrP (27 kDa), monoglycosylated PrP (30 kDa), and diglycosylated PrP (35 kDa) that are coherent with research done by Yap and Say (2011) using the same clone of antibody.

Furthermore, immunofluorescence staining has validated the assessment of PrP^C expression of LS 174T and HEK-293 cells. Immunofluorescence staining using anti-prion antibody clone 3F4 is absolutely valid as Leclerc and co-workers (2003) have demonstrated PrP^C could be detected on the cell surface using different antibodies, and clone 3F4 is one of the consistent monoclonal antibodies that binds specifically.

5.2 Role of PrP^C in Cell Growth and Proliferation

5.2.1 Anchorage-dependent Manner

Essentially, the ability of cell to survive depends on the cell response to the growth signal thereby maintaining a homeostasis of cell numbers. In anchorage-dependent growth study, overexpression of PrP^C has proven to promote LS 174T proliferation *in vitro*. Similarly, the role of PrP^C in cell growth and proliferation is coherent with the research performed by Li and co-workers (2009) who have demonstrated the down-regulation of PrP influences the *in vitro* and *in vivo* behavior of the human pancreatic ductal adenocarcinoma cell lines where the proliferation of PrP down-regulated cells is reduced as compared to control cells. After PrP^C was knocked down using siRNA in DLD-1 and SW480 colon adenocarcinoma cell lines, the proliferation of cancer cells was significantly reduced (Li et al., 2011). Furthermore, Liang and co-workers (2007a) have demonstrated that overexpression of PrP^C could promote the tumorigenesis and proliferation of gastric adenocarcinoma cells at least partially through activation of PI3K/Akt pathway. Thus, from this study of the role of PrP^C in colorectal cancer, it has

strengthened the understanding that up-regulation of PrP^C in LS 174T cells will increase cell growth and proliferation.

Meanwhile, up-regulation of PrP^C in HEK-293 cells did not increase or decrease cell growth and proliferation. Peralta and co-workers (2011) have demonstrated the positive association between PrP^C and nestin expression indicating the contribution of PrP^C in neurogenesis. Thus, explains the role of PrP^C in non-cancer cell is necessitated in the CNS and has no known effect to cell growth and proliferation in HEK-293 cells.

5.2.2 Anchorage-independent Manner

In this study, soft agar colony formation assay was opted for the evaluation of anchorage-independent. Evidently, overexpression of PrP^C in LS 174T cells has promoted the cell proliferation in soft agar colony formation assay. Not only the number of colonies formed was increased, the colonies formed were also larger. This suggests that the overexpression of PrP^C potentially increase the aggressiveness of transformed LS 174T cells. The role of PrP^C in promoting cell proliferation in anchorage-independent growth is consistent with research performed by Liang and colleagues (2009a) who have demonstrated the forced overexpression of wild-type PrP^C (1-OPRD) and PrP^C have significantly increased the colony formation in plate for SGC-7901 human gastric adenocarcinoma cell line.

To further support the role of PrP^C in promoting cell proliferation in an anchorage-independent manner, anoikis assay was performed. In a complete

suspension form of growth environment, coating the plate with poly-HEMA simulates circulation and culminating in metastatic colonization of distant organs. Overexpression of PrP^C in LS 174T cells has shown to further promote the survivability of LS 174T cells in anchorage-independent environment. The phenomenon where the colonies formed in soft agar colony formation assay have increased and grew larger which could possibly be due to PrP^C promotes cell resistance to anoikis. Thus, it is evident that PrP^C possesses a protective role in LS 174T cells during detachment-induced apoptosis.

Anchorage-independent colony formation in soft agar occurs only if the cells are transformed (Lichtenberg et al., 1995). In normal epithelial cells, the cell survival depends on the attachment of the cell to a certain surface and they are supported by basement membranes providing survival and proliferative signals (Fukazawa, et al., 1995). This also rendered to the understanding that non-cancer cell will undergo apoptosis when placed in a suspension culture. The statement is consistent with the anchorage-independent growth study of HEK-293 cells, where no colony formation was observed and a plausible explanation would be cell apoptosis. Up-regulation of PrP^C in non-cancer cell neither cause cell transformation nor affect the cell survival under anchorage-independent manner.

5.3 Role of PrP^C in Cell Migration and Invasion

5.3.1 Two-dimensional Cell Migration and Invasion

Cell migration and invasion are essential processes in various physiological events not only in embryogenesis, wound healing, tissue regeneration, but also in several patho-physiological events such as cancer and cardiovascular disease (Smart and Riley, 2008). In the present study of cell migration and invasion, scratch wound assay has revealed that overexpression of PrP^C in LS 174T cells has markedly increased the cell motility over 24 h of incubation time. Since up-regulation of PrP^C will promote cell motility, therefore conversely down-regulation of PrP^C will also reduce cell motility. Research by Li and co-workers (2010) have demonstrated that the knockdown of PrP in A7 melanoma cell line have significantly reduced its migration in wound healing assay. Similarly, Wang and colleagues (2012) have reported *in vitro* transwell migration assays showed that PrP^C promoted the migration of SW480, while inihibition of PrP^C reduced the motility of LIM2405 colorectal carcinoma cell lines.

According to Rodriguez and co-workers (2005), observation of wound healing of more than 24 h cannot distinguish between cell proliferation and changes in cell survival from cell motility. However in the present study, wound healing was performed over 96 h with the aim to observe to what extent overexpression of PrP^C in LS 174T cells will behave. As a result, from 24 h onwards, LS 174T overexpressing PrP^C continued showing significant difference in wound closure as compared to control. Therefore, observation of wound healing and migration distance throughout 96 h can be interpreted as

overexpression of PrP^C has promoted both cell motility and cell proliferation in LS 174T cells.

In the present study, scratch wound assay for PrP^C-transfected HEK-293 cells showed no significant difference in cell migration distance as compared to the control. In contrast, Watanabe and co-workers (2011) have provided evidence that PrP^C may be necessary for brain microvascular endothelial cells to migrate into injured regions of the brain. By using siRNA to down-regulate the PrP^C expression in bEnd.3 mouse brain vascular endothelial cell line, the area covered by cellular migration in the scratch wound area was significantly reduced. Thus, it is evident that PrP^C possesses no known effect in cellular motility for HEK-293 cells but instead; it has a vital role in the brain system.

5.3.2 Three-dimensional Cell Migration and Invasion

In distant metastasis, tumor cells detach from the original site and invade the surrounding extracellular matrix followed by penetration of the blood vessels or lymphatic system. The matrigel component mimics the extracellular matrix (Kramer et al., 2013); therefore it can be used to simulate the tumor cell penetration into the cellular matrix around the blood vessels. Down-regulation of PrP decreases the number of invasive cells in human pancreatic ductal adenocarcinoma cell lines *in vitro* as well as tumor growth *in vivo* (Li et al., 2009). Pan and co-workers (2006) have exhibited that down-regulation of PrP^C produced a marked inhibition of invasion of SGC-7901 and MKN-45 human gastric adenocarcinoma cell lines through matrigel on

Boyden chamber assay. Similarly, Liang and co-workers (2009a) have demonstrated PrP^C-transfected SGC-7901 human gastric adenocarcinoma cell line produced an increased cell invasion through matrigel on Boyden chamber assay. Furthermore, Wang and colleagues (2012) have also reported PrP^C mediates the process of epithelial-mesenchymal transition and promotes metastasis in SW480 and LIM2405 colorectal carcinoma cell lines.

In the present study, transwell invasion assay has revealed that overexpression of PrP^C in LS 174T cells markedly increased the number of invasive cells as compared to control. Thus, it shows that the up-regulation of PrP^C in colorectal cancer cells will increase the cell invasiveness property.

Kramer and colleagues (2013) have reviewed that the ability to migrate is a prerequisite to invade; therefore a cell cannot invade without migration but can move without invasion. In the present study, overexpression of PrP^C in HEK-293 cells did not increase the number of invasive cells. Therefore, it is evident that up-regulation of PrP^C in HEK-293 cells did not confer to any cell invasiveness properties.

5.4 Role of PrP^C in Cell Adhesion Towards Extracellular Matrix Glycoproteins

Cell adhesion and migration are two processes that are closely linked to each other. There are four distinct steps of migration as reviewed by Lauffenburger and Horwitz (1996), namely cell polarization and membrane extension, formation and stabilization of adhesion at the tip or protrusion, contraction forces pulling the cell content forward, and de-adhesion of attachment at the rear of the cell. Mange and co-workers (2002) have demonstrated the role of PrP^C in cellular adhesion using cell aggregation assay where two Neuro-2a mouse neuroblastoma subclones expressing PrP^C showed an increased cellular aggregation in comparison with the control. Down-regulation of PrP^C in SGC-7901 and MKN-45 human gastric adenocarcinoma cell lines has decreased the cell adhesive ability to matrigel in a time-dependent manner (Pan et al., 2006; Liang et al., 2009a). Furthermore, Schrock and co-workers (2009) have demonstrated the surface levels of PrP expression regulate process formation where absence of PrP elicits lamellipodia formation while increased in PrP levels induces filopodia formation and extension in Neuro-2a mouse neuroblastoma cell line. Essentially, cell adhesion is a sophisticated process that involves many different molecular interactions, including receptor-ligand binding, changes in the fluxes through intracellular signaling pathways, and modulation of cytoskeletal assembly (Humphries, 2009).

In the present study, overexpression of PrP^C in LS 174T cells has shown to significantly increase the number of adhesive cells towards both collagen type-I and fibronectin coated surfaces. Shen and Falzon (2004) have

identified the proinvasive integrin, α5β1 mediates attachment to collagen type I while α5β1 is involved in fibronectin adhesion during overexpression of parathyroid hormone-related protein in LoVo human colorectal adenocarcinoma cell line. Therefore, it is evident that the up-regulation of PrP^C in LS 174T cells potentially increases adhesiveness of cells through integrin-mediated cell adhesion.

PrP^C has previously been reported to have diverse roles including cell adhesion (Aguzzi et al., 2008). Interestingly, Malaga-Trillo and co-workers (2009) have reported involvement of PrP in regulation of cell adhesion using zebrafish embryonic cells and *Drosophilia* S2 cells. Similarly, Schrock and co-workers (2009) have also demonstrated that the PrP^C-expressing *Drosophilia S2* cells produces abundant filopodia and remarkable cell spreading. However, in the present study, overexpression of PrP^C in HEK-293 cells did not result in any significant increase of adhesive cells in both collagen type-I and fibronectin coated surfaces. Thus, this explains the role of PrP^C in cell adhesion of non-cancer cell is cell-type specific.

5.5 Role of PrP^C in Cell Death Induced by Serum Deprivation

To extrapolate the role of PrP^C in facilitating cell migration, cell scattering assay was performed in the absence of serum. FBS is a commonly used medium supplement in cell culture because of its high content of embryonic growth promoting factors. Naturally, in the event of serum deprivation, cells will undergo apoptosis. However in the present study, in LS 174T overexpressing PrP^C, strong spider-like dispersion of epithelial

scattering cells was observed upon serum cessation. Moreover, there were also less apoptotic cells that were observed in comparison with the control cells. Noteworthy, up-regulation of PrP^C in LS 174T cells will exert a protective effect against cell death induced by serum deprivation.

In the beginning, the description on cell scattering was intended for the scatter phenomenon in MRC5 human embryo fibroblasts and MDCK cells in response to stimulation of growth factor identical to hepatocyte growth factor (HGF) (Chen, 2005). Jie and co-workers (2006) have reported HGF facilitates cell colony scattering and there was no endogenous expression of HGF detected in LS 174T cells. Therefore in the present study, it shows that PrP^C potentially mimics the function of HGF to induce cell scattering in LS 174T cells in the event of serum deprivation.

It is well established that PrP-null neurons are much more susceptible to serum deprivation induced cell death (Kuwahara et al., 1999; Kim et al., 2004). In the present study, there was minor but insignificant cell scattering that was observed in HEK-293 cells. Up-regulation of PrP^C in HEK-293 cells did not exert any protective effect towards the cell survival.

5.6 Role of PrP^C in Chemotherapeutic Drugs Treatment

Resistance to apoptosis is one of the most important features for cancer cells conferring to tumorigenesis and chemotherapeutic drug resistance (Yang et al., 2014). Zhao and colleagues (2002) have identified *PRNP* being one of the up-regulated genes from SCG-7901 gastric adenocarcinoma cells line that are resistant to vincristine and adriamycin. Evidently, Meslin and colleagues (2007a) have demonstrated adriamycin-resistant MCF7 breast adenocarcinoma cell line is sensitized upon PrP^C silencing. Furthermore, Yu and co-workers (2012) have reported although the PrP knockdown in MDA-MB-435 breast ductal carcinoma cell line was more susceptible to serum deprivation, they are more resistant to adriamycin treatment. In general, doxorubicin exerts its anticancer actions as topoisomerase II inhibitor, by targeting and intercalating the DNA of rapidly dividing tumor cells, causing cell cycle arrest in the G2 phase (Momparler et al., 1976; Fornari et al., 1994; Tacar et al., 2013). The molecular mechanisms underlying doxorubicin-induced toxicity are multi-factorial and not fully characterized even until now (El-Moselhy and El-Sheikh, 2014).

In the present study, overexpression of PrP^C in LS 174T cells showed significant increased cell resistance to doxorubicin, while not to etoposide and vincristine sulfate. Meanwhile overexpression of PrP^C in HEK-293 cells did not augment cell resistant towards chemotherapeutic drugs. Zhang and co-workers (2006b) have demonstrated up-regulation of PrP^C had little or no effect on staurosporine-mediated DNA fragmentation in Neuro-2a mouse neuroblastoma cell line but it affects staurosporine-mediated apoptosis in

HEK-293 cells. Therefore, it is evident that the expression of PrP^C conferring to drug-resistant could be cell- or drug-specific.

5.7 Role of PrP^C in Cell Regulation Against Doxorubicin Insult

Apart from being a DNA-intercalating agent, doxorubicin has shown to play a role in oxidative stress (Korga et al., 2012), inflammatory cascades (Park et al., 2012), and apoptosis (Zhang et al., 2009). In the present study, fluorescence microscopy visualization of untransfected LS 174T cells and mock-transfected LS 174T cells stained with annexin-V and PI showed significantly higher number of apoptotic and necrotic cells as compared to PrP^C-transfected LS 174T cells. Necrotic cell death is usually accompanied by generation of ROS, and various anti-oxidants that can prevent necrosis or switch it to apoptosis instead (Proskuryakov and Gabai, 2010). However, upon exposure to chemotherapeutic drugs such as doxorubicin and cisplastin, the subtoxic doses of H_2O_2 were able to switch cell suicide to necrosis (Lee and Shacter, 1999; Lee and Shacter, 2000). In present study, it is evident that PrP^C-transfected LS 174T cells treated with doxorubicin tends to exert a cytoprotective effect upon doxorubicin insult. The number of apoptotic cells in LS 174T overexpressing PrP^C was significantly reduced while almost null for necrotic cells. In view of this, the finding may indicate the biological role of PrP^C in LS 174T cells despite of being anti-apoptotic, but potentially it also possesses anti-oxidative effects.

5.8 Signaling Pathways Involved in The Anti-apoptotic Property of PrP^C

5.8.1 Human Apoptosis Antibody Array for LS 174T Cells

Owing to the anti-apoptotic effect of PrP^C in LS 174T cells, proteins that are involved in the regulation of apoptosis were investigated. Human apoptosis antibody array kit revealed that SMAC/Diablo, TRAIL-R2/DR5 and pro-caspase-3 showed a higher expression in LS 174T as compared to LS 174T-pcDNA3.1-PrP. SMAC/Diablo is a mitochondrial protein released from the mitochondrial intermembrane space into the cytoplasm during apoptosis. Once released in the cytosol, it interacts directly with the IAPs such as cIAP-1, cIAP-2, XIAP, Survivin, and Livin (Vucic et al., 2002).

Survivin showed a significantly higher protein expression in LS 174T overexpressing PrP^C. Survivin is an endogenous inhibitor of caspases and they can inhibit caspases activity by binding their conserved baculovirus IAP repeat (BIR) domains to the active site of caspases, therefore promote the degradation of active caspases (Wei et al., 2008). Another protein of apoptosis, HSP60 has shown increased protein expression in LS 174T cells upon PrP^C overexpression. To date, exact role of HSP60 is still not fully understood. HSP60 may have both pro- and anti-apoptotic roles in cancer cells (Samali et al., 1999; Kirchhoff et al., 2002; Faried et al., 2004; Di Felice et al., 2005). HSPs alone are not able to activate pro-caspase-3 and require cyt-c and dATP to initiate the process (Samali et al., 1999).

In the present study, a phenomenon where higher level of pro-apoptotic agents namely FADD, HSP60, HO-2/HMOX2, and cyt-c, but uncommonly almost null expression of cleaved caspase-3 was observed in

PrP^C-transfected LS 174T as compared to untransfected LS 174T. Since apoptosis was not deliberately triggered in this case, a plausible explanation would be the involvement of these "pro-apoptotic proteins" in other cytosolic activities apart from being recognized solely as apoptosis promoting proteins. To support this statement, Matsuyoshi and co-workers (2006) have demonstrated that the phosphorylation of FADD is implicated the cell cycle regulation and metastasis of MCF7 human breast adenocarcinoma cell line. Furthermore, Huttemann and co-workers (2011) have reviewed that the involvement of cyt-c in life-sustaining functions such as cellular respiration, ROS scavenging activities, and redox coupled protein import via Erv1-Mia40; and involvement in cellular death functions such as cell apoptosis, cardiolipin peroxidation, and ROS formation via $p66^{Shc}$.

Apart from the cytoprotective effect, up-regulation of PrP^C in LS 174T cells has been shown to increase cell proliferation, migration, invasion, and adhesion. Yang and co-workers (2004) have suggested Survivin promoted cellular proliferation by facilitating accurate sister chromatid segregation and stabilization of microtubules during late mitosis of cell cycle. Kim and co-workers (2003) have demonstrated stimulation of Survivin expressing by TCF/β catenin enhanced cell proliferation with resistance to apoptosis in HCT 116 colorectal carcinoma cell lines. In addition, study of colon cancer by Hernandez and co-workers (2011) has reported Survivin-related anti-apoptotic pathways were turned on early in tumorigenesis to promote cell proliferation. Furthermore, research by Hehlgans and co-workers (2013) have discovered the function of Survivin not only as apoptosis inhibitor, but also to reduce cell proliferation, migration, and invasion upon Survivin silencing in colorectal

cancer cell lines. Therefore, it has construed the notion that Survivin could be the key protein in LS 174T overexpressing PrP^C conferring cell resistance to apoptosis.

5.8.2 Human Apoptosis Antibody Array for LS 174T Cells in Doxorubicin-induced Apoptosis

To further investigate the underlying apoptosis proteins involved in overexpression of PrP^C, apoptosis was deliberately triggered in LS 174T cells via doxorubicin exposure. In the present study, human apoptosis antibody array revealed that doxorubicin-induced apoptosis in LS 174T cells consists of more than a single pathway of death as proposed in Figure 5.1. LS 174T cells engages mainly in extrinsic pathway of apoptosis while the intrinsic pathway of apoptosis mediated by the mitochondria was partially involved. Inhibition of three IAPs, namely Survivin, XIAP, and cIAP-1 towards the semi-active caspase-3 could confer to resistance towards apoptosis.

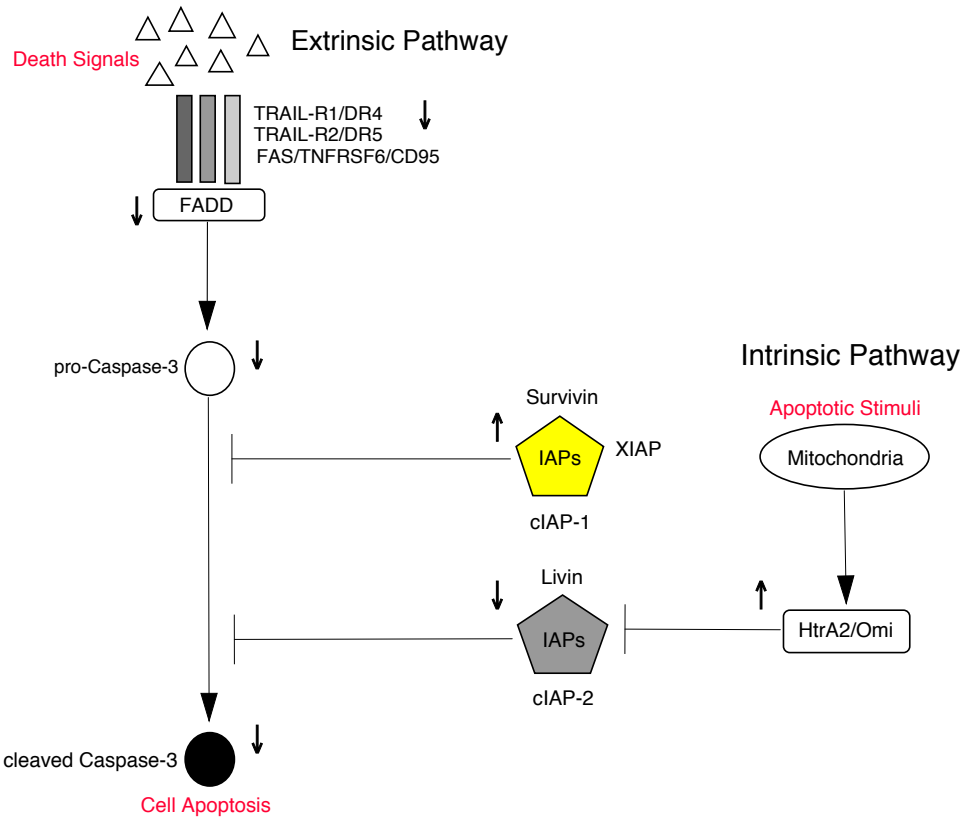

Figure 5.1: Possible apoptosis signaling pathways involved in LS 174T cell overexpressing PrP^C

Figure depicting involvement of extrinsic and intrinsic apoptotic pathway during cell apoptosis in LS 174T cells overexpressing PrP^C. TRAIL-R1/DR4, TRAIL-R2/DR5, FAS/TNFRSF6/CD95, and pro-caspase-3 were down-regulated upon exposure to doxorubicin. Three IAPs, namely Survivin, XIAP, and cIAP-1 were remarkably up-regulated upon exposure to doxorubicin. It is speculated that HtrA2/Omi antagonized only certain IAPs, namely Livin and cIAP-2 in LS 174T cell overexpressing PrP^C upon exposure to doxorubicin. Overexpression of PrP^C in LS 174T cells has mitigated cell apoptosis based on the observation that almost null expression of cleaved caspase-3 upon exposure to doxorubicin. The relative 3.7, 2.7, and 2.1-fold up-regulation of anti-apoptotic IAPs, namely Survivin, XIAP, and cIAP-1 counterbalanced the pro-apoptotic reduced Livin and cIAP-2 expression. This pathway leads to decreased doxorubicin-stimulated apoptosis in LS 174T-PrP^C cell. Illustration was created using Cytoscape software version 3.1.1.

The extrinsic apoptotic pathway begins when death signals bind to a death receptor (Wong, 2011). Upon exposure to doxorubicin, apoptotic proteins involved in extrinsic pathway namely, TRAIL-R1/DR4, TRAIL-R2/DR5, FAS/TNFRSF6/CD95, and FADD showed significantly lower expression in PrP^C-transfected LS 174T cells as compared to untransfected LS 174T cells. This finding is coherent with research by Meslin and co-workers (2007a) who have demonstrated that overexpression of PrP^C may coincide with the resistance of breast cancer cell lines to adriamycin and TRAIL-mediated cell death. During apoptosis, death receptors will bind to FADD to assemble a death-inducing signal complex (DISC) and the latter proceeds with the caspase effector cascades (O'Brien and Kirby, 2008).

Brown and co-worker (1999) have proposed two distinct mechanisms to elucidate the role of PrP^C in the cellular defense against oxidative stress, where PrP^C may act directly as a copper-dependent SOD or indirectly by up-regulating the activities of other antioxidant proteins that protect cells from oxidative stress. In present study, cyt-c is up-regulated by overexpression of PrP^C even before apoptosis induction. During pre- and post-exposure to doxorubicin, level of cyt-c in PrP^C-transfected LS 174T cells was significantly higher than untransfected LS 174T cells while its regulator the Bcl-2 family proteins, Bax, Bad, Bcl-2, and Bcl-x (Reed, 1997) were all in a relatively low expression in both untransfected LS 174T and PrP^C-transfected LS 174T cells. This finding is coherent with research by Carethers and Pham (2000) who have demonstrated LS 174T cells possesses only mutant Bax alleles, while Yap and Say (2012) reported that LS 174T cells is Bax deficient. Roucou and co-workers (2005) have demonstrated PrP^C is very specific for Bax and it

inhibits Bax conformational change in human neuronal cells and MCF7 breast adenocarcinoma cell line. Therefore, it is likely that PrP^C exerts its anti-apoptotic property via Bax-independent mechanism and this happens via the overexpression of cyt-c.

Atlante and co-workers (2000) have proposed that in the early phase of neutotoxicity, cyt-c release can be a part of cellular and mitochondrial defense mechanism against oxidative stress. In addition, Huttemann and co-workers (2011) have reviewed the diverse role of cyt-c, apart from being involved in apoptotic cascades; it also serves as important radical scavenger. To further support this speculation, Yap and Say (2011) have demonstrated that overexpression of PrP^C in LS 174T cell exhibits antioxidant activity during H_2O_2-induced oxidative stress, however, blocking of PrP^C glycosylation impedes its ROS scavenging activity. In addition, Mehrpour and Codogno (2010) have suggested due to high affinity and number of Cu^{2+}-binding sites in PrP^C, it may act as an antioxidant via copper redox cycling by quenching the generated free radicals upon binding to the potentially harmful Cu^{2+} ions. Similarly, Gonzales-Iglesias and co-workers (2002) have demonstrated the formation of PrP^C-Cu^{2+} glycosaminoglycan (GAG) complex upon binding of PrP^C octapeptide repeat region to the GAGs and the His-bound Cu^{2+} may act as a cofactor for intermolecular recognition reactions which may be crucial entities in PrP^C metabolism. Altogether, these findings has alluded to the speculation that the function of cyt-c in LS 174T cell overexpressing PrP^C was not entirely involved in apoptosis but it possesses anti-oxidant effect and serves as radical scavenger.

Activation of intrinsic pathway will result in mitochondrial permeability and the release of pro-apoptotic molecules (Danial and Korsmeyer, 2004). In comparison of both LS 174T cells, the level of SMAC/Diablo was significantly lower in PrP^C-transfected LS 174T but the level of HtrA2/Omi was significantly higher in PrP^C-transfected LS 174T. SMAC/Diablo and HtrA2/Omi are pro-apoptotic proteins that promote caspase activation that are released from the mitochondrial intermembrane space into the cytosol upon apoptotic stimuli as a negative regulator of the IAPs (Kroemer el al., 2007). In the present study, the human apoptosis antibody array consisted a total of five IAPs probes, namely Survivin, Livin, cIAP-1, cIAP-2, and XIAP. The level of Survivin, XIAP, and cIAP-1 were all significantly higher in PrP^C-transfected LS 174T as compared to untransfected LS 174T. However, the level of Livin and cIAP-2 were in a relatively low expression in both untransfected LS 174T and PrP^C-transfected LS 174T upon exposure to doxorubicin. Interestingly, despite expressing a higher level of pro-apoptotic factor such as HtrA2/Omi, LS 174T overexpressing PrP^C showed almost null expression of cleaved caspase-3. Noteworthy, the level of Survivin, XIAP and cIAP-1 in PrP^C-transfected LS 174T are remarkably high upon exposure to doxorubicin. Yang and co-workers (2004) have demonstrated that mutant cIAP-1 is resistant to Omi cleavage and Survivin was resistant to wild-type Omi cleavage even in the excessive amounts of wild-type Omi. Hence, it is speculated that HtrA2/Omi antagonized cIAP-2 and Livin, but it did not antagonize Survivin, XIAP, and cIAP-1.

Dohi and co-workers (2004) have demonstrated that Survivin and XIAP form a heterocomplex to promote cell survival against proteasomal

destruction and synergistically antagonizing apoptosome-mediated cell death in response to staurosporine treatment using MCF7 human breast adenocarcinoma cell line. In addition, Helgan and co-workers (2013) have exhibited that double knockdown of Survivin and and XIAP resulted in an enhanced apoptotic fraction in HCT-15, SW48, and SW480 colorectal adenocarcinoma cell lines upon radiation. In the present study, up-regulation of PrP^C in LS 174T cells did not overexpress XIAP protein, but when exposed to doxorubicin, XIAP was remarkably up-regulated. Upon exposure to doxorubicin, LS 174T cells overexpressing PrP^C remained refractory to apoptosis. Therefore, this finding is strong enough to substantiate Survivin, XIAP, and cIAP-1 could be the key proteins conferring to apoptosis resistance in doxorubicin treated colorectal cancer cells.

In p53-dependent modulation, doxorubicin acts by intercalating DNA and inhibiting topoisomerase II activity that leads to DNA damage and p53 activation (Gewirtz el al., 2000). In the present study, p53 was phosphorylated at serine-15 in untransfected LS 174T cells upon doxorubicin treatment. Downstream effector of p53 namely, p21/CIP1/CDKN1A and p27/KIP1 (Gartel and Tyner, 2002) showed significantly higher level of protein expression for untransfected LS 174T cells as compared to PrP^C-transfected LS 174T. Expression of p53 (S15), p21/CIP1/CDKN1A, and p27/KIP1 was almost null in PrP^C-transfected LS 174T cells. Evidently, Weiss and co-workers (2010) have demonstrated the overexpression of PrP^C in SH-SY5Y human neuroblastoma cell line disturbed cellular homeostasis, but does not alter p53 protein expression. Furthermore, Yu and colleagues (2012) have demonstrated the effect of PrP^C on doxorubicin-induced cytotoxicity in human

breast cancer cells was independent of p53 but it involved the ERK1/2 pathway. Therefore, there is a high possibility that cell death in LS 174T overexpressing PrP^C is not mediated by p53-dependent pathway.

Dysfunction of any of the several interconnected cellular pathways is sufficient to drive oxidative stress in the brain including impaired mitochondrial function, increased oxidative damage, excitotoxicity, and inflammation (Halliwell, 2006). HMOX is a rate-limiting enzyme responsible for the degradation of heme in the endoplasmic reticulum to generate an equimolar amount of biliverdin, free iron, and carbon monoxide (Tenhunen et al., 1969). HO-1/HMOX1/HSP32 and HO-2/HMOX2 possess anti-apoptotic effect through the heme catabolism into the gas carbon monoxide (Soares et al, 2002). In the present study, even before exposure to doxorubicin, the level of HO-2/HMOX2 in PrP^C-transfected LS 174T cells was significantly higher as compared to untransfected LS 174T cells. However, post-exposure to doxorubicin, the level of HO-2/HMOX2 in PrP^C-transfected LS 174T cells was significantly lower as compared to untransfected LS 174T cells. The result pre-and post-doxorubicin exposure of this protein does not tally; therefore it is not valid for discussion in this case.

HIF1-α is the major transcription factor that has been shown to promote tumor survival under hypoxia but also trigger apoptosis (Kilic et al., 2007). Liang and co-workers (2007b) have reported that PrP^C was up-regulated in MKN-28 human gastric cancer cell line upon induction of hypoxia, but HIF-1 does not appear to play a role in the induction of PrP^C under chronic hypoxia as no recognizable HIF-1 binding motif is present in

the sequence of PrP^C promoter. In contrast, Jeong and co-workers (2012) have demonstrated HIF-1α exerted its protective role on SH-SY5Y human neuroblastoma cell line upon up-regulation of PrP^C by hypoxia induction. However, in the present study, there was no significant difference in HIF1-α level between untransfected LS 174T cells and PrP^C-transfected LS 174T cells. Therefore, the protective effect of HIF1-α in cancer cell could be cell-type specific.

5.9 Concluding Remarks and Future Studies

In this study, overexpression of PrP^C in LS 174T cells has promoted cell proliferation, migration, invasion, adhesion, resistant to anoikis, survival in anchorage-independent growth, and resistance to doxorubicin. Overexpression of PrP^C in HEK-293 cells does not affect the biological role in term of cell proliferation, invasion, migration, adhesion, and cell cytotoxicity towards chemotherapeutic drugs. Understanding the key protein PrP^C associated with prion diseases in cancer is essential to shed new light in chemotherapeutic drugs development. Survivin and XIAP are considered to be a promising factor for a molecular targeted tumor therapy that is currently tested in clinical trials (Miura et al., 2011; Wong, 2011; Rodel et al., 2012). Natural IAPs namely Survivin, XIAP and cIAP-1 may be the answer to the puzzling role of PrP^C that could promote cell proliferation, migration, invasion, adhesion, MDR activities, and cell resistant to apoptosis in colorectal cancer cells.

In future study, further analyzes can be performed to make the study more comprehensive. Halogenated nucleotides for instance the pyrimidine analog bromodeoxyuridine (BrdU) are essential target for labeling nascent DNA in living cells, therefore BrdU incorporation assay can be performed to confirm increased cell proliferation by overexpression of PrP^C. To better reflect the understanding on cell invasiveness due to overexpression of PrP^C, EMT markers such as vimentin and E-cadherin can be examined. Furthermore, cell cycle analysis can be performed to examine if there is any change of cell cycle phase in cells overexpressing PrP^C under chemotherapeutic drugs treatment. Beside chemo-resistance, cells resistant to immuno-cytokine killing also provide additional information about PrP-mediated oncogenic effects.

As PrP^C overexpression has been implicated to be involved in the colorectal cancer cell resistance to apoptosis, which leads to cancer progression, the possibility of using PrP^C as a tumor biomarker to monitor cancer progression and grading of colorectal cancer could be examined. Investigation of the role of PrP^C is desirable to be extended to *in vivo* model since the development *in vivo* will greatly assist in deciphering the molecular mechanisms of the role ascribed to PrP^C, and how it may be subverted in cancer development. Noteworthy, functional roles of PrP^C are absolutely valuable when it comes to tissue transplantation. Since overexpression of PrP^C could promote cell survival in both anchorage-dependent and anchorage-independent manner, therefore this concept could be applied to xenograft transplantation in nude mice in future experiments.

CHAPTER 6

CONCLUSIONS

In summary, this study has demonstrated the overexpression of PrP^C in LS 174T cells promoted cell survival and resistance to apoptosis. Overexpression of PrP^C in LS 174T cells has shown to increase cell proliferation in both anchorage-dependent and anchorage-independent manner. While LS 174T cells remained resistant to anoikis, however, overexpression of PrP^C further exacerbated the phenomenon. Furthermore, overexpression of PrP^C in LS 174T has increased the cell attachment to fibronectin and collagen. Hence, this has facilitated the cellular adhesion to the ECM glycoproteins.

In the aspect of cancer metastasis, overexpression of PrP^C has significantly enhanced the cell migration and invasion in LS 174T cells. Not only the cells have developed a greater motility in 2D manner, but also a stronger infiltration in 3D manner. Overexpression of PrP^C was found to mitigate doxorubicin-induced cell cytotoxicity in LS 174T cells. Since LS 174T is deficient in Bcl-2 proteins, it is speculated that PrP^C engages in other defensive mechanisms in conferring to apoptosis resistant. PrP^C exerts its protective effect through up-regulation of three IAPs, namely Survivin, XIAP, and cIAP-1 that inhibits the pro-apoptotic proteins. Therefore, LS 174T overexpressing PrP^C is less vulnerable to cessation of growth upon doxorubicin triggered apoptosis.

Base on the findings, the physiological role ascribed to PrP^C observed from this study has portrayed a close connection of PrP^C to colorectal cancer progression. A plausible strategy to cease cancer deterioration, not fully, but at least partially is by targeting the IAPs. Since overexpression of PrP^C simultaneously up-regulated IAPs, therefore targeting PrP^C or in combination with anti-IAPs in chemotherapeutic and drugs development could be a promising tool in attenuating colorectal cancer progression.

REFERENCES

Aguzzi, A. and Weissmann., 1997. Prions research: the next frontiers. *Nature*, 389(6653), pp. 795-798.

Aguzzi, A., Baumann, F. and Bremer, J., 2008. The prion's elusive reason for being. *Annual Review of Neuroscience*, 31, pp. 439-477.

Aguzzi, A. and Polymenidou, M., 2004. Mammalian prion biology: one century of evolving concepts, *Cell*, 116(2), pp. 313-327.

Atlante, A. et al., 2000. Cytochrome *c* is released from mitochondria in a reactive oxygen species (ROS)-dependent fashion and can operate as a ROS scavenger and as a respiratory substrate in cerebellar neurons undergoing excitotoxic death. *The Journal of Biological Chemistry*, 275(47), pp. 37159-37166.

Barmada, S., Piccardo, P., Yamaguchi, K., Ghetti, B. and Harris, D.A., 2004. GFP-tagged prion protein is correctly localized and functionally active in the brains of transgenic mice. *Neurobiology of Disease*, 16(3), pp. 527-537.

Barrallo-Gimero, a. and Nieto, M.A., 2005. The Snail Genes as inducers of cell movement and survival: implications in development and cancer. *Development*, 132(14), pp. 3151-3161.

Bendheim, P.E. et al., 1992. Nearly ubiquitous tissue distribution of the scrapie agent precursor protein. *Neurology*, 42(1), pp.149-156.

Beraldo, F.H. et al., 2011. Metabotropic glutamate receptors transduce signals for neurite outgrowth after binding of the prion protein to laminin gamma1 chain. *Federation of American Societies for Experimental Biology Journal*, 25(1), pp. 265-279.

Berx, G. and van Roy, F., 2009. Involvement of members of the cadherin superfamily in cancer. *Cold Spring Harbor Perspective in Biology*, doi: 10.1101/cshperspect.a003129.

Borchelt, D.R. et al., 1994. Rapid anterograde axonal transport of the cellular prion glycoprotein in the peripheral and central nervous systems. *The Journal of Biological Chemistry*, 269(20), pp. 14711-14714.

Borchelt, D.R., Scott, M., Taraboulous, A., Stahl, N. and Prusiner, S.B., 1990. Scrapie and cellular prion proteins differ in their kinetics of synthesis and topology in cultured cells. *The Journal of Cell* Biology, 110(3), pp. 743-752.

Brown, D.R. et al., 1999a. Normal prion protein has an activity like that of superoxide dismutase. *The Biochemical Journal*, 344, pp. 1-5.

Brown, D.R., Schulz-Schaeffer, W.J., Schmidt, B. and Kretzschmar, H.A., 1997a. Prion protein-deficient cells show altered response to oxidative stress due to decreased SOD-1 activity. *Experimental Neurology*, 146(1), pp. 104-112.

Brown, D.R. et al., 1997b. The cellular prion protein binds copper *in vivo*. *Nature*, 390(6661), pp. 684-687.

Brown, K.L. et al., 1999b. Scrapie replication in lymphoid tissues depends on prion protein-expressing follicular dendritic cells. *Nature Medicine*, 5(11), pp. 1308-1312.

Brown, D.R., Clive, C. and Haswell, S.J., 2001. Antioxidant activity related to copper binding of native prion protein. *Journal of Neurochemistry*, 76(1), pp. 69-76.

Brown, D.R., Nicholas, R.S. and Canevari, L., 2002. Lack of prion protein expression results in a neuronal phenotype sensitive to stress. *Journal of Neuroscience Research*, 67(2), pp. 211-224.

Cairns, J., 1975. Mutation selection and the natural history of cancer. *Nature*, 255(5505), pp. 187-200.

Carethers, J.M. and Pham, T.T., 2000. Mutations of transforming growth factor beta 1 type II receptor, BAX, and insulin-like growth factor II receptor genes in microsatellite unstable cell lines. *In Vivo*, 14(1), pp. 13-20.

Caughey, B., Brown, K., Rayman, G.J., Katzenstein, G.E. and Thresher, W., 1994. Binding of the protease-sensitive form of PrP (prion protein) to sulfated glycosaminoglycan and Congo red. *Journal of Virology*, 68(4), pp. 2135-2141.

Caughey, B., Race, R.E. and Chesebro, B., 1988. Detection of prion protein mRNA in normal and scrapie-infected tissues and cell lines. *The Journal of General Virology*, 69, pp. 711-716.

Caughey, B., Race, R.E., Ernst, D., Buchmeier, M.J. Chesebro, B., 1989. Prion protein biosynthesis in scrapie-infected and uninfected neuroblastoma cells. *Journal of Virology*, 63(1), pp. 175-181.

Cavallaro, U., and Christofori, G., 2004. Cell adhesion and signaling by cadherins and Ig-CAMs in cancer. *Nature Reviews. Cancer*, 4(2), pp. 118-132.

Chakrabarti, O., Ashok, A. and Hegde, R.S., 2009. Prion protein biosynthesis and its emerging role in neurodegeneration. *Trends in Biochemical Sciences*, 34(6), pp. 287-295.

Chen, H.C., 2005. Cell-scatter assay. *Methods in Molecular Biology*, 294, pp. 69-77.

Chen, S., Mange, A., Dong, L., LehMann, S. and Schachner, M., 2003. Prion protein as trans-interacting partner for neurons is involved in neurite outgrowth and neuronal survival. *Molecular and Cellular Neurosciences*, 22(2), pp. 227-233.

Chiarugi, P. and Giannoni, E., 2008. Anoikis: a necessary death program for anchorage-dependent cells. *Biochemical Pharmacology*, 76(11), pp. 1352-1364.

Choi, C.J. et al., 2007. Normal cellular prion protein protects against manganese-induced oxidative stress and apoptotic cell death. *Toxicological Sciences*, 98(2), pp. 495-509.

Collinge, J. et al., 1994. Prion protein is necessary for normal synaptic function. *Nature*, 370(6487), pp. 295-297.

Comincini, S. et al., 2007. Diagnostic value of *PRND* gene expression profiles in astrocytomas: Relationship to tumor grades of malignancy. *Oncology Reports*, 17(5), pp. 989–996.

Criado, J.R. et al., 2005. Mice devoid of prion protein have cognitive deficits that are rescued by reconstitution of PrP in neurons. *Neurobiology of Disease*, 19(1-2), pp. 255-265.

Danial, N.N. and Korsmeyer S.J., 2004. Cell death: critical control points. *Cell*, 116(2), pp. 205-219.

DeNardo, D.G., Andreu, P. and Coussens, L.M., 2010. Interactions between lymphocytes and myeloid cells regulate pro-versus anti-tumor immunity. *Cancer Metastasis Reviews*, 29(2), pp. 309-316.

Di Felice, V., David, S., Cappello, F., Farina, F. and Zummo, G., 2005. Is chlamydial heat shock protein 60 a risk factor for oncogenesis? *Cellular and Molecular Life* Sciences, 62(1), pp. 4–9.

Diarra-Mehrpour, M. et al., 2004. Prion protein prevents human breast carcinoma cell line from tumor necrosis factor alpha-induced cell death. *Cancer Research*, 64(2), pp. 719-727.

Didier, A. et al., 2006. Cellular prion protein in the bovine mammary gland is selectively expressed in active lactocytes. *Journal of Histochemistry and Cytochemistry*, 54(11), pp. 1255–1261.

Dodelet, V.C. and Cashman, N. R., 1998. Prion protein expression in human leukocyte differentiation. *Blood*, 91(5), pp. 1556-1561.

Dohi, T. et al., 2004. An IAP-IAP complex inhibits apoptosis. *The Journal of Biological Chemistry*, 279(33), pp. 34087-34090.

Du, J. et al., 2005. Overexpression and significance of prion protein in gastric cancer and multidrug-resistant gastric carcinoma cell line SGC7901/ADR. *International Journal of Cancer*, 113(2), pp. 213-220.

Eccles, S.A. and Welch, D.R., 2007. Metastasis: recent discoveries and novel treatment strategies. *Lancet*, 369(9574), pp. 1742-1757.

El-Moselhy, M.A.M. and El-Sheikh, A.A.K., 2014. Protective mechanisms of atorvastatin in ameliorating doxorubicin-induced hepato-renal toxicity. *Biomedicine and Pharmacotherapy*, 68(1), pp. 101-110.

Faried, A. et al., 2004. Expression of heat- shock protein Hsp60 correlated with the apoptotic index and patient prognosis in human esophageal squamous cell carcinoma. *European Journal of Cancer*, 40(18), pp. 2804–2811.

Fidler, I.J., 2003. The pathogenesis of cancer metastasis: the "seed and soil" hypothesis revisited. *Nature Reviews. Cancer*, 3(6), pp. 453-458.

Ford, M.J. et al., 2002. A marked disparity between the expression of prion protein and its message by neurons of the CNS. *Neuroscience*, 111(3), pp. 533-551.

Fornari, F.A., Randolph, J.K., Yalowich, J.C., Ritke, M.K. and Gewirtz, D.A., 1994. Interference by doxorubicin with DNA unwinding in MCF-7 breast tumor cells. *Molecular Pharmacology*, 45(4), pp. 649-656.

Fukazawa, H., Mizuno, S. and Uehara, Y., 1995. A microplate assay for quantitation of anchorage-independent growth of transformed cells. *Analytical Biochemistry*, 228(1), pp. 83-90.

Gartel, A.L. and Tyner, A.L., 2002. The role of cyclin-dependent kinase inhibitor p21 in apoptosis. *Molecular Cancer Therapeutics*, 1(8), pp. 639-649.

Gewirtz, D.A., Sundaram, S. and Magnet, K.J., 2000. Influence of topoisomerase II inhibitors and ionizing radiation on growth arrest and cell death pathways in the breast tumor cell. *Cell Biochemistry and Biophysics*, 33(1), pp. 19–31.

Gibbs, C.J and Asher, D.M., 1996. Subacute spongiform unconventional virus encephalopathies. In: Baron, S. (4th eds.). Medical Microbiology. Galveston (TX): University of Texas Medial Branch at Galveston, Chapter 71.

Gonzalez-Iglesias, R. et al., 2002. Prion protein interaction with glycosaminoglycan occurs with the formation of oligomeric complexes stabilized by Cu(II) bridges. *Journal of Molecular Biology,* 319(2), pp. 527-540.

Gorodinsky, A. and Harris, D.A., 1995. Glycolipid-anchored proteins in neuroblastoma cells form detergent- resistant complexes without caveolin. *The Journal of Cell Biology*, 129(3), pp. 619–627.

Graner, E. et al., 2000. Cellular prion protein binds laminin and mediates neuritogenesis. *Brain Research. Molecular Brain Research*, 76(1), pp. 85-92.

Grivennikov, S.I., Greten, F.R. and Karin, M., 2010. Immunity, inflammation, and cancer. *Cell*, 140(6), pp. 883-899.

Halliwell, B., 2006. Oxidative stress and neurodegeneration: Where are we now? *Journal of Neurochemistry*, 97(6), pp. 1634-1658.

Hanahan, D. and Weinberg, R.A., 2000. The hallmarks of cancer. *Cell*, 100(1), pp. 56-70.

Hanahan, D. and Weinberg, R.A., 2011. Hallmarks of cancer: The next generation. *Cell*, 144(5), pp. 646-674.

Harris, D.A., 1999. Cellular biology of prion diseases. *Clinical Microbiology Reviews*, 12(3), pp. 429-444.

Harris, D.A., 2001. Biosynthesis and cellular processing of the prion protein. *Advances in Protein Chemistry*, 57, pp. 203-228.

Harris, D.A., Lele, P. and Snider, W.D., 1993. Localization of the mRNA for a chicken prion protein by in situ hybridization. *Proceedings of the National Academy of Sciences of the United States of America*, 90(9), pp. 4309-4313.

Hebert, D.N. and Molinari, M, 2007. In and out of the ER: protein folding, quality control, degradation, and related human diseases. *Physiological Reviews*, 83(4), pp. 1377-1408.

Hehlgans, S. et al., 2013. Double targeting of surviving and XIAP radiosensitizes 3D grown human colorectal tumor cells and decreases migration. *Radiotherapy and Oncology*, 108(1), pp.32-39.

Hernandez. J.M. et al., 2011. Expression of the antiapoptotic protein survivin in colon cancer. *Clinical Colorectal Cancer,* 10(3), pp. 188-193.

Hotchkiss, R.S. and Nicholson, D.W., 2006. Apoptosis and caspases regulate death and inflammation in sepsis. *Nature Reviews Immunology*, 6, pp. 813-822.

Hu, W. et al., 2008. Prion Protein: physiological functions and role in neurological disorders. *Journal of the Neurological* Sciences, 264(1-2), pp. 1-8.

Humphries, M.J., 2009. Cell adhesion assays. *Methods in Molecular Biology*, 522, pp. 203-210.

Huttemann, M. et al., 2011. The multiple functions of cytochrome c and their regulation in life and death decisions of the mammalian cell: From respiration to apoptosis. *Mitochondrion*, 11(3), pp. 369-381.

Hutter, G., Heppner, F.L. Aguzzi, A., 2003. No superoxide dismutase activity of cellular prion protein *in vivo*. *Biological Chemistry*, 384(9), pp. 1279-1285.

Jackson, G.S. et al., 2001. Location and properties of metal-binding sites on the human prion protein. *Proceedings of the National Academy of Sciences of the United States of America*, 98(15), pp. 8531-8535.

Jeffrey, M. et al., 2000. Synapse loss associated with abnormal PrP precedes neuronal degeneration in the scrapie-infected murine hippocampus. *Neuropathology and Applied Neurobiology*, 26(1), pp.41-54.

Jemal, A. et al., 2011. Global cancer statistics. *CA: A Cancer Journal for Clinicians*, 61(2), pp. 69-90.

Jeong, J.K. et al., 2012. Hypoxia-inducible factor-1 alpha regulates prion protein expression to protect against neuron cell damage. *Neurobiology of Aging*, 33(5), pp. 1006.

Jie, J., Wang, J., Qu, J and Hung, T., 2006. Effects of adenoviral-mediated gene transduction of NK4 on proliferation, movement, and invasion of human colonic LS174T cancer cells *in vitro*, *World Journal of Gastroenterology*, 12(25), pp. 3983-3988.

Jones, S. et al., 2005. Recombinant prion protein does not possess SOD-1 activity. *The Biochemical Journal*, 392(2), pp. 309-312.

Kanaani, J., Prusiner, S.B., Diacovo, J., Baekkeskov, S. and Legname, G., 2005. Recombinant prion protein induces rapid polarization and development of synapses in embryonic rat hippocampal neurons *in vitro*. *Journal of Neurochemistry*, 95(5), pp. 1373-1386.

Karnoub, A.E. and Weinberg, R.A., 2006-2007. Chemokine networks and breast cancer metastasis. *Breast Disease*, 26, pp. 75-85.

Karp, G., 2008. *Cell and molecular biology: Concepts and experiments*, 5th ed. New Jersey: John Wiley and Sons, pp. 653-657.

Kikuchi, Y. et al., 2002. G_1-Depdendent prion protein expression in human glioblastoma cell line T98G, *Biological and Pharmaceutical Bulletin*, 25(6), pp. 728-733.

Kilic, M., Kasperczyk, H., Fulda, S. and Debatin, K-M., 2007. Role of hypoxia inducible factor-1 alpha in modulation of apoptosis resistance. *Oncogene*, 26(14), pp. 2027-2038.

Kim, B.H. et al., 2004. The cellular prion protein (PrP^C) prevents apoptotic neuronal cell death and mitochondrial dysfunction induced by serum deprivation. *Molecular Brain Research*, 124(1), pp, 40-50.

Kim, P.J., Plescia, J., Clevers, H., Fearon, E.R. and Altieri, D.C., 2003. Survivin and molecular pathogenesis of colorectal cancer. *Lancet*, 362(9379), pp. 205-209.

Kim, R., Emi, M. and Tanabe, K., 2007. Cancer immunoediting from immune surveillance to immune escape. *Immunology*, 121(1), pp. 1-14.

Kirchhoff, S.R., Gupta, S. and Knowlton, A.A., 2002. Cytosolic heat shock protein 60, apoptosis, and myocardial injury. *Circulation*, 105(24), pp. 2899–2904.

Klamt, F. et al., 2001. Imbalance of antioxidant defense in mice lacking cellular prion protein. *Free Radical Biology and Medicine*, 30(10), pp. 1137-1144.

Klymkowsky, M.W. and Savagner, P., 2009. Epithelial-mesenchymal transition: a cancer researcher's conceptual friend and foe. *The American Journal of Pathology*, 174(5), pp. 1588-1593.

Korga, A. et al., 2012. The redox imbalance and the reduction of contractile protein content in rat hearts administered with L-thyroxine and doxorubicin. *Oxidative Medicine and Cellular Longevity*, doi: 10.1155/2012/681367.

Kramer, M.L. et al., 2001. Prion protein binds copper within the physiological concentration range. *The Journal of Biological Chemistry*, 37(20), pp. 7185-7193.

Kramer, N. et al., 2013. *In vitro* cell migration and invasion assays. *Mutation Research*, 752(1), pp. 10-24.

Kroemer, G. et al., 2009. Classification of cell death: recommendations of the Nomenclature Committee on Cell Death 2009. *Cell Death and Differentiation*, 16(1), pp. 3-11.

Kroemer, G., Galluzzi, L. and Brenner, C., 2007. Mitochondrial membrane permeabilisation in cell death. *Physiological Reviews*, 87(1), pp. 99-163.

Kucik, D.F. and Wu, C., 2005. Cell-Adhesion Assays. *Methods in Molecular Biology*, 294, pp. 43-54.

Kuwahara, C. et al., 1999. Prions prevent neuronal cell-line death. *Nature,* 400(6741), pp. 225-226.

LaCasse, E.C. et al., 2008. IAP-targeted therapies for cancer. *Oncogene*, 27(48), pp. 6252-6275.

Laine, J., Marc, M.E., Sy, M.S. and Acelrad, H., 2001. Cellular and subcellular morphological localization of normal prion protein in rodent cerebellum. *The European Journal of Neuroscience*, 14(1), pp. 47-56.

Lauffenburger, D.A. and Horwitz, A.F., 1996. Cell migration: a physically integrated molecular process. *Cell*, 84(3), pp. 359-369.

Le Pichon, C.E. et al., 2009. Olfactory behavior and physiology are disrupted in prion protein knockout mice. *Nature Neuroscience*, 12(1), pp. 60-69.

Leclerc, E. et al., 2003. Conformation of PrP(C) on the cell surface as probed by antibodies. *Journal of Molecular Biology*, 326(2), pp. 475-483.

Lee, Y.J. and Shacter, E., 1999. Oxidative stress inhibits apoptosis in human lymphoma cells. *The Journal of Biological Chemistry*, 274(28), pp. 19792-19798.

Lee, Y.J. and Shacter, E., 2000. Hydrogen peroxide inhibits activation, not activity, of cellular caspase-3 *in vivo*. *Free Radical Biology and Medicine*, 29(7), pp. 684-692.

Lehmann, S., Milhavet, O., and Mangé, A., 1999. Trafficking of the cellular isoform of the prion protein. *Biomedicine & Pharmacotherapy*, 53(1), pp. 39-46.

Li, C. et al., 2007. Normal cellular prion protein is a ligand of selectins: binding requires Le(X) but is inhibited by sLe(X). *The Biochemical Journal*, 406(2), pp. 333-341.

Li, C. et al., 2009. Binding of pro-prion to filamin A disrupts cytoskeleton and correlates with poor prognosis in pancreatic cancer. *The Journal of Clinical Investigation*, 119(9), pp. 2725-2736.

Li, C. et al., 2010. Pro-prion binds filamin A, facilitating its interaction with integrin beta1, and contributes to melanomagenesis. *The Journal of Biological Chemistry*, 285(39), pp. 30328-30339.

Li, Q.Q. et al., 2011. Cellular prion protein promotes glucose uptake through the Fyn-HIF-2α-Glut1 pathway to support colorectal cancer cell survival. *Cancer Science*, 102(2), pp. 400-406.

Liang, J. et al., 2007a. Cellular prion protein promotes proliferation and G1/S transition of human gastric cancer cells SGC7901 and AGS. *Federation of American Societies for Experimental Biology Journal*, 21(9), pp. 2247-2256.

Liang, J. et al., 2007b. Hypoxia induced overexpression of PrP^C in gastric cancer cell lines. *Cancer Biology and Therapy*, 6(5), pp. 769-774.

Liang, J. et al., 2009a. Function of PrP^C (1-OPRD) in biological activities of gastric cancer cell lines. *Journal of Cellular and Molecular Medicine*, 13(11-12), pp. 4453-4464.

Liang, J. et al., 2009b. Inhibition of PI3K/Akt partially leads to the inhibition of PrP^C-induced drug resistance in gastric cancer cells. *The Federation of European Biochemical Societies Journal*, 276(1), pp. 685-694.

Lichtenberg, G., Nowak, C., Gleier, K., Meckert, C. and Richter-Reichhelm, H.B., 1995. Anchorage independent colony growth of fetal hamster lung epithelial cells after treatment with diepoxybutane. *Toxicology Letters*, 75(1-3), pp. 193-199.

Linden, R. et al., 2008. Physiology of the prion protein. *Physiological Reviews*, 88(2), pp. 673-728.

Loubet, D. et al., 2012. Neuritogenesis: the prion protein controls beta1 integrin signaling activity. *FASEB Journal*, 26(2), pp. 678-690.

Majno, G. and Joris, I., 1995. Apoptosis, oncosis, and necrosis. An overview of cell death. *The American Journal of Pathology*, 146(1), pp. 3-15.

Makrinou, E., Collinge, J. and Antoniou, M., 2002. Genomic characterization of the human prion protein (PrP) gene locus. *Mammalian Genome: Official Journal of The International Mammalian Genome Society*, 13(12), pp. 696-703.

Malaga-Trillo, E. et al., 2009. Regulation of embryonic cell adhesion by the prion protein. *PLoS Biology*, 7(3), pp. 576-590.

Mange, A., Milhavet, O., Umlauf, D., Harris, D. Lehmann, S., 2002. PrP-dependent cell adhesion in N2a neuroblastoma cells. *The Federation of European Biochemical Societies Letters*, 514(2-3), pp. 159-162.

Manson, J. et al., 1992. The prion protein gene: a role in mouse embryogenesis? *Development*, 115(1), pp. 117-122.

Martin-Lanneree, S. et al., 2014. PrP^{C} from stem cells to cancer. *Frontiers in Cell and Development Biology*, 2(55), pp. 1-7.

Martin, S.S. and Leder, P., 2001. Human MCF10A mammary epithelial cells undergo apoptosis following actin depolymerization that is dependent of attachment and rescued by Bcl-2. *Molecular and Cellular Biology*, 21(19), pp. 6529-6536.

Martins, V.R., Mercadante, A.F., Cabral, A.L., Freitas, A.R. and Castro, R.M., 2001. Insights into the physiological function of cellular prion protein. *Brazilian Journal of Medical and Biological Research*, 34(5), pp. 585-595.

Masoudi-Nejad, A. et al., 2014. Cancer systems biology and modeling: Microscopic scale and multiscale approaches. *Seminars in Cancer Biology*, doi: 10.1016/j.semcancer.2014.03.003.

Masters, C.L. and Richardson, E.P. Jr., 1978. Subacute spongiform encephalopathy Creutzfeldt-Jakob disease- the nature and progression of spongiform change. *Brain: A Journal of Neurology*, 101(2), pp. 333-344.

Matsuyoshi, S., Shimada, K., Nakamura, M., Ishida, E. and Konishi, N., 2006. FADD phosphorylation is critical for cell cycle regulation in breast cancer cells. *British Journal of Cancer*, 94(4), pp. 532-539.

McEwan, J.F., Windsor, M.L. and Cullis-Hill, S.D., 2009. Antibodies to prion protein inhibit human colon cancer cell growth. *Tumor Biology: The Journal of The International Society for Oncodevelopmental Biology and Medicine*, 30(3), pp. 141-147.

McLennan, N.F. et al., 2004. Prion protein accumulation and neuroprotection in hypoxic brain damage. *The American Journal of Pathology*, 165(1), pp. 227-237.

Mehrpour, M. and Codogno, P., 2010. Prion protein: From physiology to cancer biology. *Cancer Letters*, 290(1), pp. 1-23.

Meslin, F. et al., 2007a. Silencing of prion protein sensitizes breast adriamycin-resistance carcinoma cells to TRAIL-mediated cell death. *Cancer Research*, 67(22), pp. 10910-10919.

Meslin, F. et al., 2007b. Efficacy of adjuvant chemotherapy according to prion protein expression in patients with estrogen receptor-negative breast cancer. *Annals of Oncology*, 18(11), pp.1793–1798.

Mironov, A.Jr. et al., 2003. Cytosolic prion protein in neurons. *The Journal of Neuroscience*, 23(18), pp. 7183-7193.

Miura, K. et al., 2011. Inhibitor of apoptosis protein family as diagnostic markers and therapeutic targets of colorectal cancer. *Surgery Today*, 41(2), pp. 175–182.

Momparler, R.L., Karon, M., Siegel, S.E. and Avila, F., 1976. Effect of adriamycin on DNA, RNA, and protein synthesis in cell-free systems and intact cells. *Cancer Research*, 36(8), pp. 2891-2895.

Moya, K.L. et al., 2000. Immunolocalization of the cellular prion protein in normal brain. *Microscopy Research and Technique*, 50(1), pp. 58-65.

Moya, K.L., Hassig, R., Creminon, C., Laffont, I., Di Giamberardino, L., 2004. Enhanced detection and retrograde axonal transport of PrP^{C} in peripheral nerve. *Journal of Neurochemistry*, 88(1), pp. 155-160.

Naslavsky, N., Stein, R., Yanai, A., Friedlander, G. and Taraboulos, A., 1996. Characterization of detergent-insoluble complexes containing the cellular prion protein and its scrapie isoform. *The Journal of Biological Chemistry*, 272(10), pp. 6324– 6331.

Negrini, S., Gorgoulis, V.G., and Halazonetis, T.D., 2010. Genomic instability- an evolving hallmark of cancer. *Nature Reviews. Molecular Cell Biology*, 11(3), pp. 220-228.

O'brien, M.A. and Kirby, R., 2008. Apoptosis: A review of pro-apoptotic and anti apoptotic pathway and dysregulation in diseases. *Journal of Veterinary Emergency and Critical Care*, 18(6), pp. 572-585.

O'Donovan, C.N., Tobin, D. and Cotter, T.G., 2001. Prion protein fragment PrP (106-126) induces apoptosis via mitochondrial disruption in human SH-SY5Y cells. *The Journal of Biological Chemistry*, 276(47), pp. 43516-43523.

Pan, K.M. et al., 1993. Conversion of alpha-helices into beta-sheets features in the formation of the scrapie prion proteins. *Proceedings of the National Academy of Sciences of the United States of America*, 90(23), pp. 10962-10966.

Pan, Y. et al., 2006. Cellular prion protein promotes invasion and metastasis of gastric cancer, *Federation of American Societies for Experimental Biology Journal*, 20(11), pp. 1886-1888.

Pantera, B. et al., 2009. PrP^{C} activation induces neurite outgrowth and differentiation in PC12 cells: role for caveolin-1 in the signal transduction pathway. *Journal of Neurochemistry*, 110(1), pp. 194-207.

Paoli, P., Giannoni, E. and Chiarugi, P., 2013. Anoikis molecular pathways and its role in cancer progression. *Biochimica et Biophysica Acta*, 1833(12), pp. 3481-3498.

Park, J., Kanayama, A., Yamamoto, K. and Miyamoto Y., 2012. ARD1 binding to RIP1 mediates doxorubicin-induced NF-kappaB activation. *Biochemical and Biophysical Research Communications*, 422(2), pp. 291-297.

Peralta, O.A., Huckle, W.R. and Eyestone, W.H., 2011. Expression and knockdown of cellular prion protein (PrPC) in differentiating mouse embryonic stem cells. *Differentiation, Research in Biological Diversity*, 81(1), pp. 68-77.

Pinkas, J., Martin, S.S. and Leder, P., 2004. Bcl-2-mediated cell survival promotes metastasis of EpG4 βMEKDD mammary epithelial cells. *Molecular Cancer Research*, 2(10), pp. 551-556.

Polyak, K. and Weinberg, R.A., 2009. Transitions between epithelial and mesenchymal states: acquisition of malignant and stem cell traits. *Nature Reviews. Cancer*, 9(4), pp. 265-273.

Premzl, M. et al., 2003. Shadoo, a new protein highly conserved from fish to mammals and with similarity to prion protein. *Gene*, 314(1), pp. 89–102.

Proskuryakov, Y. and Gabai, V.L., 2010. Mechanisms of tumor cell necrosis. *Current Pharmaceutical Design*, 16(1), pp. 56-58.

Prusiner, S.B., Scott, M.R., DeArmond, S.J. and Cohen, F.E., 1998. Prion protein biology, *Cell*, 93(3), pp. 337-348.

Qian, B.Z. and Pollard, J.W., 2010. Macrophage diversity enhances tumor progression and metastasis. *Cell*, 141(1), pp. 39-51.

Qin, K., Zhao, L., Ash, R.D., McDonough, W.F. and Zhao, R.Y., 2009. ATM-mediated transcriptional elevation of prion in response to copper-induced oxidative stress. *The Journal of Biological Chemistry*, 284(7), pp. 4582-4593.

Rae, T.D., Schmidt, P.J., Pufahl, R.A., Culotta, V.C. and O'Halloran, T.V., 1999. Undetectable intracellular free copper: the requirement of a copper chaperone for superoxide dismutase. *Science*, 284(5415), pp. 805-808.

Rapoport, T.A., 2007. Protein translocation across the eukaryotic endoplasmic reticulum and bacterial plasma membranes. *Nature*, 450(7170), pp. 663-669.

Ray, M.R. and Jablons, D.M., 2010. Hallmarks of Metastasis. *Lung Cancer Metastasis*, New York: Springer, pp. 29-46.

Reed, J.C., 1997. Bcl-2 family proteins: Regulator of apoptosis and chemoresistance in haematologic malignancies. *Seminars in Hematology*, 34 (4-5), pp. 9-19.

Rieger, R., Edenhofer, F., Lasmezas, C.I. and Weiss, S., 1997. The human 37-kDa laminin receptor precursor interacts with the prion protein in eukaryotic cells. *Nature Medicine*, 3(12), pp. 1383-1388.

Rodel, F. et al., 2012. Survivin as a prognostic/predictive marker and molecular target in cancer therapy. *Current Medicinal Chemistry*, 19(22), pp. 3679–3688.

Rodriguez, L.G., Wu, X. and Guan, J., 2005. Wound-healing assay. *Methods in Molecular Biology*, 294, pp. 23-29.

Roucou, X. and LeBlanc, A.C., 2005. Cellular prion protein neuroprotective function: implications in prion diseases, *Journal of Molecular Medicine, 83*(1), pp. 3-11.

Roucou, X. et al., 2005. Cellular prion protein inhibits proapoptotic Bax conformational change in human neurons and in breast carcinoma MCF-7 cells. *Cell Death and Differentiation*, 12(7), 783-795.

Sakurai-Yamashita, Y. et al., 2005. Female-specific neuroprotection against transient brain ischemia observed in mice devoid of prion protein is abolished by ectopic expression of prion protein-like protein. *Neuroscience*, 136(1), pp. 281-287.

Sales, N. et al., 2002. Developmental expression of the cellular prion protein in elongating axons. *The European Journal of Neuroscience*, 15(7), pp. 1163-1177.

Salk, J.J., Fox, E.J. and Loeb, L.A., 2010. Mutational heterogeneity in human cancers: origin and consequences. *Annual Review of Pathology*, 5, pp. 51-75.

Samali, A., Cai, J., Zhivotovsky, B., Jones, D.P. and Orrenius, S., 1999. Presence of a pre-apoptotic complex of pro-caspase-3, Hsp60 and Hsp10 in the mitochondrial fraction of jurkat cells. *The European Molecular Biology Organization Journal,* 18(8), pp. 2040–2048.

Santuccione, A., Sytnyk, V., Leshchyns'ka, I. and Schachner, M., 2005. Prion protein recruits its neuronal receptor NCAM to lipid rafts to activate p59fyn and to enhance neurite outgrowth. *The Journal of Cell Biology*, 169(2), pp. 341-354.

Sauer, H., Dadganova, A., Hescheler, J. and Wartenberg, M., 1999. Redox-regulation of intrinsic prion expression in multicellular prostate tumor spheroids. *Free Radical Biology and Medicine*, 27(11-12), pp. 1276-1283

Schmitt-Ulms, G. et al., 2001. Binding of neural cell adhesion molecule (N-CAMs) to the cellular prion protein. *Journal of Molecular Biology*, 314(5), pp. 1209-1225.

Schneider, P. and Tschopp, J., 2000. Apoptosis induced by death receptors. *Pharmaceutica acta Helvetiae*, 74(2), pp. 281-286.

Schrock, Y., Solis, G.P. and Stuermer, C.A., 2009. Regulation of focal adhesion formation and filopodia extension by the cellular prion protein (PrP^C). *The Federation of European Biochemical Societies Letters*, 583(2), pp. 389-393.

Shen, X. and Falzon, M., 2005. PTH-related protein enhances LoVo colon cancer cell proliferation, adhesion, and integrin expression. *Regulatory Peptides*, 125(1-3), pp. 17-27.

Shyng, S.L., Heuser, J.E. and Harris, D.A., 1994. A glycolipid-anchored prion protein is endocytosed via clathrin- coated pits. *The Journal of Cell Biology*, 125(6), pp. 1239–1250.

Smart, N. and Riley, P.R., 2008. The stem cell movement. *Circulation Research*, 102, pp. 1155-1168.

Soares, M.P., et al., 2002. Modulation of endothelial cell apoptosis by heme oxygenase-1-derived carbon monoxide. *Antioxidants & Redox Signaling*, 4(2), pp. 321-329.

Spudich, A. et al., 2005. Aggravation of ischemic brain injury by prion protein deficiency: Role of ERK-1/-2 and STAT-1. *Neurobiology of Disease*, 20(2), pp. 442-449.

Stahl, N. and Prusiner, S.B., 1991. Prions and prion proteins. *Federation of American Societies for Experimental Biology Journal*, 5(13), pp. 2799–2807.

Stockel, J., Safar, J., Wallace, A.C., Cohen, F.E. and Prusiner, S.B., 1998. Prion protein selectively binds copper(II) ions. *Biochemistry*, 37(20), pp. 7185-7193.

Stohr, J. et al., 2008. Mechanisms of prion protein assembly into amyloid. *Proceedings of the National Academy of Sciences of the United States of America*, 105(7), pp. 2409-2414.

Sunyach, C. et al., 2003. The mechanism of internalization of glycosylphosphatidylinositol-anchored prion protein. *The European Molecular Biology Organization Journal*, 22(14), pp. 3591–3601.

Tacar, O., Sriamornsak, P. and Dass, C.R., 2013. Doxorubicin: An update on anticancer molecular action, toxicity and novel drug delivery systems. *Journal of Pharmacology and Pharmacotherapeutics*, 65(2), pp. 157-170.

Talmadge, J.E. and Fidler, I.J., 2010. AACR centennial series: the biology of cancer metastasis: historical perspective. *Cancer Research*, 70(14), pp. 5649-5669.

Taylor, D.R. and Hooper, N.M., 2006. The prion protein and lipid rafts. *Molecular Membrane Biology*, 23(1), pp. 89-99.

Tenhunen, R., Marver, H.S. and Schmid, R., 1969. Microsomal heme oxygenase. Characterization of the enzyme. *The Journal of Biological Chemistry*, 244(23), pp. 6388-6394.

Thiery, J.P. and Sleeman, J.P., 2006. Complex networks orchestrate epithelial-mesenchymal transitions in development and disease. *Molecular Cell Biology*, 7, pp. 131-142.

Thomas, P. and Smart, T.G., 2005. HEK 293 cell line: A vehicle for the expression of recombinant proteins. *Journal of Pharmacological and Toxicological Methods*, 51(3), pp. 187-200.

Tom, B.H. et al., 1976. Human colonic adenocarcinoma cells. I. Establishment and description of a new line. *In vitro*, 12(3), pp. 180-191.

Tsui-Pierchala, B.A., Encinas, M., Milbrandt, J. and Johnson, E.M., 2002. Lipid rafts in neuronal signaling and function. *Trends in Neurosciences*, 25(8), pp. 412-417.

Vassallo, N. et al., 2005. Activation of phosphatidylinositol 3-kinase by cellular prion protein and its role in cell survival. *Biochemical and Biophysical Research Communications*, 332(1), pp. 75-82.

Vucic, D. et al., 2002. SMAC negatively regulates the anti-apoptotic activity of melanoma inhibitor of apoptosis. *The Journal of Biological Chemistry*, 277(14), pp. 12275-12279.

Waggoner, D.J. et al., 2000. Brain copper content and cuproenzyme activity do not vary with prion protein expression level. *The Journal of Biological Chemistry*, 275(11), pp. 7455-7458.

Walter, E.D., Chattopadhyay, M. and Millhauser, G.L., 2006. The affinity of copper binding to the prion protein octarepeat domain: evidence for negative cooperativity. *Biochemistry*, 45(43), pp. 13083-13092.

Wang, Q., Qian, J., Wang, F. and Ma, Z., 2012. Cellular prion protein accelerates colorectal cancer metastasis via the Fyn-SP1-SATB1 axis. *Oncology Reports*, 28(6), pp. 2029-2034.

Watanabe, T. et al., 2011. Involvement of cellular prion protein in the migration of brain microvascular endothelial cells. *Neuroscience Letters*, 496(2), pp. 121-124.

Watanabe, T. et al., 2012. Atorvastatin stimulates neuroblastoma cells to induce neurite outgrowth by increasing cellular prion protein expression. *Neuroscience Letters*, 531(2), pp. 114-119.

Watts, J.C., et al., 2007. The CNS glycoprotein Shadoo has PrP(C)-like protective properties and displays reduced levels in prion infections. *The European Molecular Biology Organization Journal*, 26(17), pp. 4038–4050.

Wei, Y., Fan, T., and Yu, M., 2008. Inhibitor of apoptosis proteins and apoptosis. *Acta Biochimica et Biophysica Sinica*, 40(4), pp. 278-288.

Weise, J. et al., 2006. Deletion of cellular prion protein results in reduced Akt activation, enhanced postischemic caspase-3 activation, and exacerbation of ischemic brain injury. *Stroke*, 37(5), pp. 1296-1300.

Wells, G.A.H. et al., 1987. A novel progressive spongiform encephalopathy in cattle. *The Veterinary Record*, 121(18), pp. 419-420.

Westergard, L., Christensen, H.M. and Harris, D.A., 2007. The cellular prion protein (PrP^c): Its physiological function and role in disease. *Biochimica et Biophysica Acta*, 1772(6), pp. 629-644.

White, A.R. et al., 1999. Prion protein-deficient neurons reveal lower glutathione reductase activity and increase susceptibility to hydrogen peroxide toxicity. *The American Journal of Pathology*, 155(5), pp. 1723-1730.

Wilson, D.A. and Nixon, R.A., 2009. Sniffing out a function for prion proteins. *Nature Neuroscience*, 12(1), pp. 7-8.

Wong, B.S. et al., 2001. Increased levels of oxidative stress markers detected in the brains of mice devoid of prion protein. *Journal of Neurochemistry*, 76(2), pp. 565-572.

Wong, R.S.Y., 2011. Apoptosis in cancer: from pathogenesis to treatment. *Journal of Experimental and Clinical Cancer Research*, 30(87), pp. 1-14.

World Cancer Research Fund International, 2014. *Worldwide data*. [Online]. Available at: http://www.wcrf.org/int/cancer-facts-figures/worldwide-data [Accessed: 8th August 2014].

Yang, D., Welm, A. and Bishop, J.M., 2004. Cell division and cell survival in the absence of survivin. *Proceedings of National Academy of Science United States of America*, 101(42), pp. 15100–15105.

Yang, X. et al., 2014. Prion protein and cancers. *Acta Biochimica et Biophysica Sinica*, 46(6), pp. 431-440.

Yap, Y.H and Say, Y.H., 2011. Resistance against apoptosis by the cellular prion protein is dependent on its glycosylation status in oral HSC-2 and colon LS 174T cancer cells. *Cancer Letters*, 306(1), pp. 111-119

Yap, Y.H. and Say, Y.H., 2012. Resistance against tumor necrosis factor α apoptosis by the cellular prion protein is cell-specific for oral, colon and kidney cancer cell lines. *Cell Biology International*, 36(3), pp. 273-277.

Yilmaz, M. and Christofori, G., 2009. EMT, the cytoskeleton, and cancer cell invasion. *Cancer Metastasis Reviews*, 28(1-2), pp. 15-33.

Yu, H. et al., 2012. Silencing prion protein in mdamb-435 breast cancer cells leads to pleiotropic cellular responses to cytotoxic stimuli. *Public Library of Sience One*, 7(11), e48146. doi: 10.1371/journal.pone.0048146.

Zainal Arrifin, O. and Nor Saleha, I.T., 2011. NCR Report 2007, *Ministry of Health*, Malaysia.

Zanata, S.M. et al., 2002. Stress-inducible protein 1 is a cell surface ligand for cellular prion that triggers neuroprotection. *The European Molecular Biology Organization Journal*, 21(13), pp. 3307-3316.

Zhang, C.C., Steele, A.D., Lindquist, S. and Lodish, H.F., 2006a. Prion protein is expressed on long-term repopulating hematopoietic stem cells and is important or their self-renewal. *Proceedings of the National Academy of Sciences of the United States of America*, 103(7), pp. 2184-2189.

Zhang, Y., Qin, K., Wan, J., Hung, T., and Zhao, R.Y., 2006b. Dividing roles of prion protein in staurosporine-mediated apoptosis. *Biochemical and Biophysical Research Communications*, 349(2), pp. 759-768.

Zhang, Y.W., Shi, J., Li, Y.J. and Wei, L., 2009. Cardiomyocyte death in doxorubicin-induced cardiotoxicity. *Archivum Immunologiae et Therapia Experimentalis (Warsz),* 57(6), pp. 435-445.

Zhao, Y. et al., 2002. Differentially expressed gene profiles between multidrug resistant gastric adenocarcinoma cells and their parental cells. *Cancer Letters*, 185(2), pp. 211-218.

APPENDIX A

Coordinates and targets of human apoptosis antibody array.

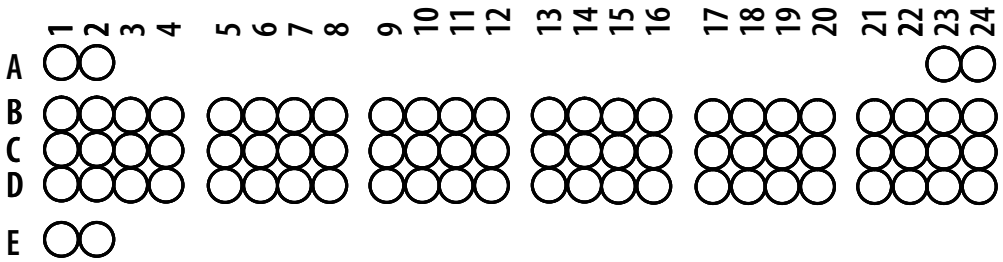

Coordinate	Target/Control	Coodinate	Target/Control
A1, A2	Reference Spots	C13, C14	HO-2/HMOX2
A23, A24	Reference Spots	C15, C16	HSP27
B1, B2	Bad	C17, C18	HSP60
B3, B4	Bax	C19, C20	HSP70
B5, B6	Bcl-2	C21, C22	HTRA2/Omi
B7, B8	Bcl-x	C23, C24	Livin
B9, B10	Pro-Caspase-3	D1, D2	PON2
B11, B12	Cleaved Caspase-3	D3, D4	p21/CIP1/CDKN1A
B13, B14	Catalase	D5, D6	p27/Kip1
B15, B16	cIAP-1	D7, D8	Phospho-p53 (S15)
B17, B18	cIAP-2	D9, D10	Phospho-p53 (S46)
B19, B20	Claspin	D11, D12	Phospho-p53 (S392)
B21, B22	Clusterin	D13, D14	Phospho-Rad17 (S635)
B23, B24	Cytochrome c	D15, D16	SMAC/Diablo
C1, C2	TRAIL R1/DR4	D17, D18	Survivin
C3, C4	TRAIL R2/DR5	D19, D20	TNF RI/TNFRSF1A
C5, C6	FADD	D21, D22	XIAP
C7, C8	Fas/TNFRSF6/CD95	D23, D24	PBS (Negative Control)
C9, C10	HIF-1α	E1, E2	Reference Spots
C11, C12	HO-1/HMOX1/HSP32		

APPENDIX B

Human apoptosis antibody array intensity analysis of LS 174T cells pre-doxorubicin treatment.

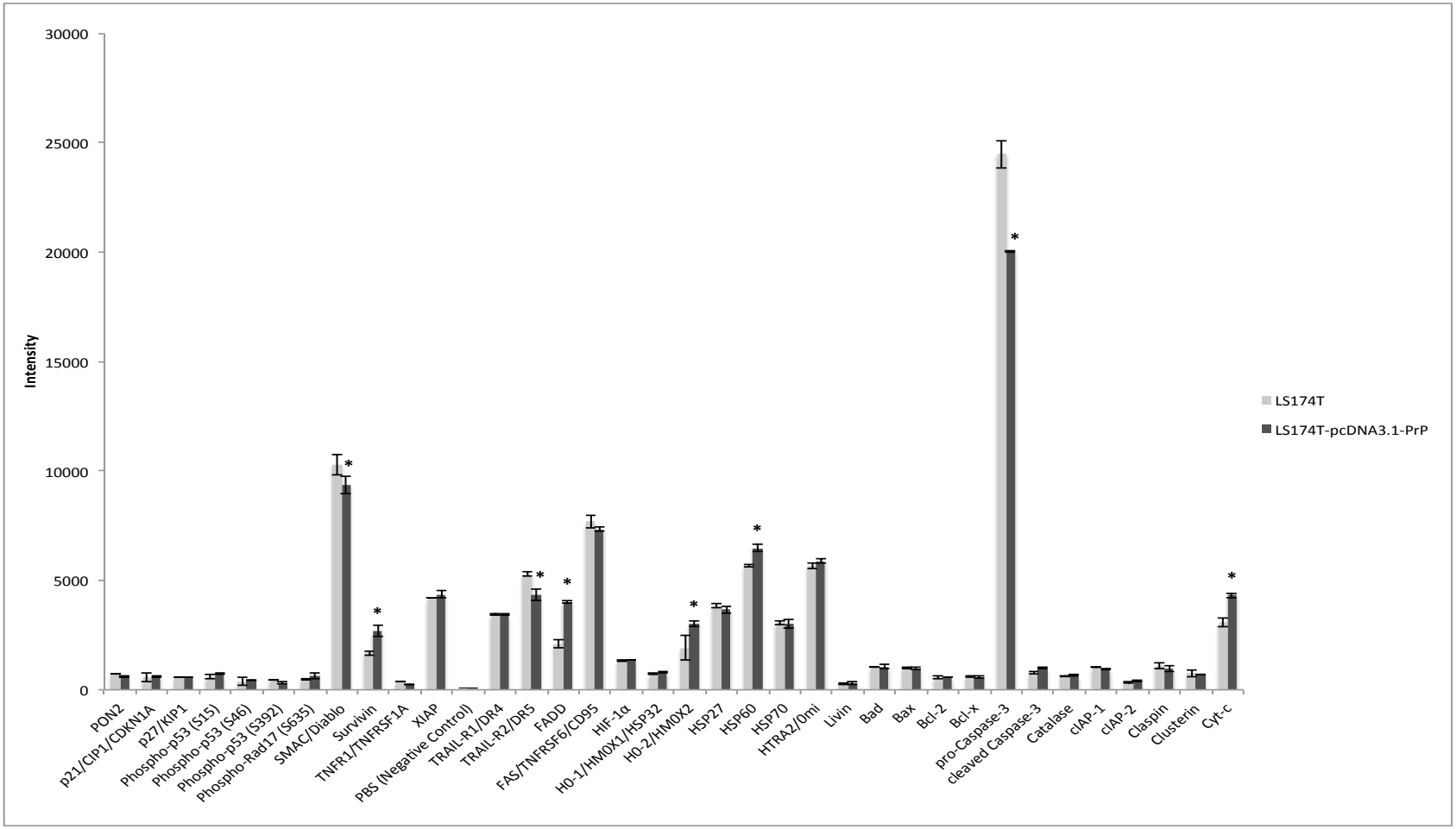

APPENDIX C

Human apoptosis antibody array intensity analysis of LS 174T cells post-doxorubicin treatment.

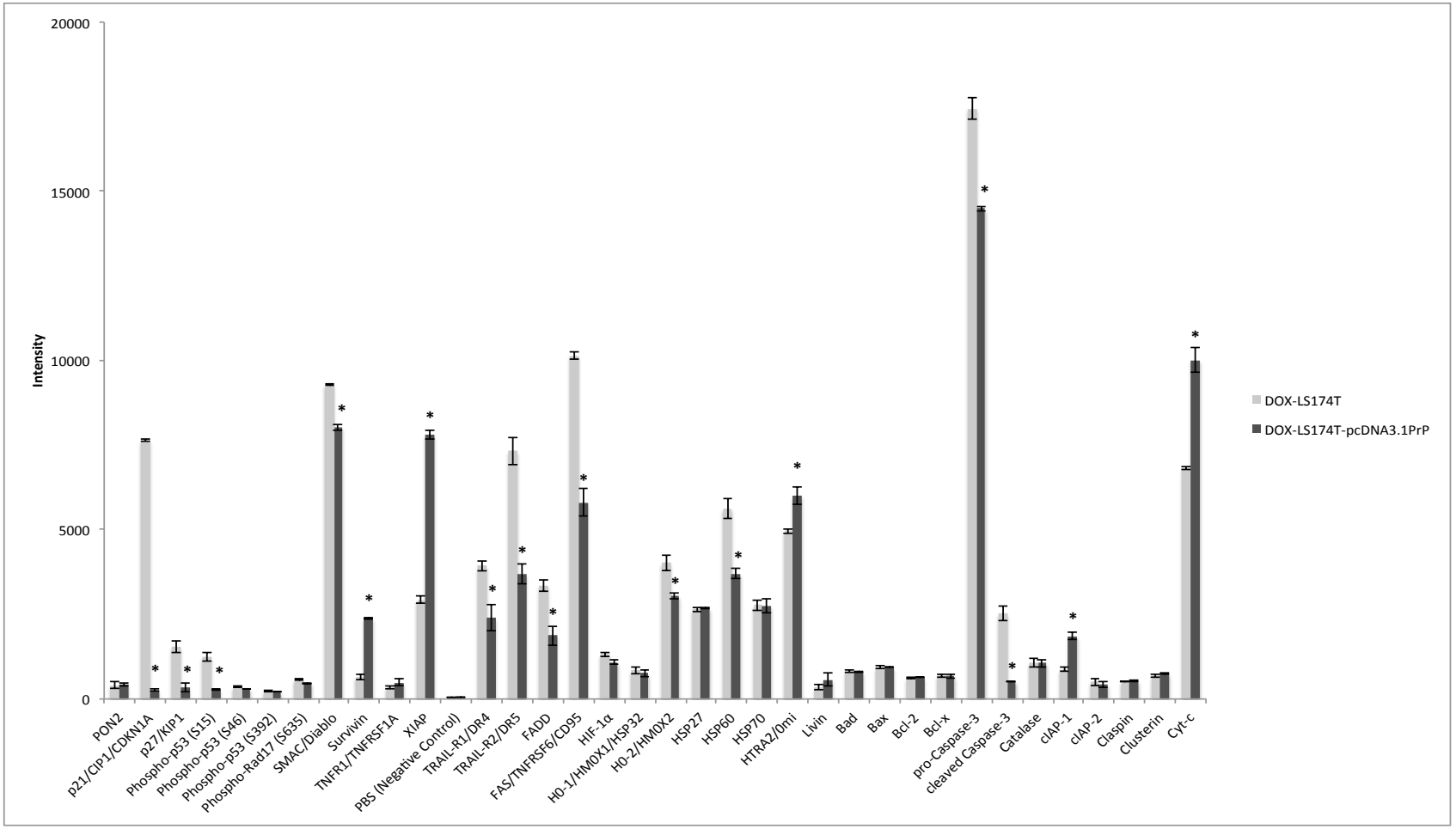

APPENDIX D

Densitometry analysis for LS 174T and DOX-LS 174T cells.